FOREST FIRE AEROSOL FORCING OF PRECIPITATION

ALONG THE U.S. SOUTH ATLANTIC COAST

by

CRAIG A. RAMSEYER

(Under the Direction of Thomas L. Mote)

ABSTRACT

This thesis uses six case days to examine the effects of aerosols produced by forest fires on the development of deep marine clouds and their ability to precipitate available cloud liquid water (CLW) along the U.S. South Atlantic coast. A proxy for precipitation efficiency (CREP) is calculated using a blended satellite precipitation product and CLW path from the Advanced Microwave Scanning Radiometer – Earth Observing System (AMSR-E), following the methodology of Jin and Shepherd (2008); Berg et al. (2006). This study finds that shallow precipitating clouds are very rare, likely due to precipitation suppression from forest fire aerosols. Upwind aerosol optical thickness (AOT) values of >1.5 are needed for a noticeable impact on precipitation in deep clouds. Cloud effective radius is decreased in all six cases. CREP shows inconsistent aerosol forcing on precipitation for high aerosol cases. The discrepancy may be related to suppression of precipitation when a high percentage of cloud condensation nuclei are thrust above the level of homogeneous nucleation by intense updrafts.

INDEX WORDS: forest fire, aerosol, precipitation, CREP

FOREST FIRE AEROSOL FORCING OF PRECIPITATION ALONG THE U.S. SOUTH ATLANTIC COAST

by

CRAIG A. RAMSEYER

B.S., James Madison University, 2009

A Thesis Submitted to the Graduate Faculty of The University of Georgia in Partial Fulfillment of the Requirements for the Degree

MASTER OF SCIENCE

ATHENS, GEORGIA

2011

FOREST FIRE AEROSOL FORCING OF PRECIPITATION

ALONG THE U.S. SOUTH ATLANTIC COAST

by

CRAIG A. RAMSEYER

Major Professor:	Thomas Mote
Committee:	Marshall Shepherd
	Yongqiang Liu

Electronic Version Approved:

Maureen Grasso
Dean of the Graduate School
The University of Georgia
August 2011

ACKNOWLEDGMENTS

Thank you to Dr. Thomas Mote (Climate Research Laboratory/UGA) for his input and assistance, as well as, Dr. Marshall Shepherd (UGA) and Dr. Yongqiang Liu (Southern Research Center/USDA Forest Service) for their participation on the thesis committee. Thank you to Dr. Scott Goodrick (Southern Research Center/USDA Forest Service) for providing access to the SMARTFIRE database. This research was partially supported by a cooperative agreement SRS 09-CA-1330138-079 between the USDA Forest Service and the University of Georgia.

TABLE OF CONTENTS

Page

LIST OF TABLES

Page

LIST OF FIGURES

Page

CHAPTER 1

INTRODUCTION

Both human and natural processes contribute to the composition of the atmosphere. Biomass burning as well as urban and industrial pollutants contribute extensively to the anthropogenic aerosol concentrations in the atmosphere and are a major constituent in climate change (Ramanathan et al. 2005). Aerosols play a large role in the global energy budget through their ability to reduce solar radiation and through their secondary effects by altering clouds and the microphysical processes within them (Koren et al. 2004, Ramanathan et al. 2005, Lohmann and Feichter 2005). The importance of aerosols in the global climate system has been recognized by the United Nations Framework Convention on Climate Change (UNFCCC) and the Global Climate Observing System (GCOS), which called aerosols, cloud properties, and precipitation essential climate variables.

The role of aerosols in cloud microphysical processes and resultant precipitation has become a focus of research during the past two decades (Stevens and Feingold 2009). The effect of aerosols on cloud microphysics and precipitation is difficult to ascertain using only *in situ* measurements or ground measurements, but this effort has been aided by the advent of multiple new sources of information from satellite observations. A combination of *in situ* and satellite measurements may provide the most promising results for observational studies. Much of the research in the area is directed toward aerosols resulting directly from human processes (industrial, urban, and agricultural), while the effects of aerosols resulting from natural or quasi-

natural processes, such as those resulting from forest fires, are still debated. Aerosols have the potential to change precipitation patterns. Aerosols can also alter the latent heat release process which has global impacts. Latent heat release is a critical input into global circulation patterns (Rosenfeld 1999).

This thesis explores the effects of forest fire aerosols on the formation of clouds as well as the effect of changing cloud microphysics that lead to precipitation. The research area is focused on the southwest Atlantic Ocean, near the south Atlantic coast of the U.S. Fires from states along the south Atlantic coastline, including Florida, North Carolina, Georgia, South Carolina, and Virginia, served as the point sources of aerosols studied (Fig. 1). This thesis examines the effects of elevated aerosol concentrations on precipitation in clouds over the southwest Atlantic Ocean due to wildfire emissions. Previous research has shown that different cloud regimes have different responses to elevated aerosols (Rosenfeld 1999, Andreae et al. 2004). This thesis will focus on cold top, deep maritime clouds which have received less attention in the scientific literature.

Aerosols have the ability to alter microphysical processes in cloud formation and precipitation. Aerosols ability to affect precipitation can have regional socio-economic impacts on crop farming and drinking water especially if there is a negative forcing. Changing precipitation patterns due to the introduction of aerosols can have impacts on the global water and carbon cycle. Because aerosols can have an impact on cloud formation and precipitation efficiency, they are important parameters in cloud and weather models. Forest fire aerosols are analyzed specifically in this study because of their frequency in the Southeast, particularly during the spring months.

The primary research objective addressed in this study is to examine the forcing of forest fire aerosols on cold, deep layer marine cloud precipitation off of the southeastern U.S. Atlantic Coast. The methodology used to address this objective made use of a suite of remote sensing data products. Moderate Resolution Imaging Spectroradiometer (MODIS) Aerosol Product data are the used to estimate smoke aerosol concentration. MODIS Cloud Product data are commonly used to determine cloud top temperature, cloud particle effective radius, and cloud phase. Forest fire spatial extent and plume height is gathered from the Satellite Mapping Automated Reanalysis Tool for Fire Incident Reconciliation (SMARTFIRE) database (www.getbluesky.org/smartfire/). North American Regional Reanalysis (NARR) wind fields as well as trajectory model output from the Hybrid Single Particle Lagrangian Integrated Trajectory Model (HYSPLIT) were utilized in order to determine the path of travel of the forest fire aerosols from the smoke plume. An infrared-passive microwave blended precipitation product from Tropical Rainfall Measuring Mission (TRMM) was used to quantify precipitation from marine clouds. Advanced Microwave Scanning Radiometer – Earth Observing System (AMSR-E) data was used to provide estimates of cloud liquid water (CLW).

This study produced a precipitation efficiency proxy for smoky and non-smoky clouds, examining cloud effective radius and cloud phase for smoky and non-smoky days, and approximating aerosol loads for class G fire days. Based on previous research, the hypothesis for the outcome of this study, was that aerosol induced deep clouds would lead to higher values of the precipitation efficiency proxy due to the initial suppression of precipitation in the clouds' early stage.

This study is novel in a few facets. A precipitation efficiency proxy is defined to analyze individual case days. Similar proxies have been used, but primarily for studies analyzing longer

periods (monthly, seasonal). The Atlantic Coast of the U.S. is an area unstudied with respect to aerosol forcing on precipitation. The spatial extent of the clouds studied is larger than most studies in the discipline. This study analyzed six case days which is a relatively large number considering the depth in which each case day is analyzed.

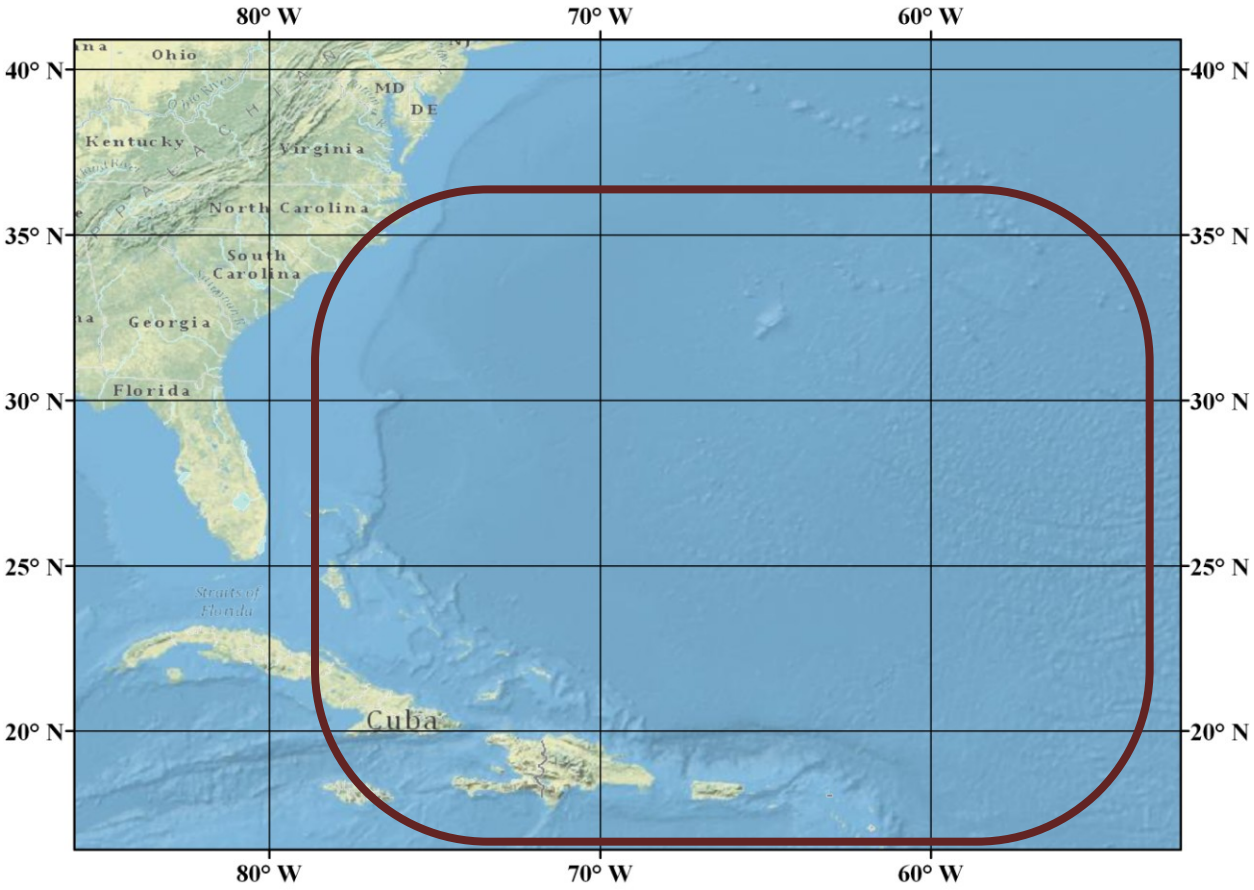

Fig. 1.1. Project study area along the U.S. South Atlantic Coast.

CHAPTER 2

LITERATURE REVIEW

The effects of aerosols on clouds and precipitation have been studied for over 50 years. The advancement of satellite technology and robust weather, climate, and cloud models over the past two decades has led to an increase in research and a better understanding of how aerosols are affecting many facets of the climate system. In order to understand how this study fits into the existing body of research, a literature review on the subject is presented in Chapter 2.

2.1. Biomass Fire Aerosols

Other than industrial pollutants, biomass burning emissions are the other main pollution source on a global scale (Levin and Cotton 2009). Some of the biomass burning emissions are the result of fires caused by direct human induced fires, for clearing land, or logging operations. The rest of the biomass burning aerosols result from naturally occurring fires. There may be some indirect human effects still associated with seemingly naturally occurring fires. These naturally occurring biomass fires are mostly caused by climatological and meteorological events such as drought and lightning, with lightning being the most common ignition source. In tropical forests, the number of human induced fires greatly outnumbers the number of natural fires (Bevan et al. 2009).

Biomass burning aerosols are mainly composed of carbonaceous species (Reid et al. 2005, Andreae et al. 1996, Sinha et al. 2003). Black carbon (BC) is one of the significant sub-

species. BC is defined as, light-absorbing or thermally refractory carbon (Levin and Cotton 2009). BC is considered to be a collection of aggregates that range in size from 20-50 nm (Levin and Cotton 2009, Smith et al. 1989). Other significant species come from high organic fraction of the emission (Andreae and Merlet 2001, Sinha et al. 2003). Biomass burning aerosols are distinctly different from industrial aerosols in that they have relatively high organic percentage of the total emissions (Andreae and Merlet 2001). Biomass burning aerosols accounts for a large percentage of the emitted organic particles into the atmosphere (Crutzen and Andreae 1990). Industrial aerosols and biomass burning aerosols contribute about equally to BC emissions, with biomass burning aerosols possibly contributing slightly more than industrial aerosols (Penner et al. 2001). Individual aerosol particles are often a mixture of aerosols with a core carbonaceous material and an organic material coating (Ramanathan et al. 2001a, Haywood and Boucher 2000).

Studies have shown that approximately half of the organic matter within biomass burning aerosols is water soluble (Reid et al. 2005). High water solubility is important because it is an indicator of the ability for these aerosols to dissolve into the solvent (i.e. water in the atmosphere). The remaining inorganic portion is minor initially, but as the aerosol ages, it can comprise a significant contribution to the soluble content of forest fire aerosols (Roberts et al. 2002, Reid and Hobbs 1998). Differences in chemical makeup of aerosols could lead to different responses in meteorological processes such as cloud formation and precipitation efficiency thus identifying the composition of an aerosol is critical for analyzing these processes.

Biomass burning is also a major source of trace gases such as NO, CO_2, O_3, NO_x SO_x, CH_4, and others (Kaufman et al. 1992, Andreae et al. 1988, Crutzen et al. 1985). Studying the effect of these individual gases on meteorological processes is beyond the scope of this thesis.

Modern technology allows for these gases and aerosols to be measured in forest fires, from *in situ* measurements and satellite data.

2.2 Radiative Effects of Aerosols

The primary direct radiative effect of carbonaceous aerosols (BC and organic) is their ability to absorb and reflect shortwave radiation. BC is particularly efficient at absorbing incoming radiation even in small quantities in the atmosphere (Grassi 1975). One consequence of large atmospheric absorption is a large negative surface forcing and local cooling effect (Ramanathan et al. 2001a). Observed trends indicate that from 1960-2000, solar radiation was decreasing -0.42 $W \cdot m^2$ per decade (Ramanathan et al. 2005)(Fig. 2.1). This surface cooling can also alter evaporation processes at the surface (Ramanathan et al. 2005). BC also has the ability to absorb radiation emitted or reflected by the surface (Ramanathan et al. 2001a). Aerosol induced changes at the top of the atmosphere is much less than the changes seen at the surface (Satheesh and Ramanathan 2000). The net aerosol forcing at the top of the atmosphere in the 1990s was within ± 1 $W \cdot m^{-2}$ whereas the net surface forcing was of the order of ± 10 to ± 15 $W \cdot m^{-2}$ (Ramanathan et al. 2005). There is a balance of evaporation, radiation, and sensible heat flux at the surface. With a decrease in surface radiation due to the introduction of aerosols, the other components will decrease in order to compensate (Ramanathan et al. 2001a). Approximately 65% of the global annual mean of absorbed surface radiation is balanced by evaporation (Kiehl and Trenberth 1997). A reduction in evaporation would be balanced by a decrease in precipitation which would lead to a ripple effect through the hydrologic cycle (Ramanathan et al. 2001a). This indicates that aerosols have a large effect on surface processes and the hydrologic cycle which can have wide reaching impacts on a number of meteorological processes.

Indirect effects refer to the role played by aerosols as cloud condensation nuclei (CCN). CCN play a prominent role in precipitation formation and efficiency by providing a nucleus with which water is able to adhere to. A positive relationship exists between the number of CCN and droplet number concentration (Fig. 2.2). This means as the number of CCN increases, the number of droplets increases. An increase in albedo results from the increase in the number of drops (Twomey 1977, Ramanathan et al. 2001a, Kaufman et al. 2002, Rosenfeld et al. 2008). This results in a brighter cloud due to the increase in reflective surface.

Another indirect effect of aerosols causes a reduction of precipitation efficiency and a subsequent increase in cloud lifetimes (Albrecht 1989). The increased lifetime of clouds leads to a further increase in the reflection of solar radiation and a cooling effect at the surface (Ramanathan et al. 2001a). This can have important ramifications for cloud formation and precipitation ability and will be discussed later.

A negative relationship exists between the number of CCN and droplet effective radius (Bevan et al. 2009). Thus, as aerosols increase they increase the number of CCN and create smaller droplets as shown in several *in situ* and satellite studies (Kaufman and Fraser 1997, Martin et al. 1994, Pawlowska and Brenguier 2000, Taylor and McHaffie 1994). These smaller drops are less efficient at precipitating in most cases (Rosenfeld 1999, Ramanathan et al. 2001a). As aerosols increase CCN counts, the available water will theoretically remain constant. As a result, the same amount of water is available but is distributed over a greater number of droplets and it changes the drop size distribution (DSD) in the cloud (Rosenfeld 1999). At any particular location, CCN vary by several orders of magnitude with time, depending on the proximity of sources, wind direction, air mass type, precipitation and cloudiness (Radke and Hobbs 1969). The land surface acts as a major source of CCN (i.e. dust, organic matter, etc.)(Radke and Hobbs

1969). Naturally, marine air masses tend to have smaller concentrations of CCN than continental air masses. Forest fires are a naturally occurring cause for increased CCN over land, and are substantial sources of CCN (Radke and Hobbs 1969, Twomey 1960). The rate of production of CCN from burning vegetation matter is on the order of 10^{12} to 10^{15} per kg of material consumed (Eagen et al. 1974).

Giant cloud condensation nuclei (GCCN) can be as large as 100μm in diameter (Levin and Cotton 2009). GCCN can have significant impacts on warm clouds by providing embryos for initiating coalescence growth in warm clouds (Johnson 1982). GCCN can cause rapid development of precipitation size particles in warm clouds in very small quantities (i.e. 1 GCCN per liter) (Johnson 1982). GCCN can also cause have effects on cold clouds by increasing the size of graupel particles (Yin et al. 2000, Teller and Levin 2006, Levin and Cotton 2009). Yin et al. 2000 showed that the inclusion of GCCN caused precipitation to initiate earlier in the cloud lifetime and total accumulation was significantly higher. GCCN are very difficult to measure and thus most studies have been theoretical in nature. Quantification of precipitation in terms of GCCN are currently unfeasible (Levin and Cotton 2009). It is still important to understand the potential impacts that GCCN have on precipitation processes in all clouds and pollution regimes.

Recent studies using remote sensing techniques have found a significant positive correlation between cloud fraction and aerosol optical thickness (AOT) (Kaufman and Koren 2006). AOT is the integral of the aerosol concentration in a column of the atmosphere whose particles intercept (by absorption and scattering) the solar radiation at the wavelength of interest (Ramanathan et al. 2001a). Subsequently there is a positive correlation between CCN and AOT (Rosenfeld et al. 2008; Fig. 2.3). The globally averaged value of AOT (at 0.55 μm) is 0.12 ± 0.04

(Roberts et al. 2001). Natural and anthropogenic sources contribute almost equally to the worldwide quantity of AOT (Radke and Hobbs 1976, Penner et al. 2001).

2.3. Effects of Aerosols on Clouds and Precipitation

The impact of aerosols on cloud formation, cloud microphysics, and precipitation efficiency has been receiving attention for over 50 years (Levin and Cotton 2009). One of the biggest issues is assessing the impact that increasing CCN has on precipitation (Levin and Cotton 2009). The most important complication arises from the fact that different aerosol types correspond to different air masses and cloud regimes. Aerosol chemical makeup can also have an impact on its ability to effect precipitation and cloud formation, as discussed earlier. The effects of aerosols on clouds and precipitation are often studied by analyzing a specific pollution source or cloud regime.

a. General Findings

As discussed earlier, increased aerosols can cause a "dimming" effect at the surface. This decreased solar radiation at the surface causes less heat to be available for evaporation and enhancement of convective rain clouds (Ramanathan 2001b). The absorbed radiation leads to a heating of air in a shallow layer just above the surface. This heating leads to a stabilization of the lower atmosphere and can limit the amount of convective activity (Koren et al. 2004). Increased CCN also has impacts on convective available potential energy (CAPE), thus aerosols have the ability to affect the amount of energy within clouds (Rosenfeld et al. 2008).

Aerosols with large concentrations of small CCN nucleate many small cloud droplets, which coalesce very inefficiently into raindrops thus leading to rain suppression over polluted

regions (Ramanathan et al. 2001b, Rosenfeld 1999). Past remote sensing studies identified a correlation between enhanced aerosol concentrations and suppressed precipitation (Rosenfeld 1999, 2000).

The microphysical properties of clouds are altered by forest fire aerosol concentration. Early studies (Warner and Twomey 1967, Warner 1971, Eagen et al. 1974) found the addition of forest fire smoke particles into clouds caused a reduction in cloud droplet number and size. These effects may impede the formation of rain droplets by coalescence (Levin and Cotton 2009). More recent studies have examined specific cloud types. Presently, cloud physicists normally classify the characteristics of clouds and aerosols into two broad regimes, maritime and continental (Rosenfeld et al. 2008).

b. Continental Cloud Studies

Studying the influence of aerosols on precipitation and storm development over land is a difficult endeavor due to the complex meteorological forces to consider (Jin and Shepherd 2008, Ntelekos et al. 2009). The difficulty comes in extracting the aerosol effect among the other forces in order to make plausible conclusions. Dynamic processes are suggested as being the prevailing factor in determining the formation and spatial extent of aerosol influenced clouds over land and subsequent rainfall (Jin and Shepherd 2008, Shepherd 2005).

Sub micrometer aerosols tend to invigorate precipitation in deep convective warm clouds over land (Ntelekos et al. 2009, Andreae et al. 2004, Koren et al. 2005, Lin et al. 2006, Rosenfeld et al. 2008, Grell et al. 2010). Convective available potential energy (CAPE) increases with increasing CCN concentrations until a threshold is met, in this study, 1000 CCN per cm^{-3} at 0.4% supersaturation (Rosenfeld et al. 2008; Fig. 2.4). One of these studies investigated aerosol

impacts on convective rainfall in the northeastern U.S. It was concluded that low levels of aerosols lead to a general decrease in extreme precipitation and organization of convection (Ntelekos et al. 2009). Also, higher aerosol concentrations led to higher maximum rainfall accumulations and larger areas of maximum accumulations. In Alaska, aerosols from forest fires caused a decrease in precipitation coverage and precipitation amounts during nighttime (Grell et al. 2010). During the afternoon, precipitation became convective and there was a significant increase in coverage and amount.

The increased energy needed to increase precipitation in these clouds must come from another source, increased aerosol loads. Model simulations of these processes suggest that the delay of rain early in a clouds lifecycle causes greater amounts of cloud water and rain later in the cloud lifecycle, thus agreeing with the observational studies (Rosenfeld et al. 2008) (Fig. 2.5).

However, models have found that the dynamic processes associated with aerosol laden deep clouds may be more complex. Models have been able to successfully resolve precipitation invigoration due to aerosols in warm base clouds (0°C) (Phillips et al. 2007). However, models do not suggest precipitation invigoration in scenarios where cloud base is below the 0°C isotherm . At 0°C isotherm almost all of the condensate freezes. The slowing of the rate of coalescing cloud droplets into rainfall (autoconversion) due to increased CCN can leave cloud droplets in the cloud. These cloud drops are elevated by strong updrafts above the -38°C level, the level at which homogeneous nucleation takes place (Rosenfeld et al. 2008). The importance of this is that these small ice particles have no efficient way of falling as precipitation. This process has been confirmed by other modeling studies (Rosenfeld and Woodley 2000, Cui et al. 2006, Khain et al. 2001). Large aerosol loads can lead to mid-tropospheric dryness which can

suppress convective activity (Cui et al. 2006). A model simulation showed that adding small radius CCN aerosols to warm-base clouds has the opposite effect on cold-base deep convective clouds (Khain et al. 2008). Thus, cold-base clouds see a decrease in precipitation by suppressing convective processes (Khain et al. 2008). This process has not yet been detected in observational studies.

c. Maritime Cloud Studies

Due to the lower number of meteorological factors that need to be considered over oceanic areas, including less significant surface-induced convection, it is generally easier to make sound conclusions on the aerosol effect over these areas (Jin and Shepherd 2008). Shallow maritime clouds normally have low CCN concentrations and few cloud droplets (Andreae et al. 2004). Marine clouds often have weak updrafts in part due to the lack of afternoon heating of the surface. Water has a high specific heat and responds slowly to the addition of heat, unlike terrestrial surfaces. The weak updrafts allow more time for raindrops to grow and precipitate before reaching the freezing level. Despite these clouds having relatively low cloud tops, the clouds develop precipitation very efficiently, which is evidenced by the growing drop size distribution with increasing height. Even modest increases in shallow cloud cover (4%) have been shown to offset 2-3 K of greenhouse warming. The addition of aerosols has a large effect on the coverage and properties of shallow marine clouds over the Atlantic Ocean (Kaufman et al. 2005). Kaufman et al. 2005 concluded that the shallow cloud cover increased systematically by 20-40% with increases in the aerosol column concentration, which was evidenced by an increase in the optical thickness from 0.03-0.50. There was a 10-30% reduction in the cloud droplet size in the study. This suggests an inhibition of precipitation in these clouds due to the introduction of

aerosols. The inhibition of precipitation plays a role in the formation and spatial extent of shallow clouds over the Atlantic (Kaufman et al. 2005). Jin and Shepherd 2008 found a detectable negative aerosol cloud droplet size relationship in liquid water clouds in maritime regimes off the China Sea (Fig. 2.6.). These findings suggest that cloud formation is closely related to aerosols while rainfall may be affected by many other processes in addition to the aerosol presence (Jin and Shepherd 2008).

Effects of aerosols on deep clouds over oceans have been given less attention. In the limited studies available, these clouds have been shown to respond somewhat differently than terrestrial deep clouds. Deep tropical clouds off the Australian coast have been shown to have a negative feedback to the introduction of forest fire aerosols (Rosenfeld 1999). This study examined smoky and non-smoky clouds and their ability to precipitate. The smoke free clouds were shown to efficiently convert cloud liquid water to precipitation size drops. This finding is consistent with the notion that deep tropical clouds with large cloud droplets rainout while growing (Rosenfeld 1999). Coalescence efficiency of cloud droplets into rainfall is greatly reduced when the radius of the largest cloud droplets is smaller than an effective radius of 14 μm (Rosenfeld and Gutman 1994). The study with Australian forest fire smoke showed that non-smoky clouds reached an effective radius threshold of 14 μm at 8°C while the smoky clouds never reached the effective radius threshold (Rosenfeld 1999). Warm rain processes in deep tropical clouds were practically shut off and the smoke induced clouds grew to heights of -10°C before the cloud began precipitating while the non-smoky clouds precipitated most of their water before freezing (Rosenfeld 1999). Aerosols have precipitation suppression potential in shallow marine warm clouds as well as deep, cold tropical clouds that are below the freezing level (Rosenfeld 1999).

d. “Smoky” Clouds

Smoky clouds are defined as clouds with high concentrations of aerosols resulting primarily from vegetation burning (Andreae et al. 2004). Pyro-clouds represent the most intense or extreme smoky clouds (Andreae et al. 2004). These clouds have seemingly conflicting aerosol forcing mechanisms. The presence of forest fire aerosols causes high concentrations of small cloud droplets which are slow to coalesce and precipitate while large ash particles act as GCCN and initiate large precipitation particles (Johnson 1982). Extreme concentrations of CCN initially suppress precipitation causing a lack of evaporative cooling which keeps energy embedded in the cloud. An injection of heat provided by the fire provides additional energy to invigorate updrafts allowing the cloud to grow vertically while further suppressing precipitation. Sensitivity to aerosols increases substantially with cloud height above the cloud base (Andreae et al. 2004). High smoke concentrations reduce surface radiational heating which would theoretically provide less energy for convective processes. Despite the decrease in surface heating, the added water and the increased depth of the cloud has been shown to allow for the production of lightning, hail, and heavy rain (Andreae et al. 2004).

e. Conclusions of Previous Studies

The present body of literature suggests that precipitation is suppressed entirely or decreased in shallow clouds due to the introduction of small aerosols. These aerosols cause a reduction in cloud effective radius and an increase in CCN leading to decreased precipitation efficiency (Rosenfeld 1999, Rosenfeld 2000, Andreae et al. 2004, Rosenfeld et al. 2006, Rosenfeld et al. 2008). Most recent research in this discipline focuses on deep clouds,

particularly convective clouds over land (Ntelekos et al. 2009, Andreae et al. 2004, Koren et al. 2005, Lin et al. 2006, Cui et al. 2006, Khain et al. 2001, Grell et al. 2010). These studies suggest the possibility of invigoration of cloud dynamics due to delaying the formation of raindrop in the initial cloud stages (Rosenfeld et al. 2008). In other words, deep clouds with long lifetimes grow to heights where they are able to overcome the aerosol forcing (Graber and Rudich 2006). These findings have been replicated by model studies for deep clouds with warm cloud bases (>0°C) (Rosenfeld et al. 2008). However, some modeling research suggests that deep clouds that are especially cold, with cloud bases < 0°C, can experience a decrease in precipitation when aerosols are introduced (Rosenfeld and Woodley 2000, Cui et al. 2006, Khain et al. 2001, Khain et al. 2008, Rosenfeld et al. 2008).

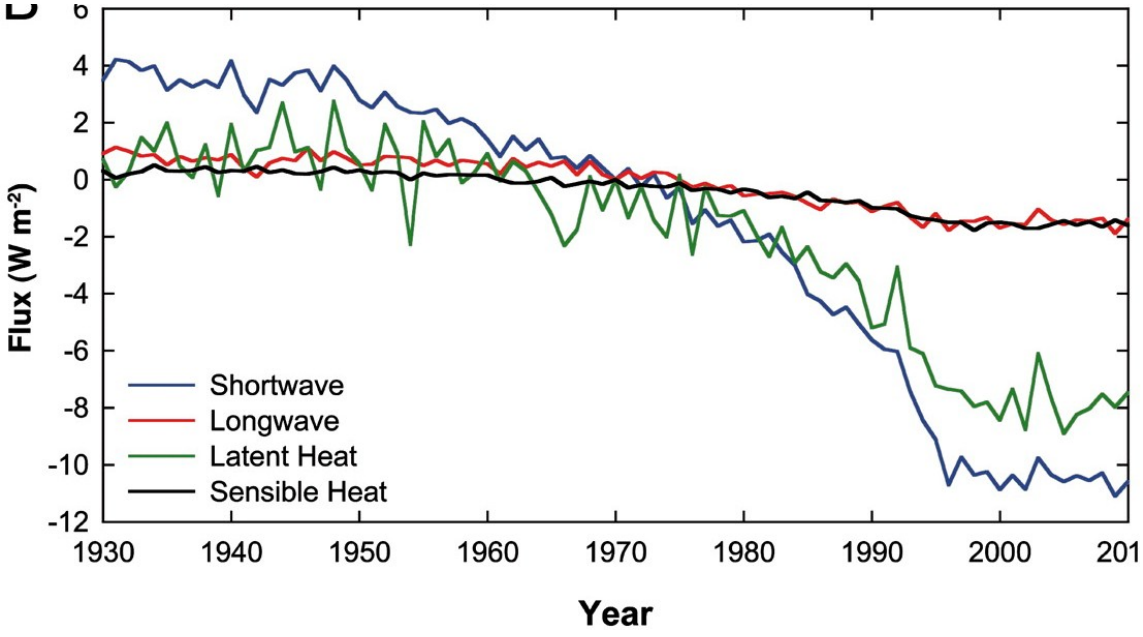

Fig. 2.1 Illustration of evidence of atmospheric dimming due to aerosols for incoming shortwave and sensible heat at the surface from Ramanathan et al. (2005).

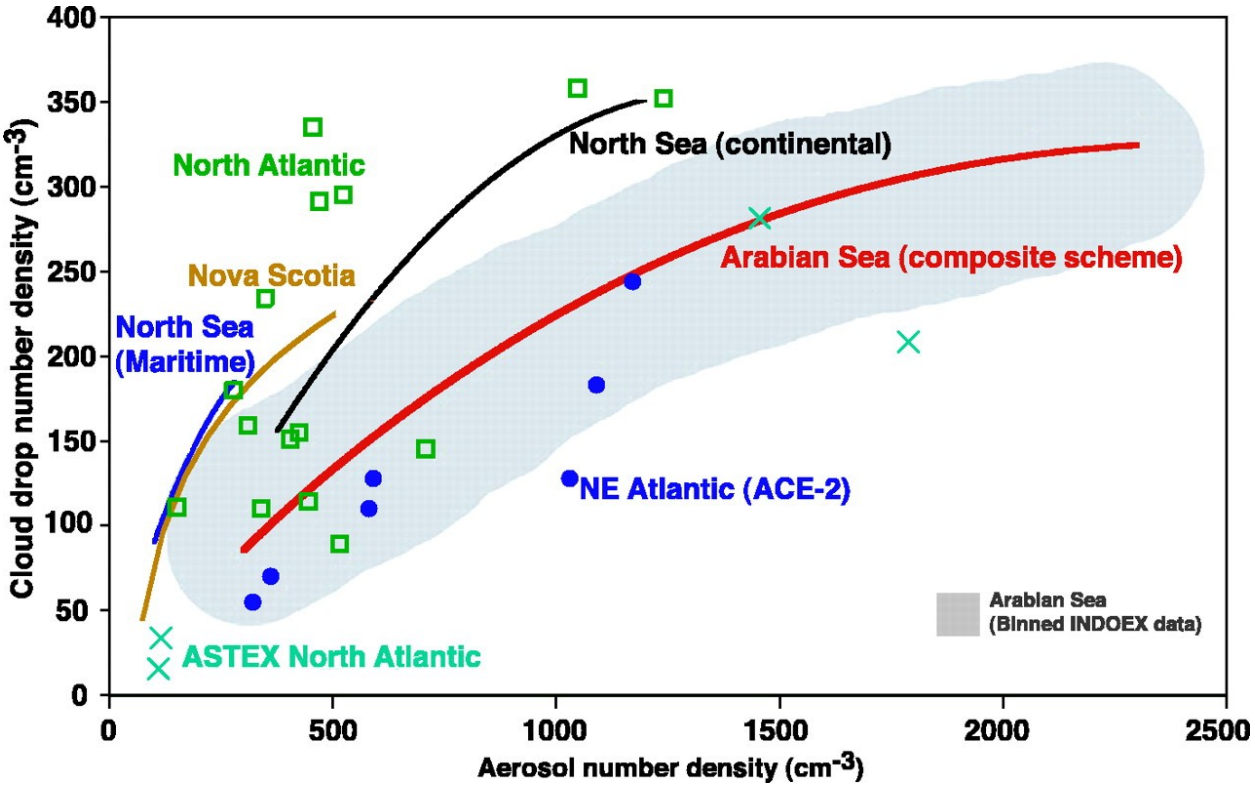

Fig. 2.2. Composite illustration from several studies comparing cloud drop number density versus aerosol number density from Ramanathan et al. (2001a).

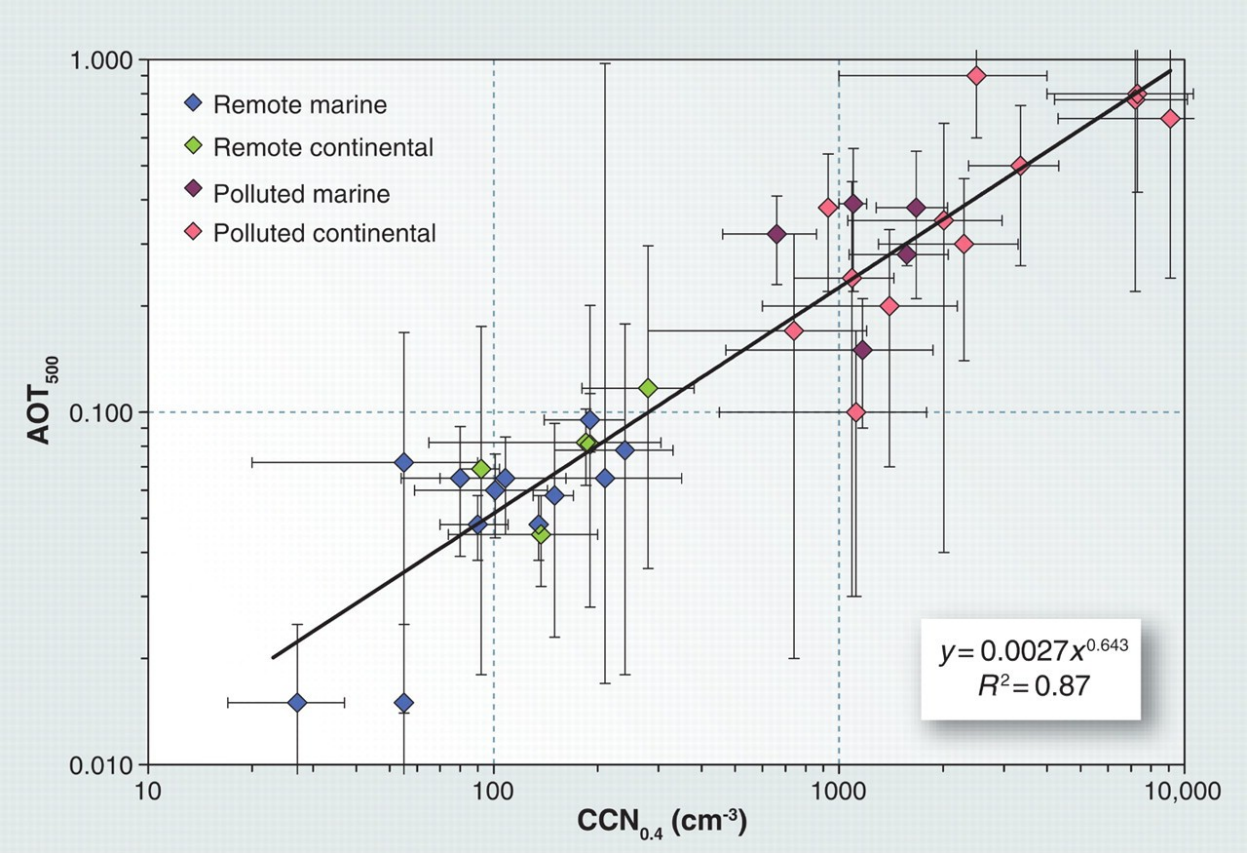

Fig. 2.3. Observed optical thickness at 500 nm and CCN concentrations at 0.4% supersaturation from studies where these variables have been measured simultaneously from Rosenfeld et al. (2008).

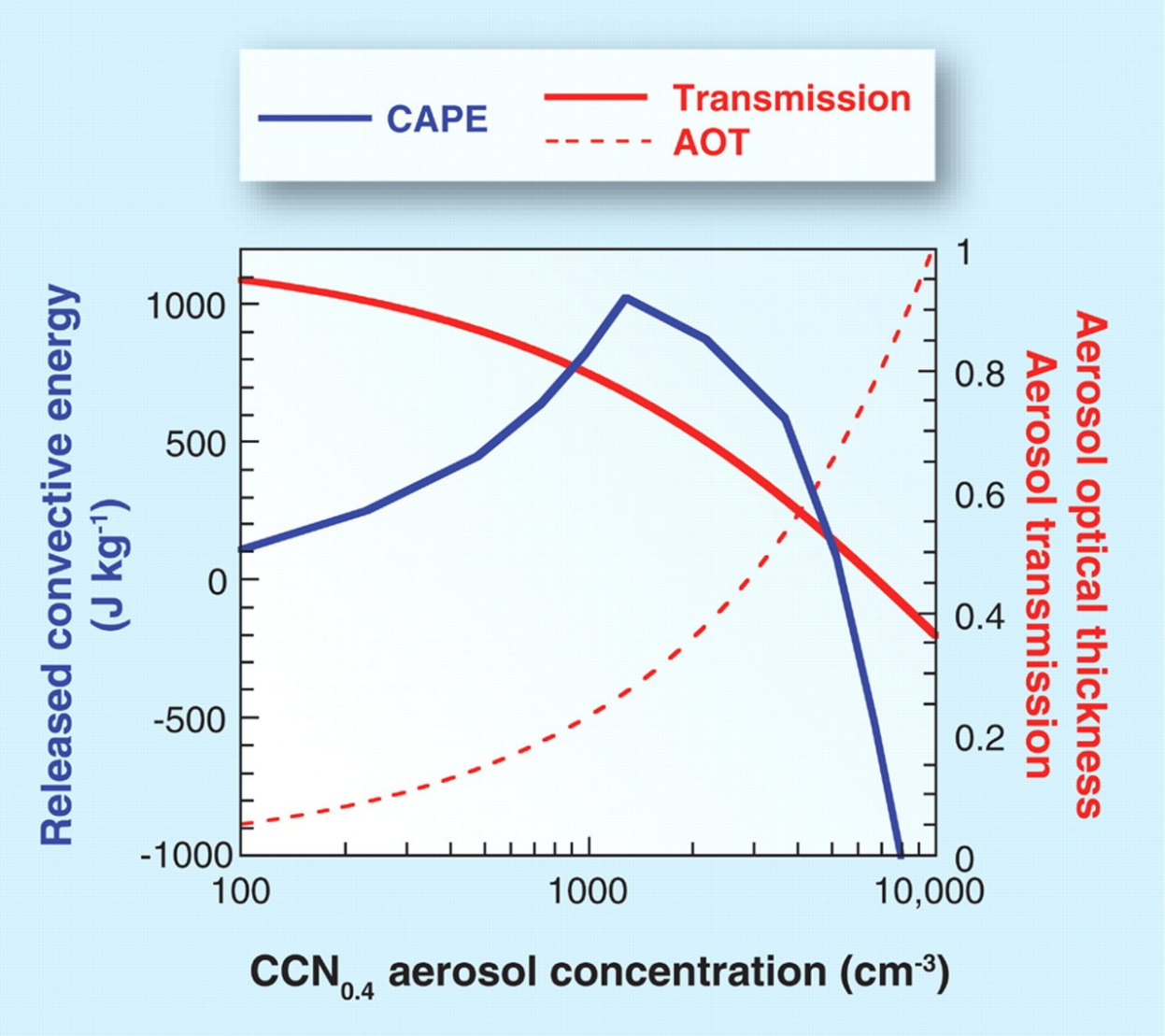

Fig. 2.4. Illustration of the relationships between CCN at 10^{-4} cm^{-3} , CAPE, and AOT from Rosenfeld et al. (2008).

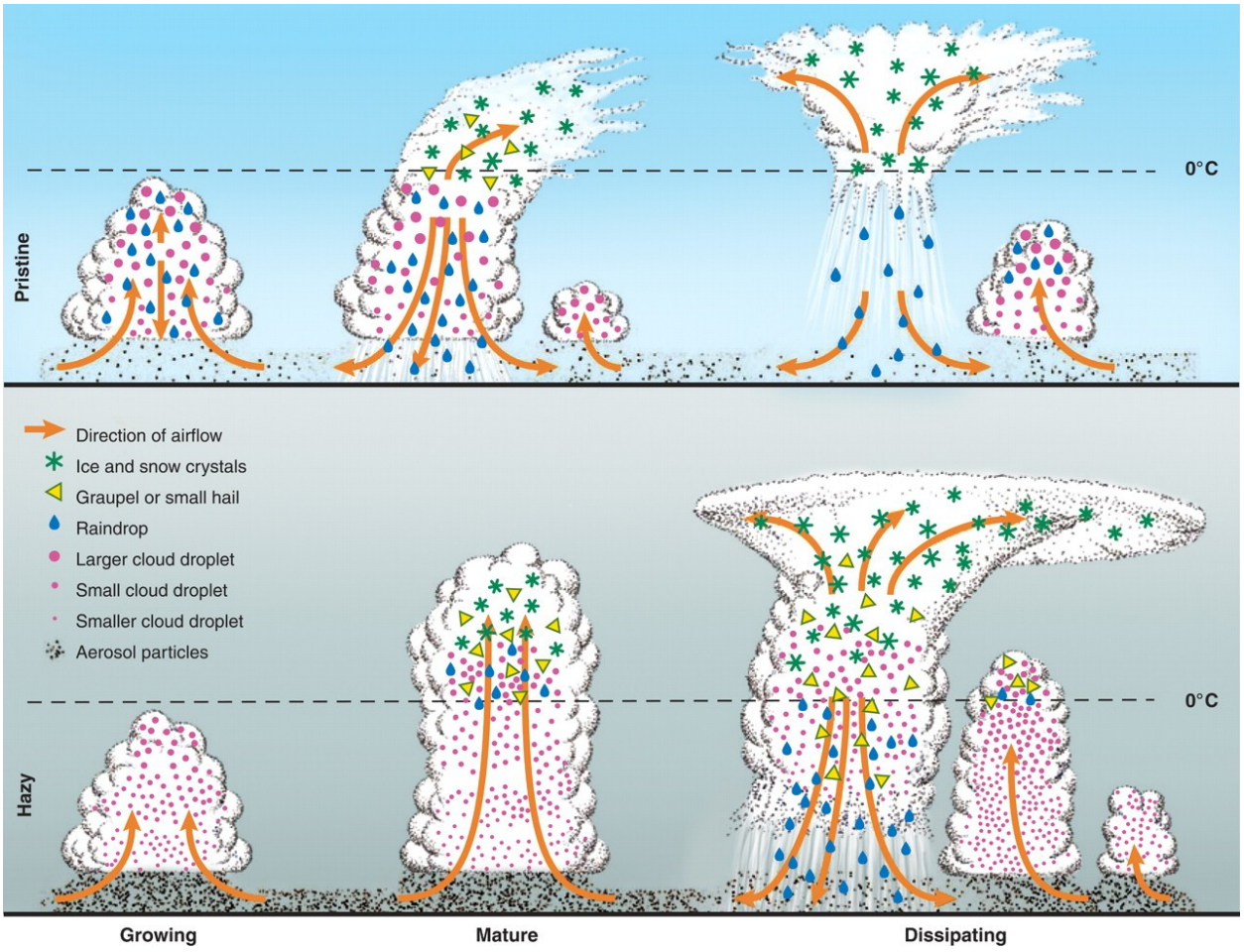

Fig. 2.5. Evolution of deep convective clouds with warm cloud bases (>0°C) in non-smoky (top) and smoky (bottom) clouds from Rosenfeld et al. (2008).

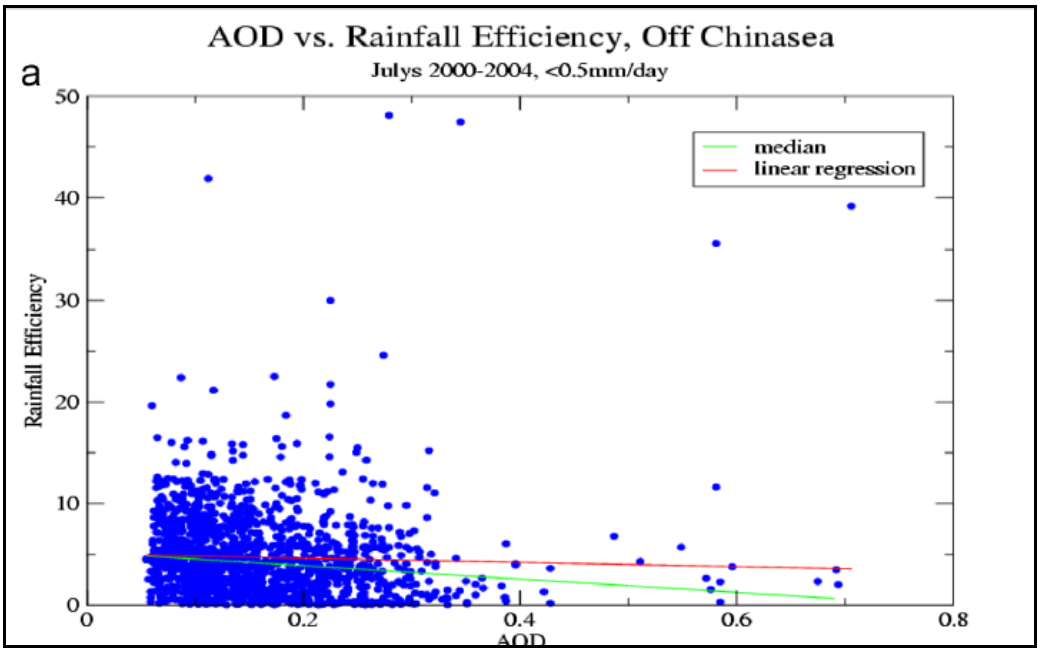

Fig. 2.6. AOT versus Rainfall Efficiency off of the China Sea Coast from Jin and Shepherd (2008).

CHAPTER 3

DATA PRODUCTS AND METHODOLOGY

This study involved the use of several data products. A methodology was developed using these data products in order to address the aerosol forcing on precipitation in the study region. The data products are discussed in section 3.1 and the methodology is discussed in detail in section 3.2.

3.1. Data Products

This study relied on remote sensing data and techniques. The advent of remote sensing techniques for analyzing aerosols and various atmospheric variables has allowed for analysis at a wide range of spatial and temporal extents. Remote sensing techniques allow for the study of remote and oceanic areas which were previously difficult to study. This study analyzes the Atlantic Ocean thus making remote sensing techniques a particularly viable option due to the lack of *in situ* data. Remote sensing techniques still have disadvantages, including relatively coarse spatial resolutions for aerosol measurements. Most remote sensing techniques cannot detect aerosols when clouds are present, making it necessary to infer aerosol concentrations through other processes.

a. MODIS Aerosol and Cloud Products

The Moderate Resolution Imaging Spectroradiometer (MODIS), launched and managed by NASA, is an Earth viewing sensor that is aboard the Earth Observing System (EOS) Aqua and Terra satellites (modis.gsfc.nasa.gov). MODIS began collecting data from Terra in February 2000 and Aqua in June 2002. MODIS provides 36 spectral bands that range in wavelengths between 0.415 and 14.235 μm (Levin and Cotton 2009). The bands vary in spatial resolution from 250 m to 1000m. MODIS has a scan swatch of 2330 kilometers that provides almost daily coverage to most of the globe (Levin and Cotton 2009). The data utilized in this study are stored in Hierarchical Data Format- Earth Observing System (HDF-EOS).

The MODIS Aerosol Product (MOD 04) monitors the ambient AOT over the oceans globally in sun glint-free, cloud-free conditions. AOT is defined as an integrated extinction coefficient value in a cross section of a column of air (Kaufman 1993). Extinction coefficient is the depletion or attenuation of radiance per unit length. AOT can also be thought of as a measure of the attenuation of radiation caused by aerosols. AOT is a unit-less measurement that is on a logarithmic scale (Kaufman 1993). As AOT values are discussed in this study, AOT values should not be compared linearly.

Over ocean scenes the aerosol type is derived while over terrestrial scenes, the aerosol size distribution is derived (Kaufman et al. 2002). The aerosol product is based on different algorithms of tropospheric aerosol over land (Kaufman et al 1997) and ocean (Tanré et al. 1997). Each of these algorithms attempts to match the observed reflectance value with a lookup table of pre-computed observed aerosol conditions and values (King et al. 2003). The land algorithm must deal with the surface reflectance and separate it from the atmospheric reflectance (Kaufman et al. 1997). The atmospheric reflectance is isolated by using lookup tables to determine the

aerosol characteristics and optical thickness in the scene, thus removing the surface reflectance. Land products are available for AOT at 0.47, 0.56, 0.65 μm at a 10-kilometer spatial resolution (King et al. 2003). The ocean algorithm is able to assume the surface reflectance is negligible. The retrieved aerosol products are provided by the best fits between the lookup table and observed reflectance. Ocean products are available at 0.47, 0.56, 0.65, 0.86, 1.24, 1.64, and 2.13 μm (King et al. 2003). This wide spectral range allows for the derivation of aerosol effective radius, which is only available over the oceans. A wide spectral range also allows for more accurate calculations of fine mode fraction than over land. Due to the wide spectral range, the uncertainty in the accuracy of the satellite estimates is lower over the ocean compared to land (King et al. 2003).

The MODIS cloud product (MOD 06) (King et al. 2003) combines visible and infrared techniques to determine physical, microphysical, and radiative cloud properties. The MODIS cloud product is a Level 2 processed data, like the aerosol product. Cloud particle phase, effective cloud particle radius, and cloud optical thickness are derived using MODIS visible and near-infrared channel radiances (modis.gsfc.nasa.gov). Cloud top properties derived using an infrared split window and longwave CO_2 absorption bands at a 5-km resolution include cloud-top temperature (CTT), cloud top pressure, and effective emissivity (Levin and Cotton 2009). Cloud top temperature (CTT) was used in this study to ensure that the vertical extent of the two cloud groups is roughly the same. Cloud phase data was utilized to determine the amount of liquid and ice clouds were included in the clouds. The effective cloud particle radius data was used to analyze changes in the cloud droplet size in the clouds between smoky and non-smoky clouds.

b. Satellite Precipitation Estimates

TRMM is a joint U.S. and Japanese effort that was launched in 1997. Aboard the TRMM satellite are five instruments including the Precipitation Radar (an electronically scanning radar operating at 13.8 GHz), the TRMM Microwave Imager (TMI) which is a passive microwave radiometer, the Visible and Infrared Scanner (VIRS), a five channel visible/infrared radiometer, the Lightning Imaging Sensor (LIS) and the Cloud and Earth Radiant Energey Sensor (CERES). TRMM also has products available that utilize data from multiple other satellites.

This study utilized a daily precipitation estimate product derived from the TRMM Multi-Satellite Analysis (TMPA). TMPA uses a suite of microwave precipitation estimates from multiple microwave sensors including the TRMM TMI, Special Sensor Microwave/Imager (SSM/I), Advanced Microwave Scanning Radiometer (AMSR), and the Advanced Microwave Sounding Unit (AMSU). Infrared estimates are also calculated based on the IR brightness values from the microwave precipitation estimates. The TMPA precipitation rate estimates are provided in 0.25° latitude by 0.25° longitude grid over 50° N-S within seven hours of observation time. Algorithm 3B42 produces daily precipitation rate estimates and root-mean-square (RMS) precipitation error estimates. The daily accumulated rainfall product (in mm) is derived from the 3-hour estimates, beginning at 0 UTC through 21 UTC. These data are available every day from 1 Jan 1997 to the present. (http://mirador.gsfc.nasa.gov/collections/TRMM_3B42_daily__006.shtml). The data utilized in this study was stored in Network Common Data Format (NetCDF).

c. AMSR CLW

The Advanced Microwave Scanning Radiometer – Earth Observing System (AMSR-E) flies aboard the NASA EOS Aqua satellite. This passive sensor provides microwave measurements of oceanic, terrestrial, and atmospheric variables. This study utilized a level 3 daily product of columnar cloud liquid water (CLW) found in the AE_DyOcn data file. AE_DyOcn files are daily global oceanic files with ascending/descending 0.25 x 0.25 decimal degree grids generated from the parent AE_Ocean level 2 files. They include SST, near-surface wind speed, columnar water vapor, and columnar cloud liquid water measurements over oceans. Data are stored in HDF-EOS and are available from 19 June 2002 to the present. The AE_Ocean parent file includes columnar liquid water measurements at a 21 km resolution. These resolutions are mapped to a 0.25 x 0.25 degree grid to produce the level 3 product used in this study (Wentz and Meissner 2004). The CLW product is available for precipitating and non-precipitating it clouds making it appropriate for use in the study. The AMSR CLW daily product is available on the same grid as the 3B42 daily TMPA product.

d. NARR Wind Data

NARR wind data was acquired for several levels of the atmosphere including at the near-surface (1000 hPa), and two lower troposphere levels (700 hPa and 500 hPa). These data have a resolution of about 32 km. Analysis of the NARR wind data aided determining the predominant wind pattern and thus the predominant direction of aerosols from the smoke plumes emitted by forest fires. These data were obtained from NOAA's National Center for Environmental Prediction (NCEP) in Graphics Interchange Format (GIF). NCEP created the NARR dataset in 2004 which has a wide variety of climate and meteorological fields available from 1979-present.

NARR is a high-resolution, high-frequency, land surface and atmosphere dataset that improved on the Global Reanalysis project. NARR has greatly improved analysis of land hydrology, surface-atmosphere interaction, and overall atmospheric circulation in the troposphere since its inception (Mesinger et al. 2006).

e. SMARTFIRE Smoke and Fire Data

Fire data for the thesis were acquired from the SMARTFIRE, a database system that combines multiple sources of fire information including space-borne sensors (ex. NOAA Hazard Mapping System fire detection) and ground-based reports (Fig. 3.1). It was developed through a NASA cooperative research agreement between the USDA Forest Service AirFire Team and Sonoma Technology, Inc. These data cover every day during 1 Jan 2007 – 31 Dec 2009. The data are organized into data files for each day of the year and the fires occurring on those days. Hourly data are also available for fire events. For the purposes of this study, the daily and hourly data were utilized. The database has several variables available for each fire event entry (Table 3.1). The data fields of use for this thesis are the total emissions fields for various chemical species, fire position (latitude/longitude), fuel loading, fire size and smoke plume height (Larkin et al. 2009, http://www.getbluesky.org/smartfire/). The smoke plume height is found in the hourly data files (Table 3.2). The plume height is updated roughly every hour for each fire listed in the database. These data are important for analyzing the trajectories of the smoke plumes as wind direction and speed may differ greatly with height.

f. HYSPLIT Forward/Backward Trajectories

The online version of the Hybrid Single-Particle Lagrangian Integrated Trajectory (HYSPLIT) model from NOAA's Air Resources Laboratory (ARL) was utilized in this study in order to compute model trajectories of each fire point source. The HYSPLIT model has many functions, for this study only the forward/backward air parcel trajectories will be used. The model uses a hybrid calculation method that uses both a Lagrangian (moving frame of reference) and Eulerian (fixed three-dimensional grid frame of reference) approach. A Lagrangian framework is used when making advection and diffusion calculations to follow the transport of the air parcel. Aerosol concentrations are calculated using an Eulerian framework. This model data will be accessed using the NOAA ARL READY website (Draxler and Rolph 2003).

3.2. Methodology

This study analyzed the effect of forest fire aerosols on precipitation off the Southeast Atlantic Coast. The methodology of the study involved the use of a suite of satellite products and extensive fire data. The study was highly dependent on the availability of the various satellite products needed for this study. Obstacles were introduced when using products from different orbiting satellites, such as insufficient spatial coverage and timing issues. For every case day, an area of precipitating smoky clouds and precipitating non-smoky clouds was needed. Non-smoky clouds were diagnosed by low aerosol concentrations being present. The areas of non-smoky precipitating clouds closest to the smoky clouds were used. These non-smoky clouds provide a theoretical baseline for clouds in the region in terms of their ability to produce precipitation given the cloud liquid water available. These two sets of clouds (smoky and non-smoky) were compared. A precipitation efficiency proxy was defined in order to

analyze clouds from different case studies and different aerosol regimes (smoky and non-smoky). The methodology used in this study is explained in detail in this section.

a. Study Region

This study examines the effect of forest fire aerosols from fires in the Southeast on AOT and the ability for clouds with elevated levels of forest fire aerosols to precipitate as they would in the presence of no (or very low) forest fire aerosols for clouds over the adjacent Atlantic Ocean. The southeastern U.S. is a region with frequent controlled burns and wildfires, particularly during the spring season. This study includes clouds in an area bounded by 81ºW-55ºW longitude and 15ºN-38ºN latitude. The smoky clouds in all of the case days are near the coastline. However, the non-smoky clouds in some cases are a good distance from the U.S. Atlantic coast in order to prevent smoke intrusion in those clouds. This study area was selected to provide sufficient size to capture two types of clouds on the same day, smoky and non-smoky clouds for all of the case days.

b. Selection of Case Days

The case days were selected based on two main premises. The first was that there was a sufficient load of aerosols being produced by a forest fire in the study area states. The second premise was that the forest fire aerosols interacted with precipitating clouds. The clouds had to be precipitating after the aerosols had been introduced to the cloud(s). A substantial obstacle of finding days that fit these criteria was the availability and coverage of the satellite data sources used in the methodology. The MODIS aerosol product needed to be available upwind from the precipitating clouds to estimate aerosol concentrations and the average AOT value for the smoky

clouds had to be 0.75 or greater, which is roughly five times the average AOT value for the study area when no forest fires are burning in the Southeast. The aerosol product is only available for cloud-free areas. MODIS has roughly two daily satellite overpasses. Aerosol product data had to be available upstream from the areas of precipitating clouds at the time they were precipitating. Aerosol product data availability was determined by analyzing the TMPA precipitation rate data to find the area the clouds precipitated at. TMPA precipitation was used to determine if precipitating non-smoky clouds were available nearby. The non-smoky clouds had to have an average AOT value of 0.25 or less which is roughly two times the average AOT value for the study area when no forest fires are burning in the Southeast. The MODIS cloud product CTT fields were analyzed to make sure the smoky and non-smoky clouds were roughly the same height. If the data was available, the HYSPLIT model was run to determine if the aerosols were on a trajectory that introduced them to the precipitating clouds. If all of these data products and criteria were met, the day was confirmed as a case day.

c. SMARTFIRE forest fire data

The fire data came from the SMARTFIRE database, and was provided by the Southern Research Station, USDA Forest Service, Athens, Georgia. The fire database was used to select potential case days, based on the size of fires and subsequent smoke output in the Southeast. A potential smoky case day was defined by the presence of at least one Class F (405-2023 ha, 1000-5000 acres, 4-20 km^2) or Class G (>2023 ha, >5000 acres, >20 km^2) fire.

The SMARTFIRE database has three types of data files: fire_events, fire_location, and fire_hourly. The fire_events data were not used in this project. Data from the fire_location file were used in this project include the location (latitude/longitude) and fire size (acres) (Table 3.1).

The fire location files are daily files that have one entry per day for each fire. Thus a fire will appear on multiple days if it burned for multiple days. This study used a term defined here as fire days. Location files have multiple entries for each fire, and the number of the entries depends on the number of days the fire burned. If a fire burns for five days, there are five entries in the database. The term "fire day" is used hereafter to discuss an entry in the database. The fire_location files are used with the understanding that multiple fire days may be attributed to the same point source fire.

It is important to note that SMARTFIRE is highly dependent on satellite data. Therefore, the data collected by SMARTFIRE should be considered estimates. The plume height data used here are only approximations. Several of the case days suggest that the plume heights are the same. However, it is very unlikely these plumes were the same height. The methodology used for making the plume height estimates analyzes plume height thresholds. The 5600 m threshold is met for a few of the fires analyzed. The SMARTFIRE database records that a smoke plume reached 5600 m, but the plume height may be slightly higher or lower in reality. The Georgia Bay Complex fire analyzed in a few of the case days is the term given to a group of simultaneous fires in close proximity to one another in South Georgia and extreme North Florida. The Georgia Bay Complex fire is recorded in the SMARTFIRE database as several smaller fires due to them having different point sources. This study sums the acreage of the smaller fires included in the Georgia Bay Complex when discussed in the case days.

The most important data in the hourly files are the estimated plume heights (Table 3.2). The plume height was used to assess which vertical levels should be examined to ascertain the direction of smoke transport for a particular fire. The plume height fields include a plume top and plume bottom. The plume data and the location were used in HYSPLIT to estimate plume

transport over the Atlantic Ocean. The plume data are estimated and a few case days have the same plume top height estimate.

The fire_locations files were processed to only include the study area in the Southeast states (Florida, Georgia, South Carolina, North Carolina, and Virginia). These states were chosen because they are in the southeastern region of the U.S. and border the Atlantic Ocean. It was assumed that fires in these states have the best opportunity for their smoke plumes to interact with the Atlantic Ocean. The yearly files were queried and fires in any other states or provinces were removed from the file. The result was three yearly files that included all fires from Florida, Georgia, South Carolina, North Carolina, and Virginia for each year from 2007-2009.

The yearly files needed to include only class F and G fire days. The area field was used to find only those fires that had an area of greater than 1000 acres or 4 km^2 (Class E) on a given day. As a result of the previous actions, each yearly file only included fire days from the five southeastern U.S. study states and fire days greater than 1000 acres or 4 km^2 in area. Fires of this size often burn for several days and emit large amounts of aerosols into the atmosphere. Aerosols from these fires travel large distances as is seen in the case days discussed below. Thus, intact plumes of aerosols from one class F or G fire may stretch hundreds of kilometers from a fire in the Southeast to far over the Atlantic Ocean.

d. Smoke Influenced Clouds and AOT

Wind data was acquired from NARR for three primary pressure levels including the near-surface (1000 hPa.), a lower troposphere level (700 hPa), and a mid-troposphere level (500 hPa). The plume height information from SMARTFIRE (Table 3.2) was used to determine which levels are most appropriate to use for smoke transport. The three levels were used to assess

smoke transport direction. These data was used in conjunction with the HYSPLIT model output to determine smoke transport. HYSPLIT model forward/backward trajectories were also used to track the plume as it moved in time. This model incorporates wind speed and direction at multiple levels of the atmosphere. The HYSPLIT output helped ensure that the air interacting with the smoky clouds contained forest fire aerosols. It is likely that in some cases the aerosols entered the atmosphere on a previous day.

The MODIS aerosol product was used to identify the location and transport of the smoke plume. Clouds that intersect the smoke plumes were selected based on a manual interpretation of the available satellite imagery. NASA's Goddard Space Flight Center maintains an online MODIS Level 1 and Atmospheric Archive and Distribution (LAADS) data and image archive (http://ladsweb.nascom.nasa.gov/) that was used to pre-screen for presence of clouds before extracting MODIS imagery. LAADS was also used for downloading all MODIS data and imagery.

MODIS aerosol product (MOD 04) satellite data was acquired for non-smoky and smoky clouds. The aerosol product (Kaufman et al. 1997, Tanré et al. 1997) provides detailed aerosol properties with a resolution of 0.5-1.0 km. The aerosol product includes AOT and aerosol size distribution. The AOT is used as an indicator of the concentration of aerosol that interacts with the cloud layer. A daily AOT product was acquired for all clouds included in a case day. The AOT products are only available for cloud-free, glint-free regions. The importance of the use of the HYSPLIT trajectories is that this modeled data are available for cloudy areas as well. AOT measurements were taken from cloud-free regions immediately upwind from the cloud location as estimated by HYSPLIT trajectories. The AOT measurements in closest proximity to the cloud were used, assuming that the aerosols from this measurement will be interacting with the cloud

layer due to the prevailing wind pattern (Kaufman et al. 2005). AOT values greater than 0.750 were used for the computation of the median AOT. This value well exceeds the AOT global average of .12 ± 0.04 (Roberts et al. 2001). It is important to note that the AOT values directly upwind from the areas of precipitation may not be associated with fires from the same day. The aerosols may be from the same fire from previous days. The number of AOT values used varied from case to case due to the presence of clouds, but the least number of AOT values for any one case day was 12. The greatest number of AOT values used for a case day was 80 (for the smokiest case day). The combination of the SMARTFIRE fire data, HYSPLIT model output, NARR wind speed and direction at 3 levels of the atmosphere, and the AOT measurements were sufficient for estimating the location and estimations of the density of aerosols in the smoky clouds. Ideally, aerosol data would be acquired from within the study clouds either through *in situ* measurements or Light Detection and Ranging (LIDAR) data. *In situ* measurements would have to be acquired through airborne retrievals due to the location of the study area. LIDAR data are primarily available through proprietary sensors and has relatively poor spatial and temporal coverage at this time. Both of these methods would give better estimates of aerosol concentrations but are expensive and difficult to acquire.

Maritime clouds are often stratified between shallow and deep clouds. There are several ways deep and shallow clouds can be defined. Deep clouds, as discussed in this study, have a large vertical extent (cloud base to cloud top) and, in general, have stronger updrafts leading to the potential for heavy precipitation. A -10°C threshold was used to define a deep cloud. This level indicates the level where the glaciation process begins (Rogers et al. 2001). Shallow clouds have a much smaller vertical extent and have weaker updrafts. These clouds have light precipitation, if any at all. This distinction is important because of the differing precipitation

potential these clouds physically posses. In each of the case days presented here, it is important to study smoky and non-smoky clouds that have roughly the same vertical composition. It would be inappropriate to compare clouds that are physically different and make conclusions about the effects of the aerosols. In order to prevent this, MODIS cloud top temperature (CTT) of the clouds were used. CTT were averaged over the smoky and non-smoky area for each case day to ensure they are roughly the same height. This work follows a similar process presented in (Rosenfeld 1999). These data were collected from the MODIS MOD 06 cloud product, which produces cloud top temperature estimates through the use of infrared retrieval methods.

e. Precipitation Efficiency Proxy

Precipitation efficiency (PE) is simply defined as a ratio between the total precipitation and the total water available to a cloud or system (Tao et al. 2004). However, there are many variations of how PE is calculated in the literature. There are instances where greater PE can be achieved due to greater pressure perturbation within a particular thunderstorm, preventing evaporative cooling by minimizing cloud contact with unsaturated air, and longer cloud system lifetimes (Newton 1966).

This study defined a PE proxy using a ratio of a precipitation estimate and a CLW estimate. TMPA 3B42 daily microwave/infrared blended satellite precipitation rate data was acquired for the smoky clouds that are influenced by aerosols originating from the forest fires defined earlier, as well as the non-smoky clouds. The algorithm retrieves 3-hourly precipitation rate data that is combined to produce a daily precipitation product. The daily precipitation rate is used as the rainfall rate (RR_{rate}) for the areas where the forest fire induced clouds are situated.

The daily data are used in this study because we are stratifying the smoke events at a temporal resolution of one day.

AMSR-E CLW stage three daily products were acquired in order to provide coverage of the smoky and non-smoky clouds for each case day. The CLW and satellite precipitation data were used to calculate a rainfall efficiency proxy. This proxy is similar to a rainfall precipitation proxy (G) defined by Jin and Shepherd (2008), who followed Berg et al (2006). The proxy used in this study is defined as the comparative rainfall efficiency proxy (CREP). CREP is the ratio between the TRMM TMI rainfall rate (RR) and the AMSR-E CLW:

$$\text{CREP} = \text{RR}/\text{AMSR-E CLW} \tag{3.1}$$

CREP was calculated for each area of clouds (smoky and non-smoky). For this study, CREP was calculated by taking the ratio between the median RR and the median CLW values for all of grid cells for a particular case day. The use of median values is aimed at reducing the amount of bias that the outliers introduce. The actual number of cases was dependent on the number of forest fires available in the 3 year SMARTFIRE database that fall into size class F or G. More importantly, the number of cases was dependent on the availability of the various satellite products.

The CREP ratio in equation form:

$$\text{CREP Ratio} = \text{CREP}_{\text{smoky}} / \text{CREP}_{\text{non-smoky}} \tag{3.2}$$

The raw data was acquired using IDL programs to read and query the MODIS, TRMM, and AMSR products all in HDF and NetCDF format. The output data was verified by importing the files into ARCGIS 10, which has the capability of visualizing HDF and NetCDF.

f. Cloud Analysis

Two cloud properties were analyzed to determine if they have any impact on precipitation in the case days. Cloud effective particle radius and cloud phase are both important for analyzing the microphysical properties of the cloud. Cloud effective particle radius gives an indication as to the size of the cloud droplets in the clouds which can impact precipitation. Cloud effective particle radius data for both smoky and non-smoky clouds were compared. Cloud phase is an important property to study because it indicates whether the cloud is comprised of liquid water droplets or ice nuclei. This provides two things, an indication of predominate water phase in the cloud, and the approximate stage in the life cycle of a deep cloud (initial, mature, dissipating; Fig. 2.5). In the initial stage of a cloud, liquid water droplets dominate in cloud tops. A mature, deep cloud top will be dominated by ice particles. These differences in water phase could have important impacts on the effect aerosols have on precipitation at the surface.

The primary research objective addressed in this study is to examine the forcing of forest fire aerosols on cold, deep layer marine cloud precipitation off of the southeastern U.S. Atlantic Coast. The preceding methodology was designed and followed in order to address this objective. The following chapter presents the results of the study followed by a discussion of how the results help address the objectives of this study.

Table 3.1. SMARTFIRE fire_location variables and descriptions.

Variable	Description
id	Unique identifier for this fire location
event_id	Event ID to look up in fire_events.csv
latitude	Location of this fire (latitude in decimal degrees)
longitude	Location of this fire (longitude in decimal degrees)
elevation	Elevation of fire (meters)
slope	Slope at fire location
state	Location information
county	Location information
country	Location information
date_time	Time fire occurred (ignition time or local midnight)
duration	Ignition duration
snow_month	Days since last snow (rarely provided)
rain_days	Days since last rain (rarely provided)
wind	Wind (mph) at fire (rarely provided)
type	WF=wildfire, WFU=wildland fire use, RX=prescribed
area	Area of this fire in acres
fuel_1hr	Total loading of 1-hr fuels (tons)
fuel_10hr	Total loading of 10-hr fuels (tons)
fuel_100hr	Total loading of 100-hr fuels (tons)
fuel_1khr	Total loading of 1,000-hr fuels (tons)
fuel_10khr	Total loading of 10,000-hr fuels (tons)
fuel_gt10khr	Total loading of > 10,000-hr fuels (tons)
shrub	Total loading of shrub fuels (tons)
grass	Total loading of grassy fuels (tons)
rot	Total loading of rotted fuels (tons)
duff	Depth of fuel loading in the duff layer (inches)
litter	Total loading of litter fuels (tons)
fuel_moisture_10hr	Moisture (%) of 10-hr fuel
fuel_moisture_1khr	Moisture (%) of 1000-hr fuel
consumption_flaming	Total moisture in the flaming phase (tons)
consumption_smoldering	Total consumption in the smoldering phase (tons)
consumption_residual	Total consumption in the residual phase (tons)
consumption_duff	Total consumption of the duff layer (tons)
heat	Total heat or sum of hourly heat released (BTU)
pm25	Total $PM_{2.5}$ or sum of hourly PM $_{2.5}$ (tons)
pm10	Total PM_{10} or sum of hourly PM_{10} (tons)
pm	Total PM or sum of hourly PM (tons)
co	Total CO or sum of hourly CO (tons)
co2	Total CO_2 or sum of hourly CO_2 (tons)
ch4	Total CH_4 or sum of hourly CH_4 (tons)
nmhc	Total NMHC or sum of hourly NMHC (tons)
nox	Total NO_x or sum of hourly NO_x (tons)
nh3	Total NH_3 or sum of hourly NH_3 (tons)

Table 3.1 (cont.)

so2	Total SO_2 or sum of hourly SO_2 (tons)

Table 3.2. SMARTFIRE fire_hourly variables and descriptions.

Variable	Description
fire_id	Location ID to look up in fire_locations.csv
hour	Hour of data
area_fract	Area fraction for the given hour (total sums to 1)
flame_profile	Flaming fraction for the hour (total sums to 1)
smolder_profile	Smoldering fraction for the hour (total sums to 1)
residual profile	Residual fraction for the hour (total sums to 1)
heat_emitted	Total emission this hour of heat (BTU)
pm25_emitted	Total emission this hour of $PM_{2.5}$ (tons)
pm10_emitted	Total emission this hour of PM_{10} (tons)
pm_emitted	Total emission this hour of PM (tons)
co_emitted	Total emission this hour of CO (tons)
co2_emitted	Total emission this hour of CO_2 (tons)
ch4_emitted	Total emission this hour of CH_4 (tons)
nmhc_emitted	Total emission this hour of NMHC (tons)
nox_emitted	Total emission this hour of NO_x (tons)
nh3_emitted	Total emission this hour of NH_3 (tons)
so2_emitted	Total emission this hour of SO_2 (tons)
pm25_flame	Flaming emission this hour of $PM_{2.5}$ (tons)
pm10_flame	Flaming emission this hour of PM_{10} (tons)
pm_flame	Flaming emission this hour of PM (tons)
co_flame	Flaming emission this hour of CO (tons)
co2_flame	Flaming emission this hour of CO_2 (tons)
ch4_flame	Flaming emission this hour of CH_4 (tons)
nmhc_flame	Flaming emission this hour of NMHC (tons)
nox_flame	Flaming emission this hour of NO_x (tons)
nh3_flame	Flaming emission this hour of NH_3 (tons)
so2_flame	Flaming emission this hour of SO_2 (tons)
pm25_smold	Smoldering emission this hour of $PM_{2.5}$ (tons)
pm10_smold	Smoldering emission this hour of PM_{10} (tons)
pm_smold	Smoldering emission this hour of PM (tons)
co_smold	Smoldering emission this hour of CO (tons)
co2_smold	Smoldering emission this hour of CO_2 (tons)
ch4_smold	Smoldering emission this hour of CH_4 (tons)
nmhc_smold	Smoldering emission this hour of NMHC (tons)
nox_smold	Smoldering emission this hour of NO_x (tons)
nh3_smold	Smoldering emission this hour of NH_3 (tons)
so2_smold	Smoldering emission this hour of SO_2 (tons)
pm25_resid	Residual emission this hour of $PM_{2.5}$ (tons)
pm10_resid	Residual emission this hour of PM_{10} (tons)
pm_resid	Residual emission this hour of PM (tons)
co_resid	Residual emission this hour of CO (tons)
co2_resid	Residual emission this hour of CO_2 (tons)
ch4_resid	Residual emission this hour of CH_4 (tons)

Table 3.2 (cont.)

nmhc_resid	Residual emission this hour of NMHC (tons)
nox_resid	Residual emission this hour of NO_x (tons)
nh3_resid	Residual emission this hour of NH_3 (tons)
so2_resid	Residual emission this hour of SO_2 (tons)
voc_resid	Residual emission this hour of VOC (tons)
plume_bottom_meters	Estimated Plume Bottom (meters)
plume_top_meters	Estimated Plume Top (meters)

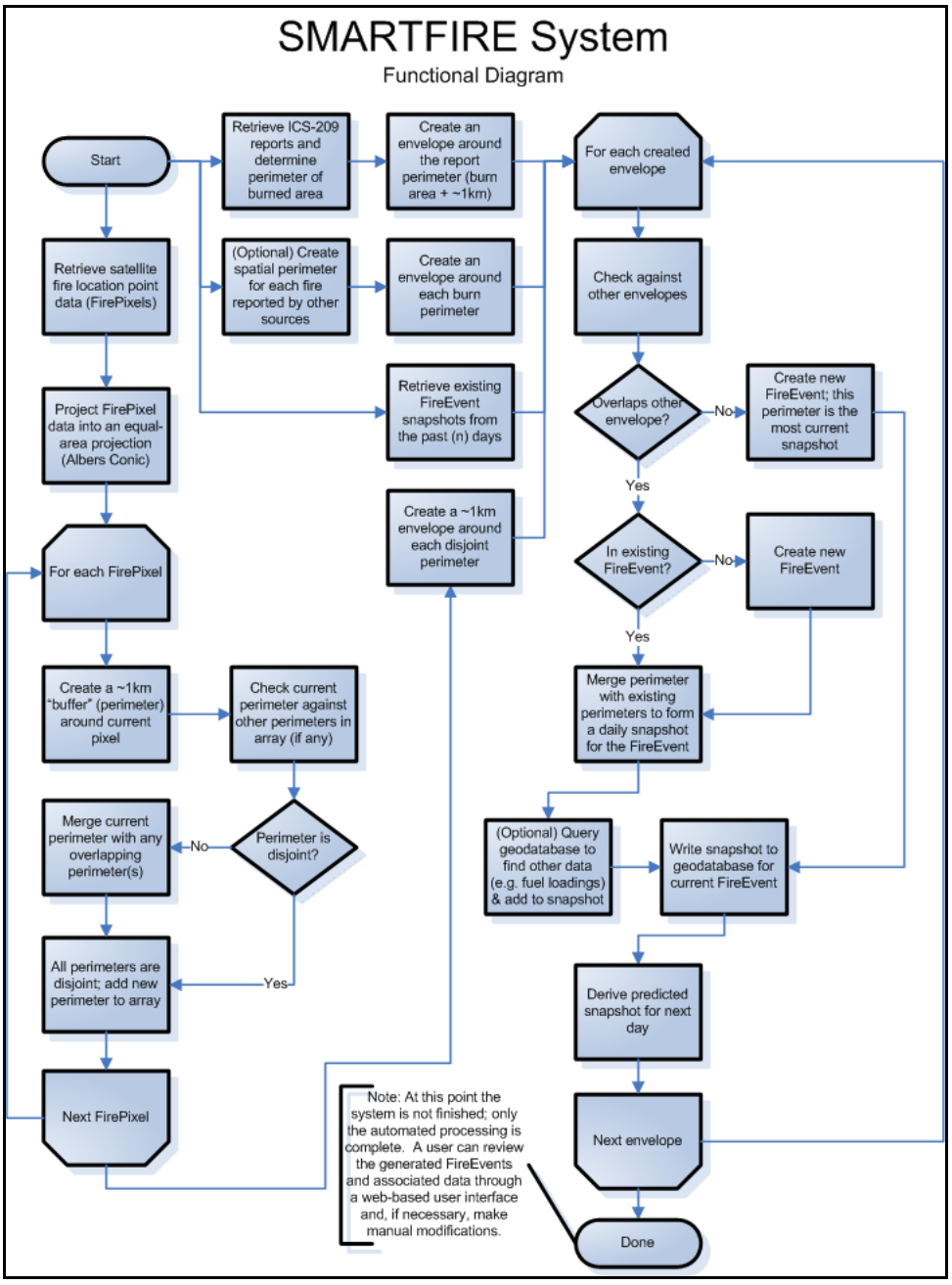

Fig. 3.1. Schematic showing operation of SMARTFIRE system (www.getbluesky.org/smartfire).

CHAPTER 4

RESULTS AND DISCUSSION

The methodology used in this study is aimed at addressing the primary objective of the thesis which is to analyze forest fire aerosol forcing of precipitation along the southeastern U.S. Atlantic Coast. This objective was addressed by locating appropriate forest fires in the Southeast through examination of the SMARTFIRE database, analyzing a comparative rainfall efficiency proxy for smoky and non smoky clouds, and analyzing cloud particle effective radius and cloud phase data from MODIS cloud product. The results and findings of the methodology are presented below.

4.1. Fire Data Analysis

The SMARTFIRE database used in this study contained data on fires from 2007-2009. It was used to analyze the trends of class E and F fires and then select potential case day days. The number of fires differed greatly between each year, mostly due to the varying climatic conditions during this time period. The Southeast averages 1000-1600 mm of precipitation on an annual basis (Fig. 4.1), but was experiencing one of the worst droughts in recorded history in 2007. Signs of the drought began in late 2005 and extended through the 2007 fire season (Fig. 4.2). The state of Georgia was particularly dry in 2007, which led to extremely high fire potential and consequently several large fires, particularly in southern Georgia (Fig. 4.2). The largest fires in the Southeast from 2007-2009 occurred in southern Georgia, the largest being the Georgia Bay

Complex fire in May 2007. The Georgia Bay Complex fire was the name given to multiple fires that burned in South Georgia and North Florida during the 2007 fire season. This particular fire burned more than 440,000 acres (1780 km^2) in Georgia alone (Georgia Forestry Commission 2007). By the 2009 forest fire season, climatic conditions had improved and the southeastern U.S. had slowly pulled out of drought conditions (Fig. 4.2). The result of this was a minor forest fire season in 2009. This pertains to this study as case days were not completed for 2009 due to small number of fire days and the paucity of available satellite data for those days. There were very few class F and G fire days (<100) in 2009 and many of these fires were short lived and small class F fires (Fig. 4.3). This is compared to 2007 where 252 class F and G fire days occurred. 2008 was a moderately active class F and G fire year with 147 class F and G fires (Fig. 4.3).

The data were also analyzed on a monthly time scale. In 2007, May was by far the most active month for class F and G fires with 140 fires (Fig. 4.3). April was the second most active month with 32 fires. In 2008, June was the most active month with 48 and May was second most active with 32 fires (Fig. 4.3). There is a secondary peak in February and March of 2008. The 2008 distribution does not have a historical fire bias like 2007 does. This allows for a smoother distribution as no month has a dramatic amount of activity. An active period is evident from March-July. In 2009, there were only 93 class F and G fires in the study area. The 2009 distribution by month looks much different than 2007 and 2008 with a primary peak in February-April (Fig. 4.4). February was the most active month with 32 fires followed by March with 18 fires and April with 17 fires. Perhaps the most interesting finding in the 2009 distribution is the lack of May and June class F and G fires, with only four total fires in these two months that were extremely active in the previous two years. When the fires from 2007-2009 were distributed by

month, there is a large primary peak in May, in part due to the bias of the Georgia Bay Complex fire during the drought of 2007 (Fig. 4.4). There is also a secondary peak in February due to the low amount of precipitation in the Southeast region during the winter months of 2007 and 2008. Class F and G fires are infrequent during the late summer and fall months in the Southeast region. This is likely due to an increase in precipitation can be attributed to afternoon/evening thunderstorms caused by an influx of moisture from the Gulf of Mexico and intense surface heating as well as drenching rains from tropical storms.

Some of the May 2007 fires, including the Georgia Bay Complex, burned for weeks. There were also several days in May 2007 with a large class G fire. This provided many more opportunities for case days to be conducted. The entire month of May 2007 was examined for case days as the Georgia Bay Complex and a few large Florida fires lasted several days during the month. One result of a very active May 2007 was a significant aerosol load in the atmosphere. These aerosols affected a large area of the eastern U.S. and the Atlantic Ocean, depending on the wind profile. The output of aerosols led to the possibility of several case days during the month, dependent on the availability of precipitating clouds and other satellite products. Four of the case days presented here are from May 2007. The other two case days presented here are from fires in eastern North Carolina in June 2008.

4.2. Case day Results

Six case days were found in the region being analyzed from 2007-2009. Each case day is discussed in detail in this section 4.2.

a. Case Day 1: South Georgia Fires 6 May 2007

The first case day is from 6 May 2007. The primary fire being analyzed for this day is still the fire centrally located in Atkinson County in southeastern Georgia. The fire had grown rapidly over a 24-hour period. SMARTFIRE recorded the size on 6 May 2007 at 24 km^2. This fire had a maximum plume top height of 6351 m and a minimum plume top height of 1032 m in the early morning hours. There were two other substantial fires reported in nearby Ware County that were small fires the day before. One of the fires was reported at 6 km^2 and the other at 8 km^2. Cumulatively, these fires were actively burning over 34 km^2. There were several smaller fires still burning in Florida as well which emitted additional aerosols into the study area. The large scale mechanism responsible for forming the precipitation clouds analyzed in this case day is a surface low pressure system that move eastward from the Tennessee Valley off the North Carolina coast between 5 May 2007 and 6 May 2007.

The MODIS visible imagery for the smoky clouds does not clearly show the smoke attributed to these fires (Fig. 4.5). This is mostly caused by the large swath of clouds over the Southeast. There is a swath of precipitating clouds centrally located at 32°N and 75°W that was used for the smoky clouds for this case day (Fig. 4.5). NARR 12 UTC winds indicate that near-surface winds were light and variable. NARR 700 hPa winds indicate northwest winds over the areas being burned while 500 hPa winds were primarily north-northwest (Fig. 4.6). HYSPLIT 48 hour forward trajectories from the South Georgia fires indicate that the smoke from the three large fires was interacting with the area used for the smoky clouds primarily at the upper levels of the smoke plumes (>3000 m) (Fig. 4.7). The non-smoky precipitation clouds used are centrally located at 27°N and 67°W (Fig.4.8).

When considering the size of the South Georgia fires burning during this time period, it would be expected that AOT values in the area would be very large. However, MODIS AOT values from 6 May 2007 are very similar in magnitude to the day before, when the size of the fires was substantially smaller. MODIS visible imagery indicates the smoke is widespread, even reaching parts of the Midwest as well as the Atlantic Ocean (Fig. 4.5). The wide dispersion of the smoke may help explain the lack of increase in AOT over the Atlantic Ocean from 5 May to 6 May. The median of the highest MODIS AOT values interacting with the smoky clouds was 0.81 (Fig. 4.5). There were only 11 AOT values over 0.75 in our study area with the highest AOT measurement being 0.93. Not only were values relatively low for the size of the fires burning in Georgia, but there was not a widespread area of high AOD values interacting with the study clouds. AOT values upwind from the non-smoky clouds were low between 0.10-0.30 (Fig. 4.5).

Tables 4.1 and 4.2 summarize the raw model output for Case Day 1. The smoky clouds median CTT is 221 K (-42°C) while the non-smoky clouds median CTT is 250 K (-23°C). The non-smoky clouds have warmer cloud tops. This discrepancy should be considered when analyzing this case day. The smoky CREP using median values is 92 while the non-smoky CREP is 82, resulting in a CREP ratio between smoky and non-smoky clouds of 1.12. This value indicates that the smoky clouds precipitated a slightly higher amount of the available CLW than the non-smoky clouds did. The smoky cloud phase data indicates that the ice phase to water phase ratio is 16.32, thus ice phase clouds were much more prevalent than liquid water clouds in the smoky clouds. The non-smoky cloud phase data indicates that the ice phase to water phase ratio is 0.12, meaning water phase clouds were much more prevalent than ice clouds. The discrepancy between the ice/liquid ratios between the smoky and non-smoky clouds is likely due

to the difference in cloud top temperature. The non-smoky clouds were much warmer than the smoky clouds, leading to less ice formation.

b. Case Day 2: Florida and Georgia Fires 9 May 2007

The second case day analyzes 9 May 2007 when numerous fires were actively burning in the Southeast. The largest of these fires was in Lafayette County, Florida. SMARTFIRE documented the fire at 54 km^2. For the Lafayette fire, the maximum plume height top at peak afternoon heating was 6350 m while the plume height at sunrise was 251 m. Lafayette County is in extreme northern Florida near the Georgia-Florida border. There were three class F Florida fires burning on May, and other notable fires were located in Ware County, Georgia. SMARTFIRE recorded five fires burning in Ware County totaling over 16 km^2. The largest of the Ware County fires had a minimum plume height top of 208 m at sunrise and 5098 m at peak heating. According to SMARTFIRE, the large Florida fires and the Ware County, Georgia fires were burning over 80 km^2 during this case day day.

This case day is particularly intriguing due to an extratropical storm moving into the study area. This allowed for a heavy precipitation event to occur in conjunction with the presence of a large amount forest fire aerosols. On 9 May 2007 this storm was designated Subtropical Storm Andrea by the NWS National Hurricane Center (NWS NHC 2011). This storm was symmetrical as seen in visible imagery and had moved in from the northeast. 9 May was the first interaction the Andrea had with the aerosol loads from the fires in Georgia and Florida (Fig. 4.9). Due to prevailing wind speeds associated with tropical storms and the center of circulation of Andrea, the southeast quadrant of the storm had inflow from the heavy aerosol load areas while the northwest quadrant of the storm had inflow from the North Carolina and Virginia coasts. The

North Carolina and Virginia coasts had no substantial forest fire activity leading to very low aerosol loads.

The result of these widespread fires was large aerosol loads in the atmosphere over Florida, Georgia, and the Atlantic Ocean. MODIS visible imagery confirmed the large amount of smoke located just south of Subtropical Storm Andrea (Fig. 4.9). This area was used as the smoky study clouds. These clouds are centrally located at 29°N and 77°W. NARR winds indicate 10-15 ms^{-1} surface winds out of the northwest and west over South Georgia and North Florida. NARR 700 hPa and 500 hPa winds indicate 15-20 ms^{-1} winds out of the north and northwest (Fig. 4.10). HYSPLIT 24-hour forward trajectories from the Lafayette County, Florida fire confirmed that the smoke plume interacted with the southeast quadrant of Subtropical Storm Andrea (Fig. 4.11). All three trajectories (10 m, 2000 m, 6300 m) indicated the smoke at all levels was flowing into the smoky clouds. HYSPLIT trajectories were also calculated for the northwest quadrant of the storm (Fig. 4.12). The trajectory indicated the origin of the inflow at 2000 m into this area was off of the coast of North Carolina. The trajectories validated the designation of this area as the non-smoky study clouds.

Large aerosol loads are further evidenced by AOT values from the area. Using a AOT threshold of 2.00, 35 values in an area bounded by 26°N-29.5°N and -78°W- 80°W were identified (Fig. 4.9). The median AOT in this area was 2.53, which is 10-20 times higher than AOT values found here during non-smoky days. There are three AOT values greater than 3.00 in this area. The AOT values were especially large due to the large acreage burning and the winds were allowing the plume to remain relatively narrow leading to low dispersion of the plume. The Florida fire of 54 km^2 was the primary source of the high aerosol loads. Southwest winds blowing across Florida caused the largest AOT values to be near the Atlantic coast of Florida.

The southeast quadrant of the storm was influenced by the smoke and high AOT values. As a result, clouds within the lower-right quadrant were designated the smoky study clouds. The non-smoky study clouds were located in the upper-left quadrant of the storm where inflow was from north and northeast. The median AOT interacting with these clouds was 0.35 (Fig. 4.9). This was eight times less than the AOT values from the smoky clouds.

Tables 4.1 and 4.3 summarize the raw model output for Case Day 2. TRMM 3B42 and AMSR CLW illustrations are shown to identify regions of precipitation and elevated cloud liquid water (Fig. 4.13). The smoky clouds median CTT was 222 K (-41°C) while the non-smoky clouds median CTT was 228 K (-35°C). The smoky CREP using median values was 93 while the non-smoky CREP was 132 resulting in a CREP ratio between smoky and non-smoky clouds of 0.70. This value indicates that the non-smoky clouds precipitated a higher amount of the available CLW than the smoky clouds did. The smoky cloud phase data indicates that the ice phase to water phase ratio was 6 compared to the non-smoky ice/water phase ratio of 3. Both areas of clouds had a greater amount of ice phase clouds, but smoky clouds had a slightly higher ratio. The smoky clouds having greater ice phase clouds was somewhat expected given the slight discrepancy in the median CTT, where smoky clouds on average are slightly colder.

c. Case Day 3: Georgia Bay Complex 12 May 2007

This case day was the most impressive when considering the size of area being burned and the resultant aerosol output. SMARTFIRE recorded the Georgia Bay Complex fire as centered over Emanuel County, Georgia, on 12 May 2007, and the size of the fire was 230 km^2. This was the largest area recorded in SMARTFIRE for all case days. In this case day, SMARTFIRE likely combined the individual fires burning in multiple counties into one entry.

There were other small class F and G fires that are not discussed in this case day because of the magnitude of the primary Georgia Bay Complex fire. SMARTFIRE recorded the maximum plume height top at 6351 m during peak afternoon heating and a minimum plume height of 259 m at sunrise. This fire was impressive in size and emissions. At peak emissions during this case day, this fire emitted over 214,000 tons of CO_2 per hour, 586 tons of CH_4 per hour, 1284 tons of PM_{10} per hour, and over 11,000 of CO per hour.

MODIS visible imagery indicates that the smoke was widespread (Fig. 4.14). Smoke can be seen over much of Florida, the eastern Gulf of Mexico, and over the Straits of Florida. Visible imagery also shows the location of precipitation that is used as the smoky clouds for the case day. This area is centrally located in the MODIS imagery at 29°N and 77°W. This area encompassed the remnants of Subtropical Storm Andrea. By 12 May 2007 the remnants of Andrea had been smoke influenced for a couple of days. Therefore, precipitating areas of the remnants were designated smoky clouds. NARR reanalysis winds were light and variable at all three levels analyzed over South Georgia and North Florida (1000 hPa, 700 hPa, 500 hPa) (Fig. 4.15). However, strong west winds at all three levels were found over Central and South Florida. The area over Central and South Florida had high AOT values due to winds out of the north on days prior to this case day. These strong winds were transporting forest fire emissions directly into the smoky clouds. HYSPLIT 48 hour backward trajectories from the smoky clouds indicates that smoke from the lower and middle levels of the smoke plumes were interacting with the smoky clouds (Fig. 4.16). The upper level trajectory indicates a northward origin, thus not originating in the smoke plumes of Georgia and Florida. To the southeast of the smoky clouds there was another area of heavy precipitation. This area was out of the influence of the smoke. The non-smoky clouds are centrally located at 25°N and 69°W (Fig. 4.14). HYSPLIT 24-hour

backward trajectories from the non-smoky clouds indicate that the trajectories at all levels originated south and southwest of the non-smoky clouds, out of range of the smoke from the Georgia and Florida fires (Fig. 4.17).

Upwind AOT values for this case day were the highest out of all of the case days. Due to the size of the fire and the emissions output, an AOT threshold of 3.00 was used, and 82 AOT values were returned for the area immediately upwind from the smoky clouds. The median AOT of these 82 values was 3.33, roughly 15-30 times a non-smoky AOT in this area (Fig. 4.14). Five of the AOT values were over 4.00. The MODIS AOT image shows that AOT values upwind from the non-smoky clouds ranged from 0.10-0.30 (Fig. 4.14).

Tables 4.1 and 4.4 summarize the raw model output for Case Day 3. TRMM 3B42 and AMSR CLW illustrations are shown to identify regions of precipitation and elevated cloud liquid water (Figure 18). The smoky clouds median CTT was 220 K (-43°C) while the non-smoky clouds median CTT was 222 K (-41°C). The smoky CREP using median values was 167 while the non-smoky CREP was 473 resulting in a CREP ratio between smoky and non-smoky clouds of 0.35. This value indicates that the non-smoky clouds precipitated a significantly higher amount of the available CLW than the smoky clouds did. The smoky cloud phase data indicated that the ice phase to water phase ratio was 68 compared to the non-smoky ice/water phase ratio of 5. Both areas of clouds had a greater amount of ice phase clouds, but smoky clouds had a significantly higher ratio. To further illustrate the discrepancy, of over 1400 MODIS measurements from within the smoky clouds, only 20 were returned as water phase clouds. For the non-smoky clouds, MODIS returned over 1700 measurements with 307 designated water phase clouds. The ice phase returns were almost identical with 1366 ice phase returns for the smoky clouds and 1371 ice phase returns for the non-smoky clouds. Considering these clouds

had almost the same vertical extent, this difference suggests other physical reasons for the difference in the cloud phase ratio, such as the changing of dynamic processes due to increased CCN.

d. Case Day 4: Georgia Bay Complex 13 May 2007

This case day analyzes the same fires that were analyzed in Case Day 4, but a day later, on 13 May 2007. The area consumed by the South Georgia and North Florida fires was roughly the same as the previous day (~200 km^2). The fire was affecting several counties but centered near Emanuel County, Georgia. The highest plume height top value recorded in SMARTFIRE for this day was 5098 m. The lowest plume height top value was at sunrise at 208 m. The total emissions from the fires were similar to the previous day.

MODIS visible imagery visualizes the vast area of smoke emitted from the fires (Fig. 4.19). Thick smoke stretched from the entire Gulf Coast of Florida to a 200 km east of central Florida over the Atlantic Ocean. The smoke was located in approximately the same area as the day before (Case Day 3). The area of clouds located in an area from 30.8°N-32°N and 75.4°W-70.6°W were used as the smoky clouds for this case day. These smoky clouds were associated with the same synoptic scale forcing mechanisms as the clouds analyzed in Case Day 4, but the smoky clouds are located farther east then the day before. NARR winds indicate predominately western winds at 1000 hPa, 700 hPa, and 500 hPa (Fig. 4.20). At 500 hPa, 10-15 ms^{-1} winds advanced these smoky clouds farther east. This area of deep clouds was the remnants of subtropical storm Andrea and had been nearly stationary for several days prior to 13 May. Mid-tropospheric winds strengthened beginning on 12 May which aided in transporting the clouds eastward. The westerly winds also sustained aerosol interaction with the smoky clouds.

HYSPLIT 24-hour backward trajectory model output confirmed that the forest fire aerosols were interacting with the smoky clouds, particularly at a height of 4000-5000 m (Fig. 4.21). The 5000 m backward trajectory indicated a path from the smoky clouds to north central Florida where extremely high AOT values are found.

MODIS visible imagery indicates the location of the non-smoky clouds in an area from 22.1°N-24°N and 64.7°W-61.1°W (Fig. 4.19). This area of deep clouds was located just east of the non-smoky clouds used for the day before. These clouds were likely associated with the same disturbance that caused the precipitating clouds on 12 May. HYSPLIT 24-hour backward trajectory output indicates that the 5000 m trajectory originated southwest of the clouds area, while 2000 m and 10 m trajectories originated south and southeast of the clouds (Fig. 4.22). The forest fire plumes were to the northwest of these clouds. Thus, the trajectories indicate that these clouds were free of significant aerosol loads.

Upwind AOT values were not as impressive in terms of the median AOT value compared to 12 May; however, large AOT values covered a larger spatial area. There were 241 AOT values greater than 1.50 for this case day, with a median AOT value of 1.80. The large AOT values stretched from Tampa Bay, Florida to the boundary between the smoky clouds and the aerosols (Fig. 4.19). AOT values upwind from the non-smoky clouds were between 0.10-0.40 (Fig. 4.19)

Tables 4.1 and 4.5 summarize the raw model output for Case Day 4. TRMM 3B42 and AMSR CLW illustrations are shown to identify regions of precipitation and elevated cloud liquid water (Fig. 4.23). The smoky clouds median CTT was 231 K (-42°C) while the non-smoky clouds median CTT was 222 K (-52°C).The smoky CREP using median values was 100 while the non-smoky CREP was 67. The CREP ratio between smoky and non-smoky clouds was 1.48.

This value indicates that the smoky clouds precipitated a higher amount of the available CLW than the non-smoky clouds did. These results contradict the findings from the day before. The smoky cloud phase data showed an ice phase to water phase ratio of 46; thus ice phase clouds were much more prevalent than liquid water clouds in the smoky clouds. About 7 % of all the smoky cloud phase retrievals indicated a mixed phase cloud. The non-smoky cloud phase data showed an ice phase to water phase ratio of 3, meaning ice phase clouds were 3 times more prevalent than liquid water phase clouds. Only 1 % of the non-smoky cloud retrievals indicated clouds in mixed phase.

e. Case Day 5: Eastern North Carolina Fires 5 June 2008

This case day examines fires in eastern North Carolina during the 2008 fire season. On 5 June 2008 there were two major fires burning in extreme eastern North Carolina. The two fires were burning in Hyde County and Tyrrell County. The Hyde County fire was the larger of the two. SMARTFIRE recorded the fire at over 134 km^2. The Tyrrell County fire was about 25% the size at just over 20 km^2. Together they encompassed over 154 km^2. SMARTFIRE estimated a maximum plume height top of 6351 m and a minimum plume top height of 259 m for the Hyde County fire. The precipitating clouds analyzed in Case Day 5 were located northeast of the Outer Banks and were associated with a surface low off the coast of Cape Cod. The predominantly west winds caused the forest fire smoke to blow into the area of precipitation centered at 37°N and 73°W (Fig. 4.24). NARR winds indicate west winds at all three levels analyzed (1000 hPa, 700 hPa, 500 hPa) (Fig. 4.25). HYSPLIT 24-hour forward trajectories from the North Carolina fires indicate the smoke was interacting with the smoky clouds (Fig. 4.26). This area of precipitation was selected to be the smoky clouds for the case day. The non-smoky clouds are to

the south, well out of the range of the forest fire smoke. The non-smoky clouds are centered at 21°N and 67°W (Fig. 4.24).

22 AOT values were returned from upwind of the smoky clouds with a value greater than 0.75 (Fig. 4.24). The median AOT value was 0.84 with 5 values greater than 1.00. The AOT values for this case day are 4-8 times larger than under non-smoky conditions. The AOT imagery shows that the plume was relatively narrow and not well dispersed. AOT values upwind from the non-smoky clouds are between 0.10-0.20 (Fig. 4.24).

Tables 4.1 and 4.6 summarize the raw model output for Case Day 5. TRMM 3B42 and AMSR CLW illustrations are shown to identify regions of precipitation and elevated cloud liquid water (Figure 4.27). The smoky clouds median CTT was 218 K (-45°C) while the non-smoky clouds median CTT was 225 K (-38°C). The smoky CREP using median values was 64 while the non-smoky CREP was 57 resulting in a CREP ratio between smoky and non-smoky clouds of 0.70. This value indicates that the smoky clouds precipitated a slightly higher amount of the available CLW than the non-smoky clouds did. The smoky cloud phase data showed an ice phase to water phase ratio of 81 compared to the non-smoky ice to water phase ratio of 53. Both areas of clouds were almost entirely ice phase clouds. This was in part due to these clouds having the coldest cloud tops studied. Despite a median CTT below the temperature needed for homogenous nucleation in smoky clouds, they appear to be precipitating the available CLW as effectively as the non-smoky clouds. This contradicts previous model studies that suggest the possibility of precipitation suppression in especially cold clouds where homogenous nucleation is occurring (Rosenfeld and Woodley 2000, Cui et al. 2006, Khain et al. 2001, Khain et al. 2008, Rosenfeld et al. 2008). However, these modeling studies indicate a cloud base of < 0°C is needed for precipitation suppression to occur.

f. Case Day 6: Eastern North Carolina Fires 16 June 2008

This case day examines a collection of small class F fires in eastern North Carolina and one small class F fire in Virginia. The Hyde County fire that burned during Case Day 5 was still active during this case day 10 days later. However, the fire had greatly decreased in size. SMARTFIRE reported the Hyde County fire was just over 12 km^2. The Tyrrell County fire in Case Day 5 had diminished in size to below class F classification. There was a fire burning in nearby Suffolk County, Virginia (VA) that was nearly 6 km^2 in size. This fire was not reported by SMARTFIRE 10 days earlier. All the fires burning in Eastern North Carolina and Eastern Virginia combined to be roughly 20 km^2. The Hyde County fire was estimated to have a maximum plume top height of 5098 m and a minimum plume top height of 208 m. There was an area of precipitating clouds to the east of these fires over the Atlantic Ocean (Fig. 4.28). This area of precipitation was associated with a cold front from a surface low located off of the Delmarva Peninsula coast. NARR winds indicate due west winds at all levels analyzed (Fig. 4.29). HYSPLIT 24-hour forward trajectories from the eastern North Carolina fires confirm the smoke from the fires was interacting with the precipitating clouds, especially at middle and upper layers (>2000 m) (Fig. 4.30). This area of precipitation was used as the smoky clouds for this case day. They are centrally located at 34°N and 71°W (Fig. 4.28). The non-smoky clouds were located at 25.5°N and 68°W well out of range of the forest fire aerosols (Fig. 4.28).

AOT values for this case day were relatively low, likely due to the limited size of these fires. There were 23 values returned over 0.75 for the area upwind of the smoky clouds (Fig. 4.28). None of these values were over 1.00. The median AOT value was 0.80, which was similar

to the value from Case Day 5. The AOT values for the non-smoky clouds ranged from 0.10-0.20 (Fig. 4.28).

Tables 4.1 and 4.7 summarize the raw model output for Case Day 6. TRMM 3B42 and AMSR CLW illustrations are shown to identify regions of precipitation and elevated cloud liquid water (Figure 4.31). The smoky clouds median CTT was 245 K (-28°C), while the non-smoky clouds median CTT was 234 K (-39°C). The smoky CREP using median values was 248, while the non-smoky CREP was 240, resulting in a CREP ratio between smoky and non-smoky clouds of 1.03. A value close to one indicates that the smoky and non-smoky clouds precipitated approximately the same given the available CLW. The smoky cloud phase data indicates that the ice phase to water phase ratio was about 3 for each cloud set. Both sets of clouds have roughly the same ice to liquid phase ratio. These clouds have some of the warmer clouds examined in this study, thus they both have a higher mixed phase percentage. The smoky clouds were comprised of 17 % mixed phase clouds while non-smoky clouds were comprised of 15 % mixed phase clouds. This case day seems to be largely unaffected by the presence of aerosols. All of the cloud characteristics examined were similar. Either the smoky clouds were able to overcome the initial suppression of precipitation or that the aerosol loads were light enough to minimize the impact on precipitation output.

4.3. Discussion of Results

The overarching objective of this study was to examine the effects of southeastern U.S. forest fire aerosols on the ability of clouds to precipitate during the 2007-2009 time period. The results of this study help address this issue but the results also bring to light other issues. In the initial stages of this study, a proposed objective involved being able to stratify between warm

and cold clouds while also stratifying them as smoky and non-smoky. However, through the selection of case days, it was discovered that warm cloud precipitation events over the Atlantic Ocean interacting with forest fire aerosols were very rare during the period data was examined (2007-2009). Shallow, warm top clouds being introduced to the aerosols was fairly common; however, these clouds were not precipitating. The inability to find warm cloud case days may be due to the limited temporal resolution available, but it may also be due to precipitation suppression as found by past studies. Several studies have shown that warm maritime clouds have suppressed precipitation due to introduction of forest fire aerosols into the cloud layer. A more thorough microphysical study of shallow clouds would be necessary to answer the question of why so few warm maritime clouds were precipitating. As a result of the lack of warm cloud case days, all of the case days presented here were cold cloud cases, with average CTT values near -40°C.

One of the most difficult aspects of this study was finding case days that met the selection criteria and had sufficient satellite data to complete the analysis. Approximately 100 days were examined, and only 6 case days resulted. Identifying a class F or G fire burning with prevailing winds blowing the aerosols into precipitating clouds is fairly difficult. This was in part due to the limited temporal resolution of the forest fire data available as well as the limited record of some of the satellite products. The selection process yielded six different case days. Case Days 1, 5, and 6 had lower AOT values interacting with the smoky clouds. They also had a lower spatial distribution of the highest AOT values. In Case Days 1 and 5 the reason for the lower spatial distribution was highly dispersed smoke plumes. There was significant acreage being burned during these case days but changing wind directions and speeds over time caused lower AOT values over a large area. Case Day 6 was a little different because there was relatively low

acreage burning. The AOT values were high given the smaller size of the fires burning due to the low dispersion of the plumes.

Case Days 2, 3, and 4 had the highest AOT values of the days examined. This was primarily due to the massive Georgia Bay Complex fire that was nearing its peak spatial extent during this time. The other reason for extremely high AOT values was the presence of Subtropical Storm Andrea. This storm was very slow moving and was stationary at times. The center of the storm stayed just off the Georgia-Florida-South Carolina coast for several days in early and mid-May. This allowed for consistent winds at the surface, lower troposphere, and mid-troposphere. The consistent winds allowed for smoke and aerosols to follow a similar trajectory and helped to focus the smoke along a specific path. On 9 May, 12 May, and 13 May, the consistent winds allowed for extremely high AOT values over Florida, South Georgia, the eastern Gulf of Mexico, and the Bahamas (Fig. 17, 22, and 27). These high AOT values also covered a large swath and appeared to be well organized. The AOT values on all three days were 15-30 times larger than a non-smoky day in the region. The differences in AOT magnitude, plume dispersion, and winds may contribute to the discrepancies in some of the data products discussed below.

a. CREP Analysis

The CREP value was used in this study to have a relative value that would allow for analysis of smoke and non-smoky clouds ability to precipitate the available cloud liquid water. CREP can be analyzed between smoky and non-smoky clouds but can also be used to compare all the smoky case days or all of the non-smoky case days. CREP values are not intended to be

used independently. The use of the CREP ratio was developed as a way to quickly determine the difference in CREP between smoky and non-smoky clouds for a case day.

The CREP ratio varied significantly through the six case days. The three lower aerosol cases showed very little difference in the CREP ratios. There was a substantial difference with the CREP ratios for the three high aerosols cases. In Case Days 2 and 3, the smoky clouds precipitated significantly less of the available CLW than the non-smoky clouds. However, in Case Day 4, the smoky clouds precipitated significantly more of the available CLW than the non-smoky clouds. This apparent contradiction is addressed in Chapter 5.

Because only 6 case days are presented here, this thesis lacks a sufficiently large sample size to examine the statistical relationship between the cases. Future research may attempt to find additional case days to use statistical tests for differences in mean values.

The median AOT vs. CREP ratio relationship brings to light an important point pertaining to AOT influence on precipitation. The lower aerosol cases have CREP ratios close to 1.00. A CREP ratio of 1.00 indicates that the smoky and non-smoky clouds precipitated the available CLW equally. All of these cases had median AOT values of less than 1.00. Thus it appears, based on the CREP ratio, that AOT values of less than 1.00 have little influence on a precipitation. However, CREP values differed greatly for the three higher aerosol cases. These cases all had median AOT values greater than approximately 1.50. This suggests an increasing impact precipitation as median AOT values increase in deep clouds over oceanic regions. In case days 2 and 3, the highly smoky clouds had much lower CREP values than the non-smoky clouds. These results is very similar to a study by Rosenfeld (1999).

There are several other factors that need to be considered when analyzing AOT and CREP. The distribution of AOT values must be examined. It appeared that plumes with high

AOT and low dispersion have the most ability to impact precipitation given the available CLW based on the CREP ratios. Case Days 2, 3 and 4 were examples of this. No case days presented here showed high AOT plumes with significant dispersion. The reason no case days are presented with high AOT values and high dispersion is due to the amount of aerosols that would be needed in order to produce high AOT values in this situation. A massive amount of burning acreage would be needed, on the order of nothing seen in recorded wildfire history in the Southeast. According to the data presented here, AOT values of this magnitude (>1.50) only occur when there is a large class G fire burning in the Southeast. The three high aerosol days in this study had at least 100 km^2 burning. The case days from 12 May and 13 May had more than 200 km^2 being burned daily.

The three case days with relatively low median AOT values provide important information as well. Case Days 1, 5, and 6 had median AOT values around 0.85. This was roughly 4-8 times the regular AOT values reported in the case day area. However, based on CREP ratios, AOT values of 0.85 are not enough to have a noticeable impact on a clouds' ability to precipitate in deep clouds. Conclusions on the lighter aerosol day's impact on shallow clouds cannot be appropriately discussed in this study. However, shallow clouds likely respond differently than deep clouds to even modest increases in aerosols as seen in the lighter aerosol days discussed here. CREP and AOT values alone were not enough to adequately address the objectives of this study. Particle size and cloud phase are two important microphysical measurements that may help providing a better understanding of the effects of forest fire aerosols on precipitation.

b. Cloud Particle Effective Radius

Cloud particle effective radius (ER) provides this study with the ability to analyze the particle size in the study clouds. In all six case days, despite the difference amongst case days in aerosol amounts, the smoky clouds had a smaller average ER than the non-smoky clouds. The smoky case day clouds averaged an ER of 16.59 μm while the non-smoky case day clouds averaged an ER of 20.43 μm. This is an important finding because it demonstrates the microphysical impact that the forest fire aerosols have on cloud particles. It also provides affirmation that the smoky clouds used in the case days were influenced by the forest fire aerosols. As would be expected based on previous research, the increased condensation nuclei provided by the aerosols caused a decrease in the size of the CCN. When the smoky cases were analyzed individually, there was not a wide range of discrepancy in size.

c. Cloud Phase Analysis

The cloud phase analysis was included in this study in an attempt to determine the water phase of each cloud (ice, liquid, mixed phase). The previous literature has shown that differences exist between aerosol forcing on liquid clouds versus aerosol forcing in ice clouds. Cloud phase is important as it can provide indications on cloud lifespan (Fig. 2.5). Based on the CTT retrievals for the case days, it was expected that there would be more ice than liquid in the case day clouds analyzed here. The percentage of ice to liquid phase differs between smoky and non-smoky clouds as well as amongst smoky clouds despite similarities in CTT. Two of the highest aerosol days, 12 May and 13 May, saw the most significant difference in ice to liquid phase ratios. 12 May smoky clouds had a median CTT of 220 K (-43°C) and a non-smoky CTT of 222 K (-41°C). Yet there was a difference in ice/liquid phase ratios of 68 for the smoky clouds and 5

for non-smoky clouds. Considering each set of clouds had over 1400 data retrievals for the cloud phase, the difference is significant. A similar difference is seen in the 13 May cloud phase retrievals. The smoky clouds in this case had a median CTT of 231 K (-42°C) and the non-smoky clouds were colder at 222 K (-52°C). Despite the warmer median temperatures, ice to liquid cloud phase ratios were still substantially different with a cloud phase ratio of 46 for smoky clouds and 3 for non-smoky clouds. The smoky clouds in this case had a mixed phase percentage of 7 %, which was a 5 % increase from the previous day. Despite the smoky clouds having a warmer median CTT, they still had a substantially higher ice to liquid cloud phase ratio. In all three high aerosol cases, the ice to liquid ratio was higher for the smoky case, despite the similarity in median CTT. The 9 May case day had a smaller difference in ice to liquid phase ratios, but the smoky clouds still had a higher ratio.

These cases suggest the possibility that the aerosols are affecting the ice to liquid cloud ratios in clouds. More case days need to be examined in order to understand if the trend persists. It has been documented in previous research that the initial suppression of precipitation can allow for stronger updrafts later in the cloud cycle, which lifts CCN to higher levels in the atmosphere. This could help explain the phenomenon seen in these clouds. The difficulty with this analysis is the difference in CREP ratios between the 9 May, 12 May, and the 13 May case. The 9 May and 12 May cases indicate a substantial decrease in CREP ratios, while the 13 May indicates an increase in CREP ratio. What is further complicated when observing the CREP values for each of the smoky cloud sets. On 9 May, the average CREP value was 87, while the 12 May average CREP value was 94, and the 13 May average CREP value was 105. This makes it difficult to draw any conclusions on the effect of the difference in ice to liquid cloud phase ratios. One difference that exists is the increase in mixed phase percentage in the 13 May and an

increase in the CTT. The 13 May median CTT was 8-11 K warmer than the 9 May and 12 May median CTT. This difference in CTT may indicate that clouds that elevate a higher percentage of their CCN above the level of homogeneous nucleation see a decrease in CREP. This hypothesis can be better analyzed with additional case days.

Table 4.1. Number of TRMM and AMSR-E 0.25° x 0.25° grid cells used for each case day.

	Smoky	**Non-smoky**
Case Day 1	42	48
Case Day 2	58	65
Case Day 3	98	100
Case Day 4	114	120
Case Day 5	63	91
Case Day 6	57	88

Table 4.2. Case Day 1 summary of raw data output.

	Median	**Average**
Smoky AOT	.806	.822
Smoky TRMM PR_{rate}	12.360 mm/hr	15.345 mm/hr
Smoky AMSR CLW	0.134 mm	0.181 mm
Smoky MODIS CTT	220.93 K	225.76 K
Smoky CREP	92.27	84.57
Non-smoky TRMM PR_{rate}	13.31 mm/hr	15.65 mm/hr
Non-smoky AMSR CLW	.162 mm	.277 mm
Non-smoky MODIS CTT	226.25 K	232.82 K
Non-smoky CREP	82.10	56.61
CREP Ratio	1.12	1.49
Smoky Ice/Liquid Cloud Ratio	16.316	
Smoky Mixed Phase Cloud %	5.58%	
Non-smoky Ice/Liquid Ratio	0.124	
Non-smoky Mixed Phase Cloud %	5.58%	
Smoky Effective Radius Avg.	14.70 μm	
Non-smoky Effective Radius Avg.	17.42 μm	

Table 4.3. Case Day 2 summary of raw data output.

	Median	**Average**
Smoky AOT	2.531	2.560
Smoky TRMM PR_{rate}	20.835 mm/hr	22.357 mm/hr
Smoky AMSR CLW	0.224 mm	0.256 mm
Smoky CREP	93.16	87.22
Smoky MODIS CTT	224.54 K	236.28 K
Non-smoky TRMM PR_{rate}	35.923 mm/hr	42.099 mm/hr
Non-smoky AMSR CLW	0.272 mm	0.322 mm
Non-smoky CREP	132.22	130.68
Non-smoky MODIS CTT	230.72 K	235.63 K
CREP Ratio	.70	.66
Smoky Ice/Liquid Cloud Ratio	5.547	
Smoky Mixed Phase Cloud %	3.90 %	
Non-smoky Ice/Liquid Ratio	3.091	
Non-smoky Mixed Phase Cloud %	1.37 %	
Smoky Effective Radius Avg.	16.16 μm	
Non-smoky Effective Radius Avg.	16.49 μm	

Table 4.4. Case Day 3 summary of raw data output.

	Median	**Average**
Smoky AOT	3.327	3.387
Smoky TRMM PR_{rate}	15.840 mm/hr	21.560 mm/hr
Smoky AMSR CLW	0.095 mm	0.229 mm
Smoky CREP	166.82	94.32
Smoky MODIS CTT	218.58 K	221.58 K
Non-smoky TRMM PR_{rate}	24.15 mm/hr	33.199 mm/hr
Non-smoky AMSR CLW	0.051 mm	0.071 mm
Non-smoky CREP	476.33	467.65
Non-smoky MODIS CTT	216.82 K	221.84 K
CREP Ratio	.35	.20
Smoky Ice/Liquid Cloud Ratio	68.300	
Smoky Mixed Phase Cloud %	2.26 %	
Non-smoky Ice/Liquid Ratio	4.466	
Non-smoky Mixed Phase Cloud %	7.69 %	
Smoky Effective Radius Avg.	16.48 μm	
Non-smoky Effective Radius Avg.	20.20 μm	

Table 4.5. Case Day 4 summary of raw data output.

	Median	**Average**
Smoky AOT	1.807	1.992
Smoky TRMM PR_{rate}	22.380 mm/hr	25.706 mm/hr
Smoky AMSR CLW	0.225 mm	0.247 mm
Smoky CREP	99.55	104.17
Smoky MODIS CTT	230.61 K	230.34 K
Non-smoky TRMM PR_{rate}	37.74 mm/hr	50.541 mm/hr
Non-smoky AMSR CLW	0.560 mm	0.635 mm
Non-smoky CREP	67.39	79.56
Non-smoky MODIS CTT	221.92 K	221.69 K
CREP Ratio	1.48	1.31
Smoky Ice/Liquid Cloud Ratio	46.167	
Smoky Mixed Phase Cloud %	6.91 %	
Non-smoky Ice/Liquid Ratio	2.586	
Non-smoky Mixed Phase Cloud %	1.47 %	
Smoky Effective Radius Avg.	17.25 µm	
Non-smoky Effective Radius Avg.	20.70 µm	

Table 4.6. Case Day 5 summary of raw data output.

	Median	**Average**
Smoky AOT	.839	.878
Smoky TRMM PR_{rate}	39.180 mm/hr	40.225 mm/hr
Smoky AMSR CLW	0.617 mm	0.566 mm
Smoky CREP	63.52	71.12
Smoky MODIS CTT	208.55 K	209.55 K
Non-smoky TRMM PR_{rate}	20.73 mm/hr	21.682 mm/hr
Non-smoky AMSR CLW	0.322 mm	0.383 mm
Non-smoky CREP	64.46	56.60
Non-smoky MODIS CTT	208.50 K	209.62 K
CREP Ratio	.99	1.26
Smoky Ice/Liquid Cloud Ratio	80.700	
Smoky Mixed Phase Cloud %	0 %	
Non-smoky Ice/Liquid Ratio	53.389	
Non-smoky Mixed Phase Cloud %	6.49 %	
Smoky Effective Radius Avg.	19.94 μm	
Non-smoky Effective Radius Avg.	25.3 μm	

Table 4.7. Case Day 6 summary of raw data output.

	Median	**Average**
Smoky AOT	.803	.814
Smoky TRMM PR_{rate}	14.37 mm/hr	17.689 mm/hr
Smoky AMSR CLW	0.058 mm	0.104 mm
Smoky CREP	249.91	169.50
Smoky MODIS CTT	215.03 K	217.42 K
Non-smoky TRMM PR_{rate}	19.905 mm/hr	21.471 mm/hr
Non-smoky AMSR CLW	0.083 mm	0.165 mm
Non-smoky CREP	239.39	129.77
Non-smoky MODIS CTT	218.55 K	223.14 K
CREP Ratio	1.04	1.30
Smoky Ice/Liquid Cloud Ratio	3.097	
Smoky Mixed Phase Cloud %	17.47 %	
Non-smoky Ice/Liquid Ratio	3.350	
Non-smoky Mixed Phase Cloud %	15.19 %	
Smoky Effective Radius Avg.	14.99 μm	
Non-smoky Effective Radius Avg.	22.44 μm	

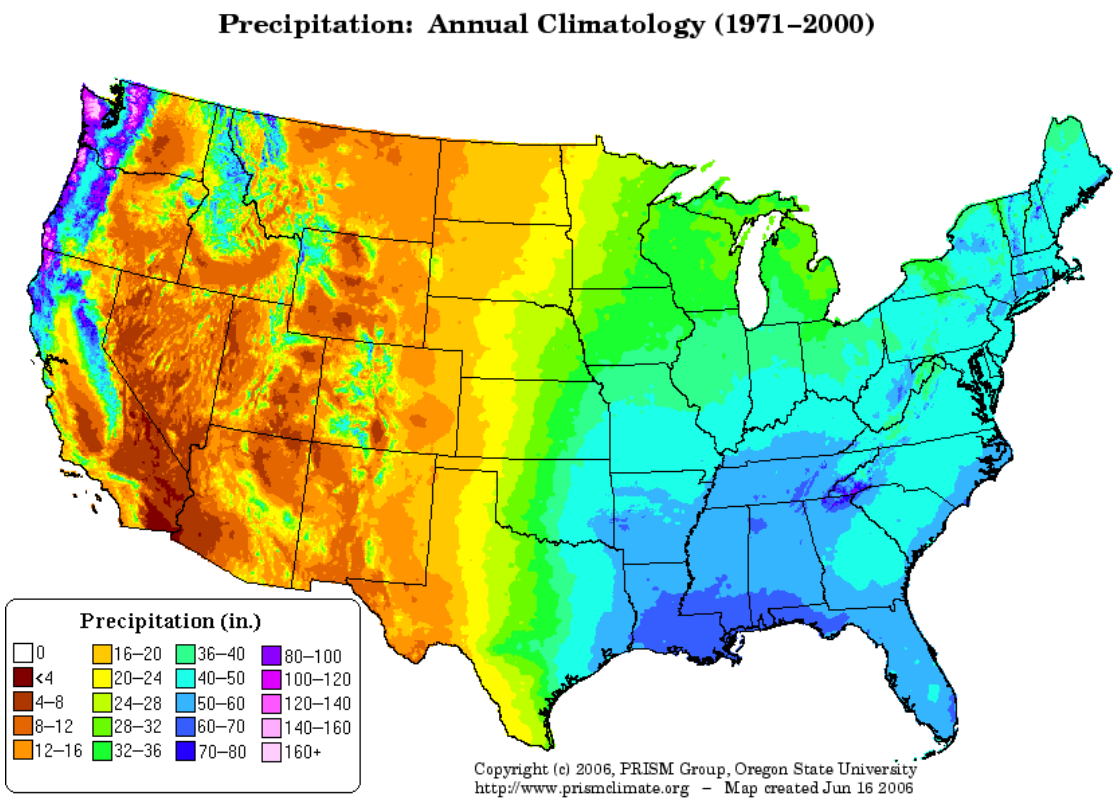

Fig. 4.1. Illustration of average annual precipitation from 1971-2000 from PRISM Group.

(a)

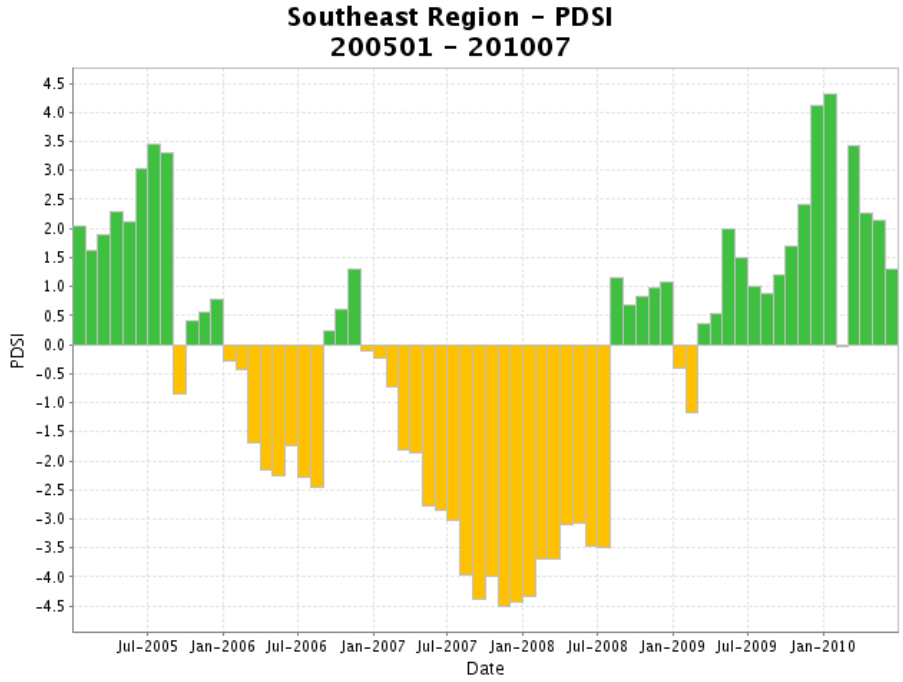

(b)

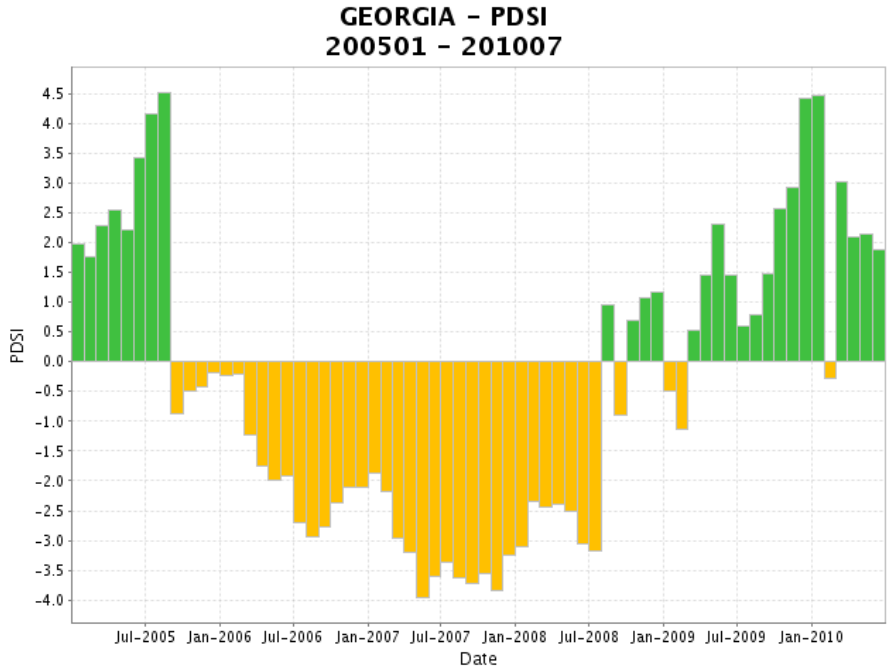

Fig. 4.2. Palmer Drought Severity Index (PDSI) for Southeast states from Jan. 2005- Jul. 2010 (a) and Palmer Drought Severity Index (PDSI) for Georgia from Jan. 2005-Jul. 2010 (b).

(a)

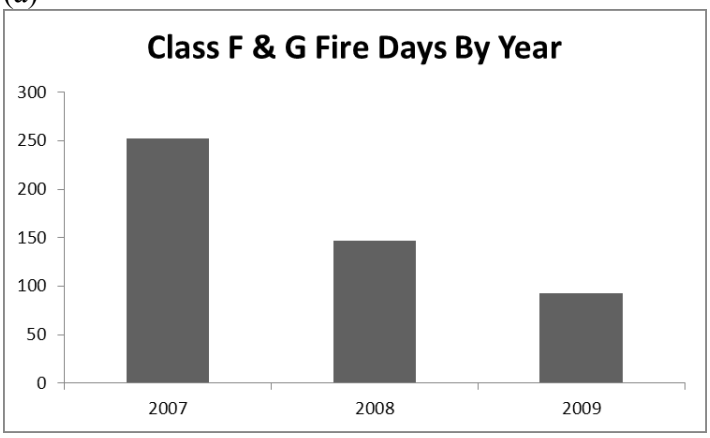

(b)

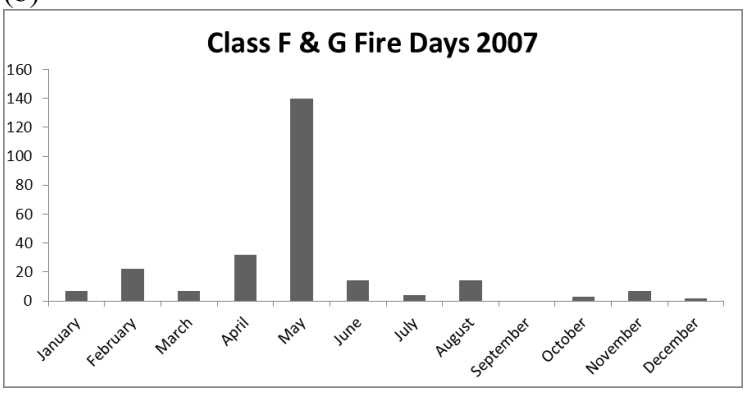

(c)

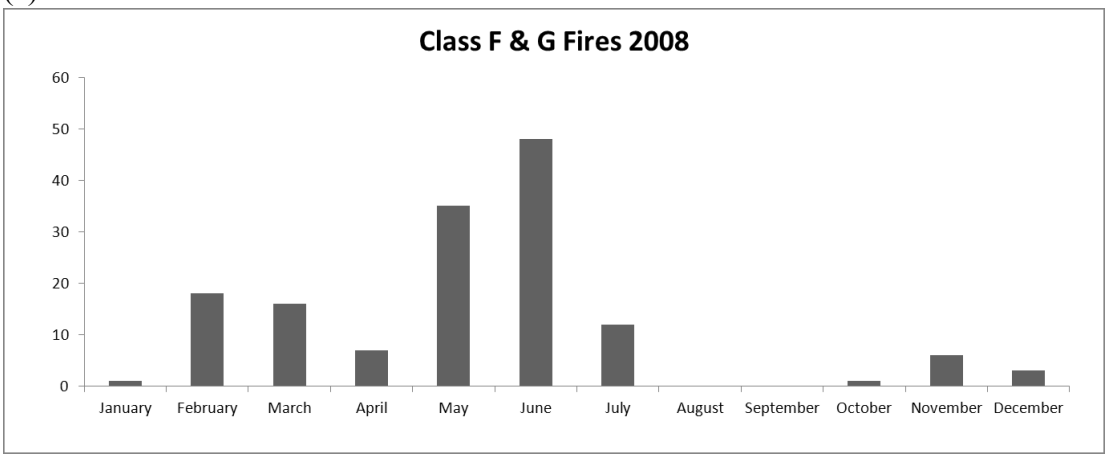

Fig. 4.3. Displays (a) the number of class F and G fire days for each year from 2007-2009 and (b) the number of class F and G fire days by month for 2007 as well as (c) the number of class F and G fire days by month for 2008.

(a)

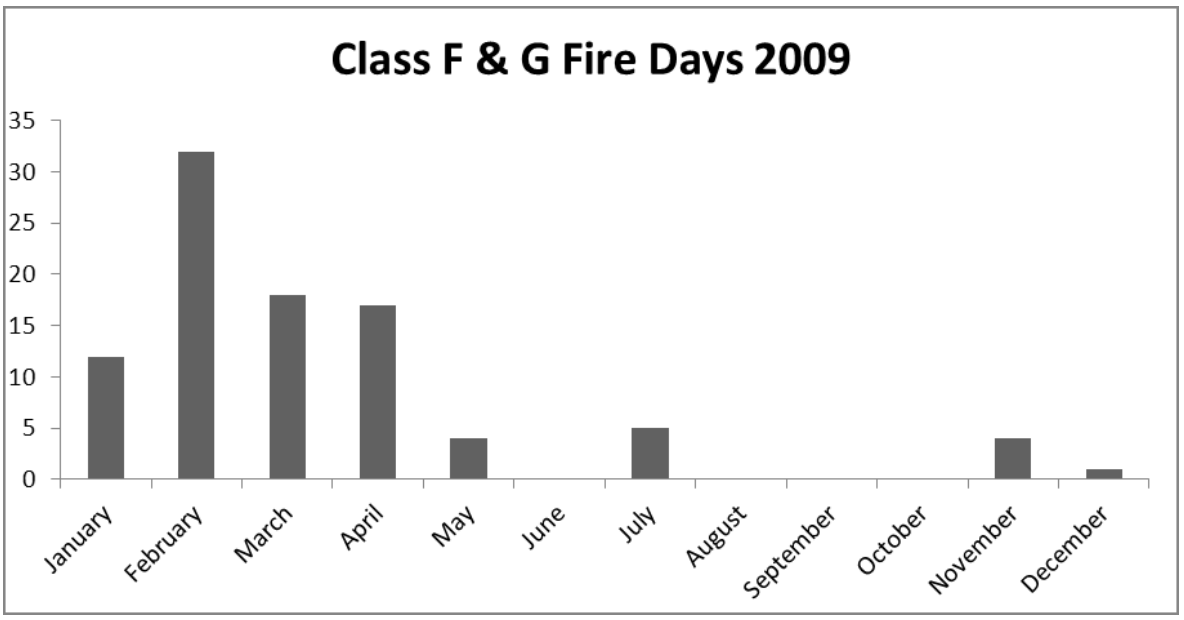

(b)

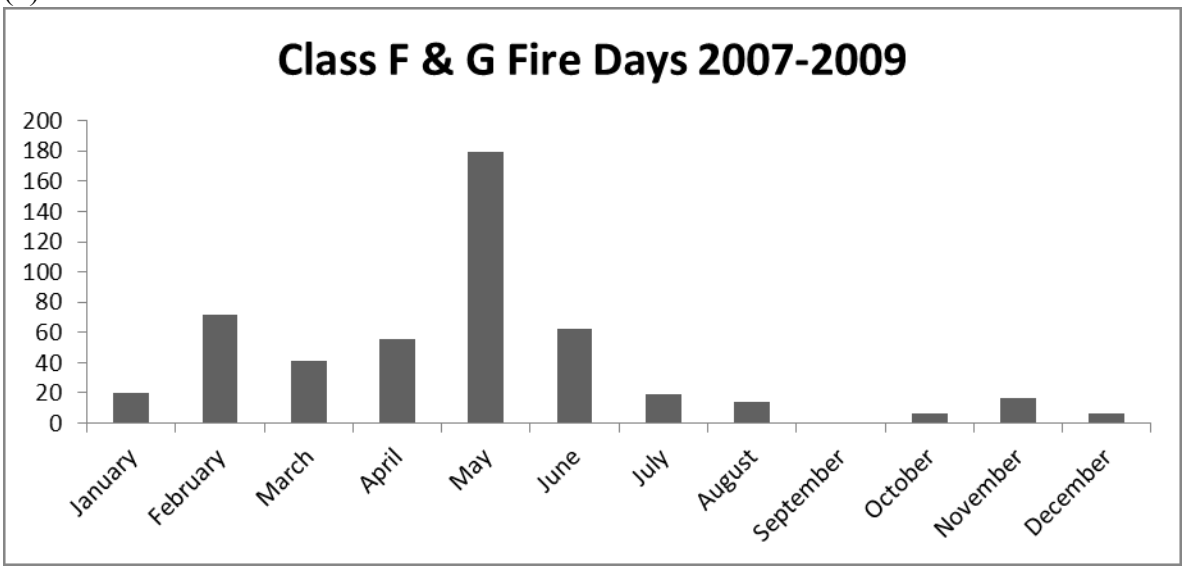

Fig. 4.4. Displays (a) the number of class F and G fire days by month for 2009 and (b) the number of class F and G fire days by month for 2007-2009.

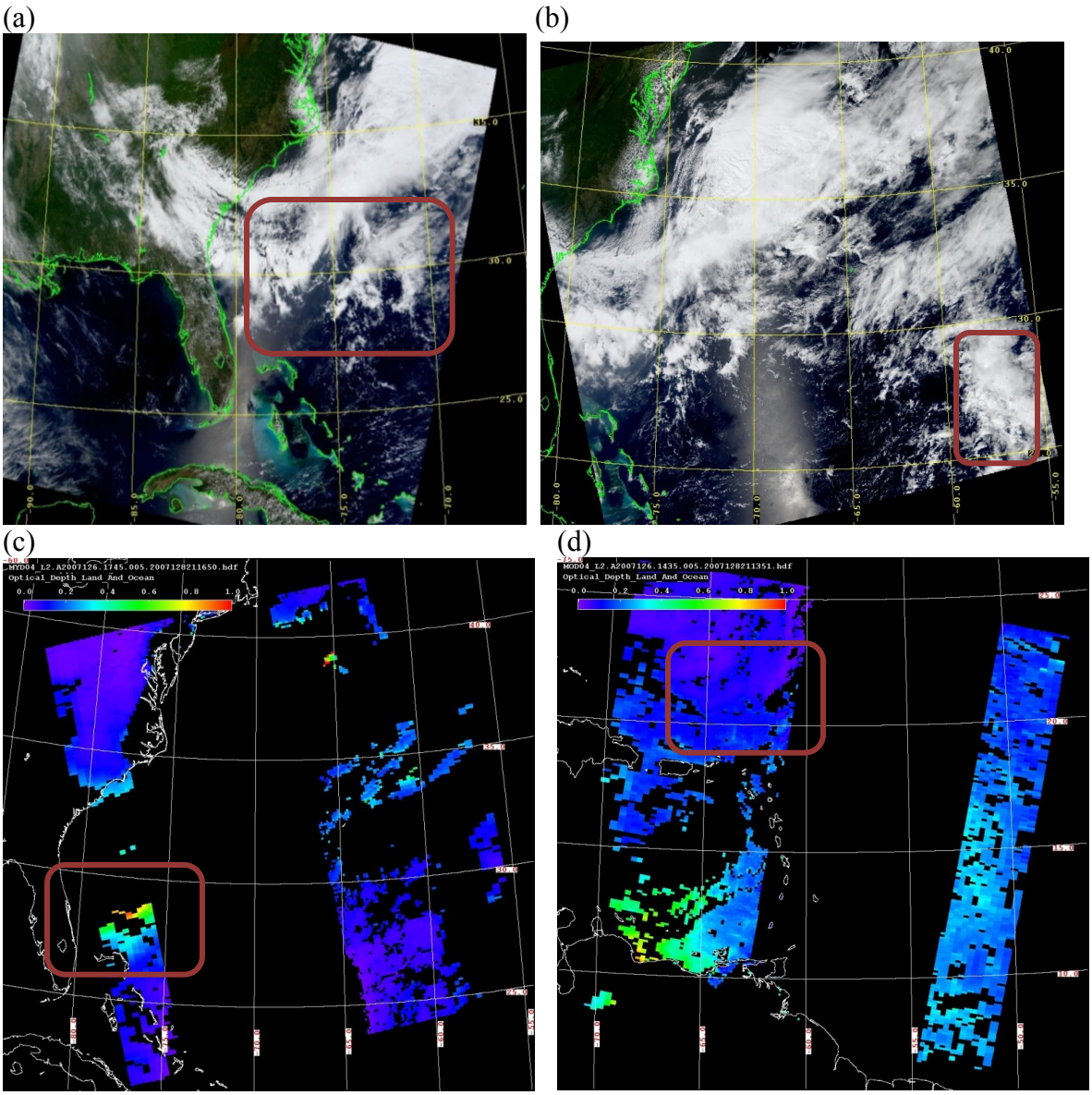

Fig. 4.5. Case Day 1 MODIS Visible imagery for (a) smoky clouds and (b) non-smoky clouds and MODIS AOT upwind from (c) smoky clouds and (d) non-smoky clouds.

(a)

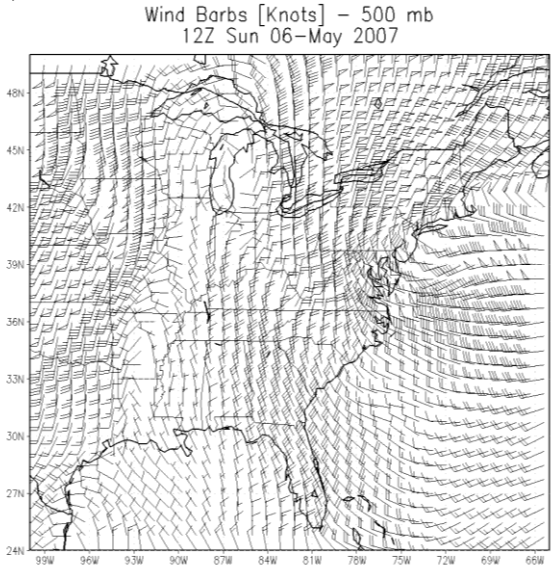

(b)

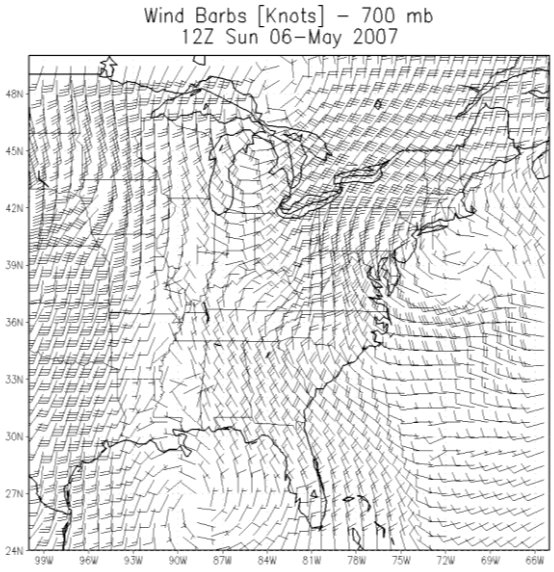

(c)

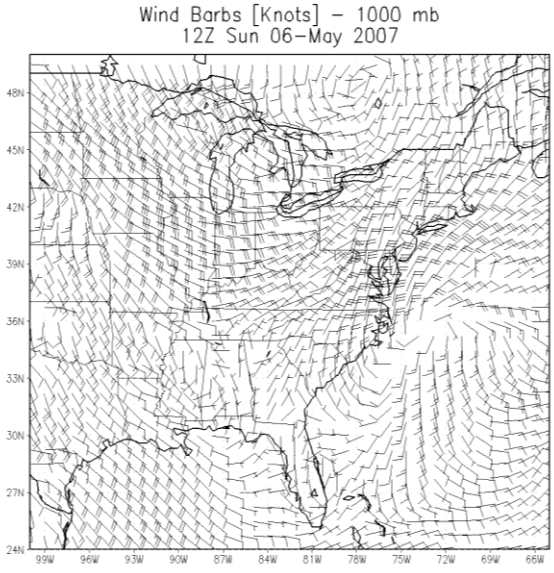

Fig. 4.6. Case Day 1 NARR wind barbs at (a) 500 hPa, (b) 700 hPa, and (c) 1000 hPa

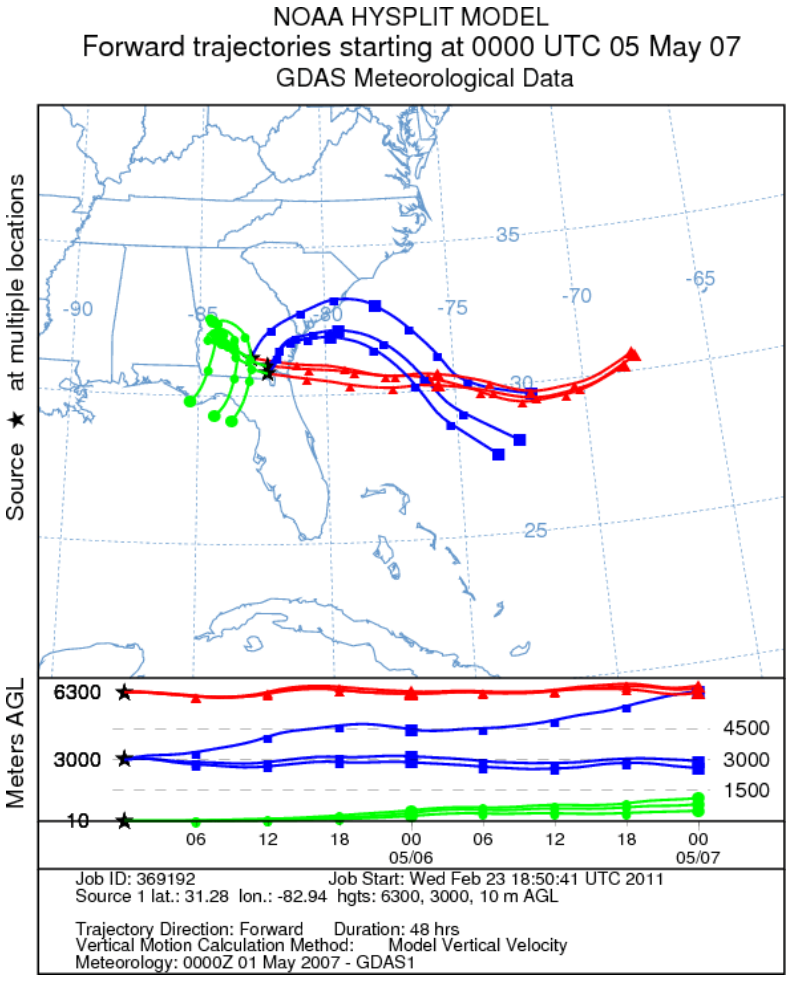

Fig. 4.7. Case Day 1 HYSPLIT model 48 hour forward trajectories from three South Georgia fires.

(a)

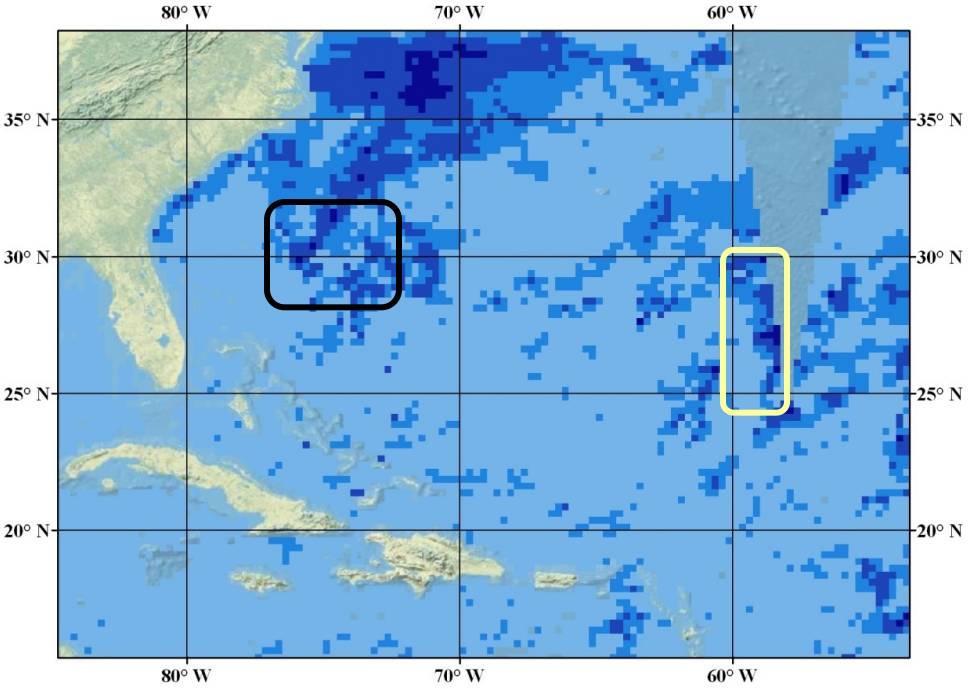

(b)

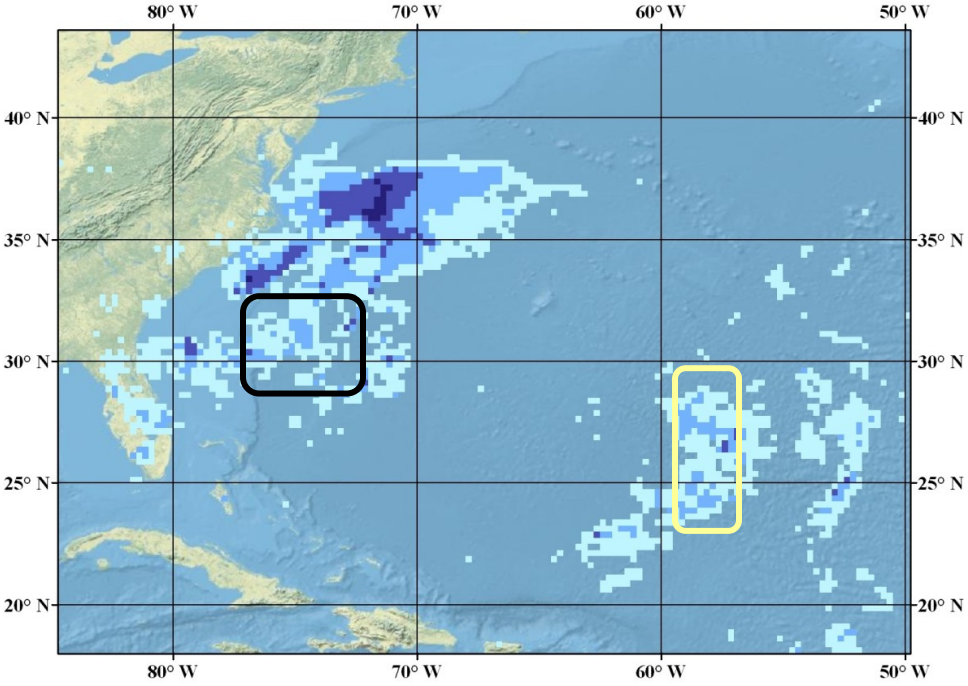

Fig. 4.8. Case Day 1 (a) AMSR Daily CLW Product and (b) TRMM TMI 3B42 Daily Product with smoky clouds in darker outline.

(a)

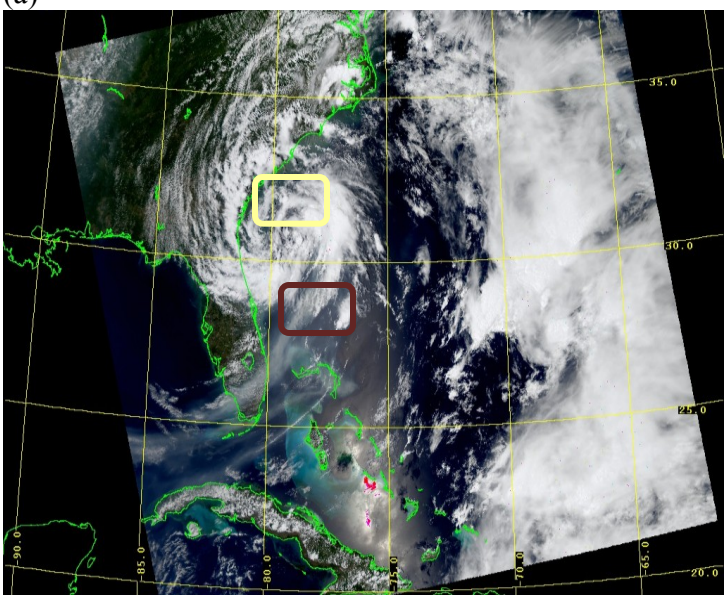

(b)

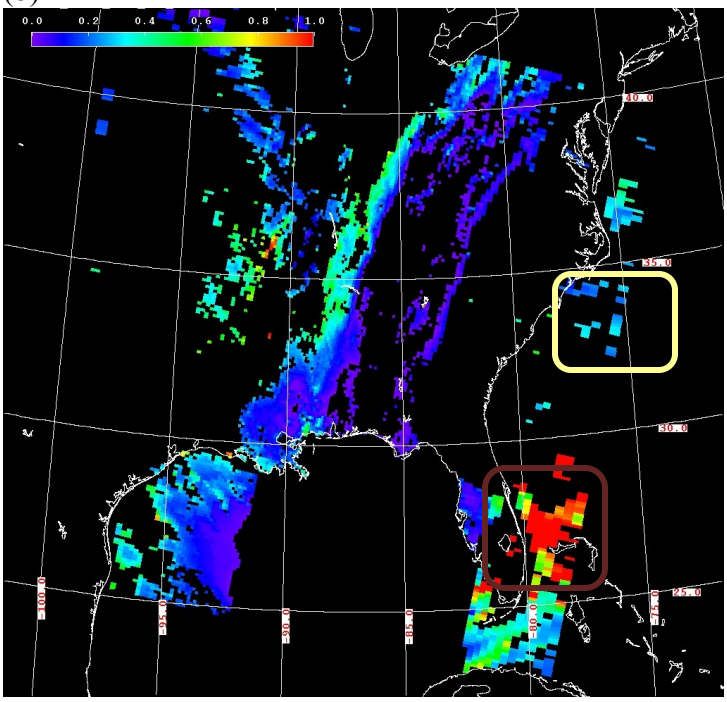

Fig. 4.9. Case Day 2 (a) MODIS Visible Imagery of smoky and non-smoky clouds and MODIS AOT upwind from smoky and (b) non-smoky clouds with smoky clouds in darker outline.

(a)

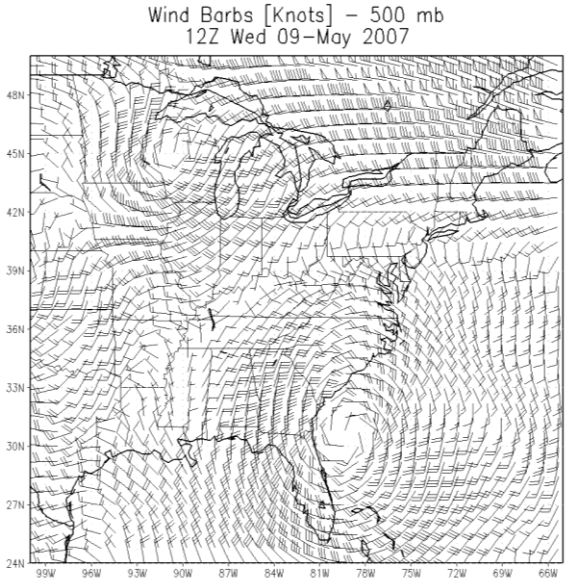

(b)

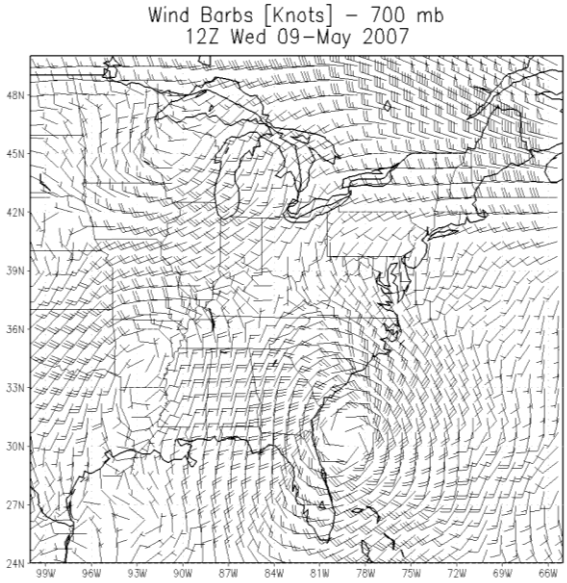

(c)

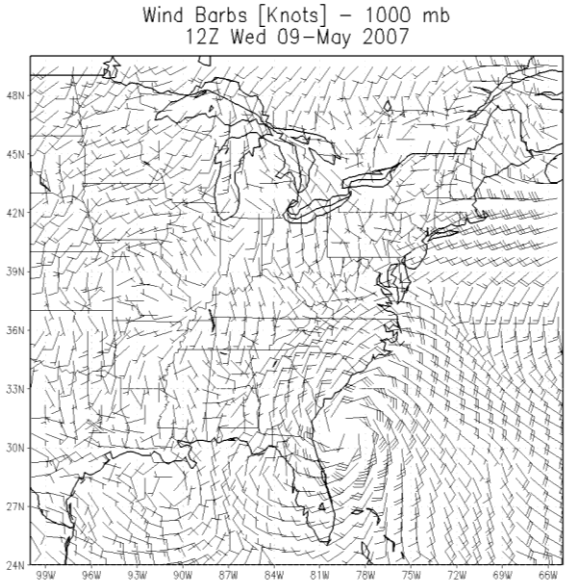

Fig. 4.10. Case Day 2 NARR wind barbs at (a) 500 hPa, (b) 700 hPa, and (c) 1000 hPa.

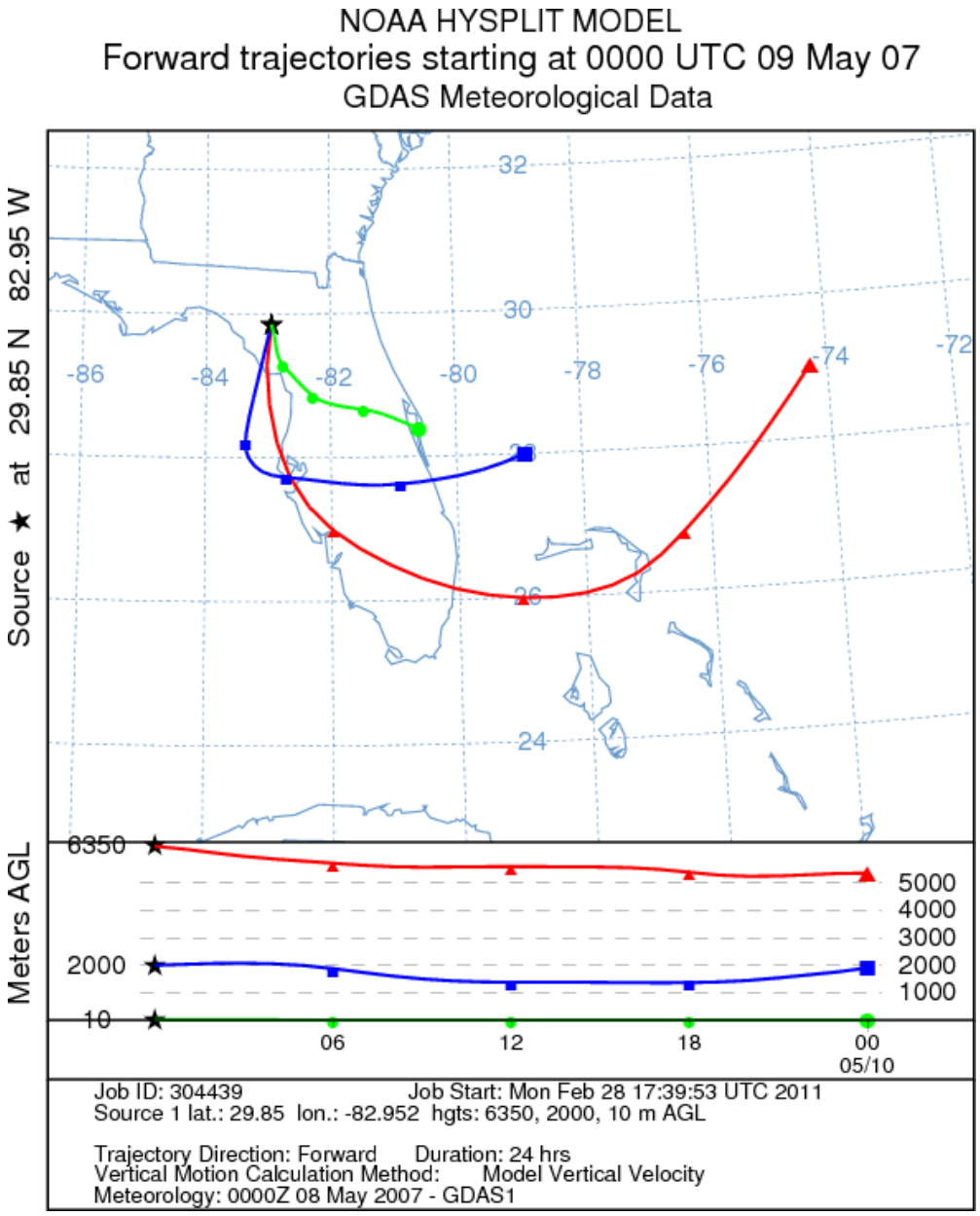

Fig. 4.11. Case Day 2 HYSPLIT model 24-hour forward trajectories from Lafayette County, FL fire.

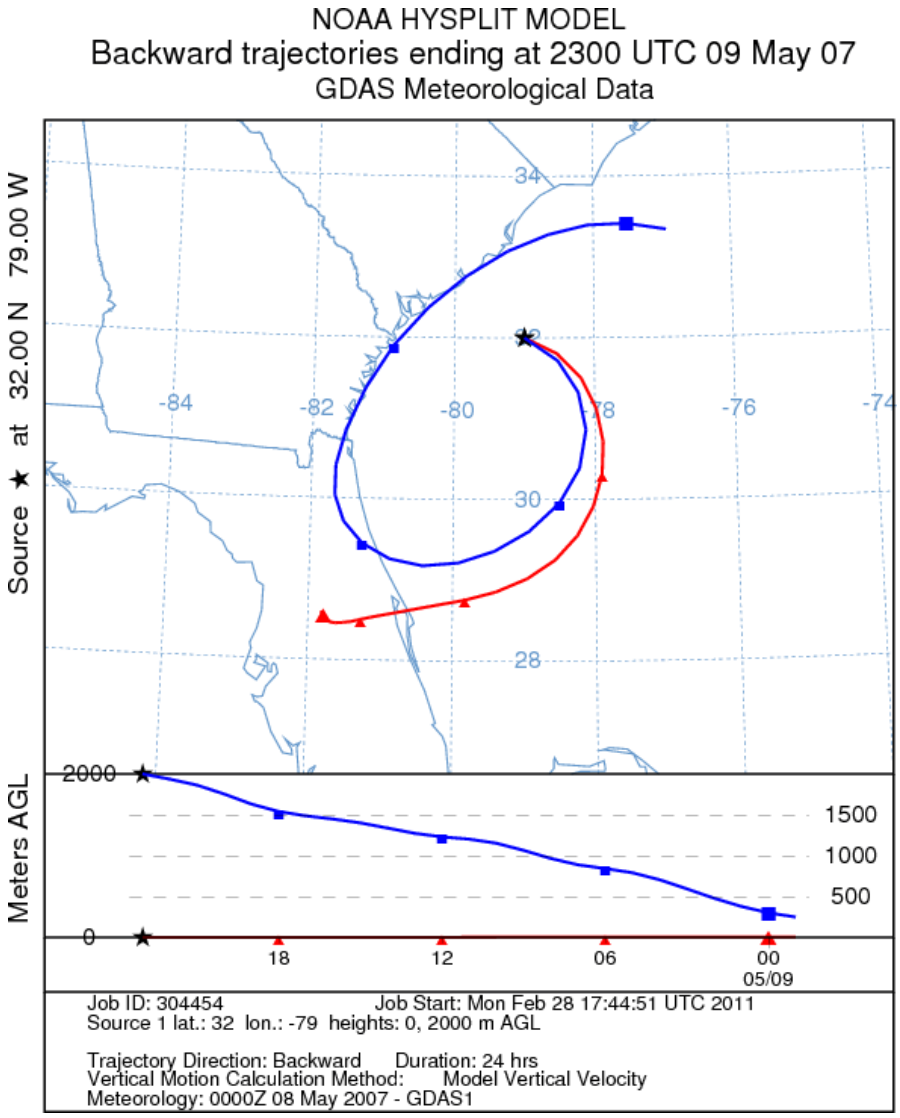

Fig. 4.12. Case Day 2 HYSPLIT model 24-hour backward trajectories from non-smoky clouds.

(a)

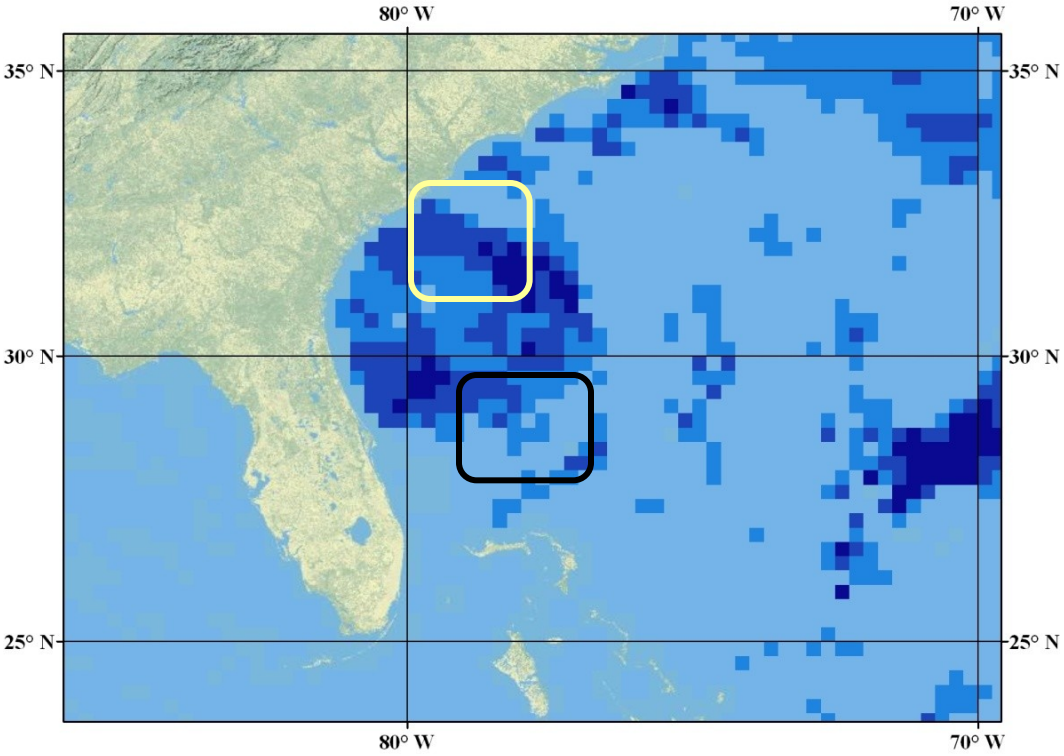

(b)

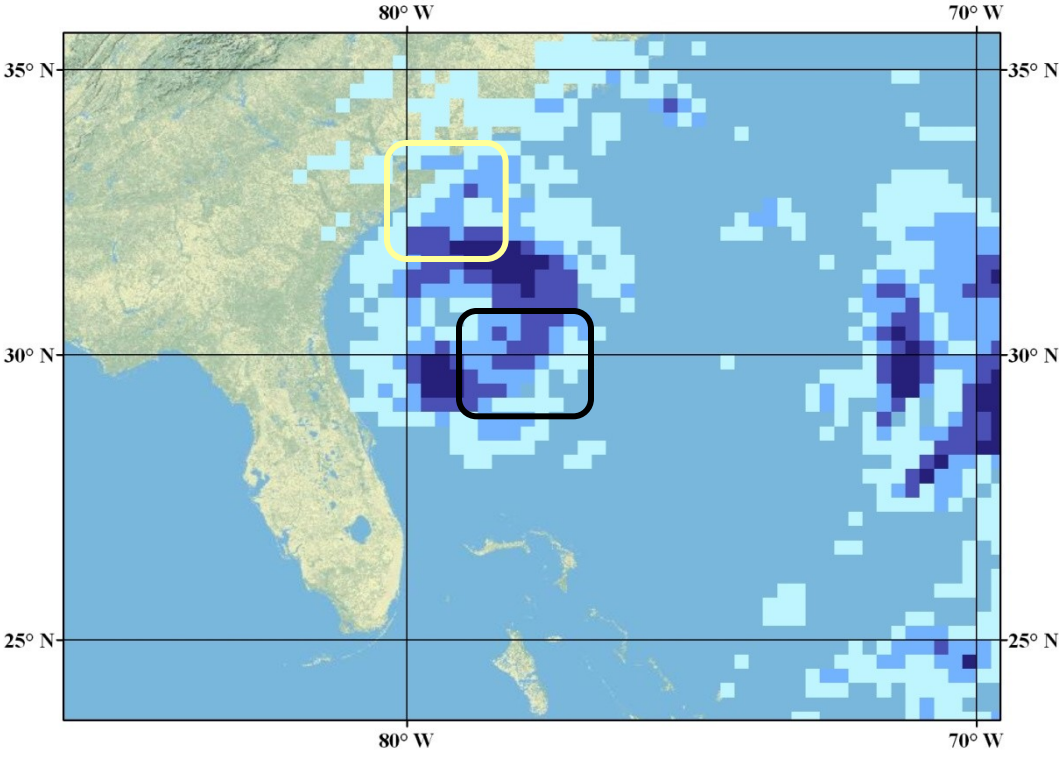

Fig. 4.13. Case Day 2 (a) AMSR CLW and (b) TRMM TMI 3B42 Daily Product (smoky clouds in darker outline).

(a)

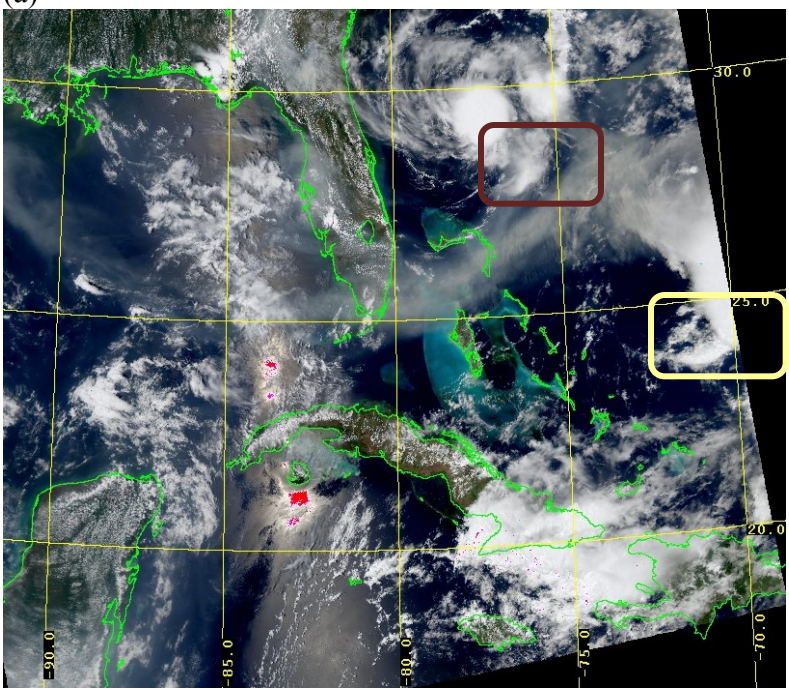

(b)

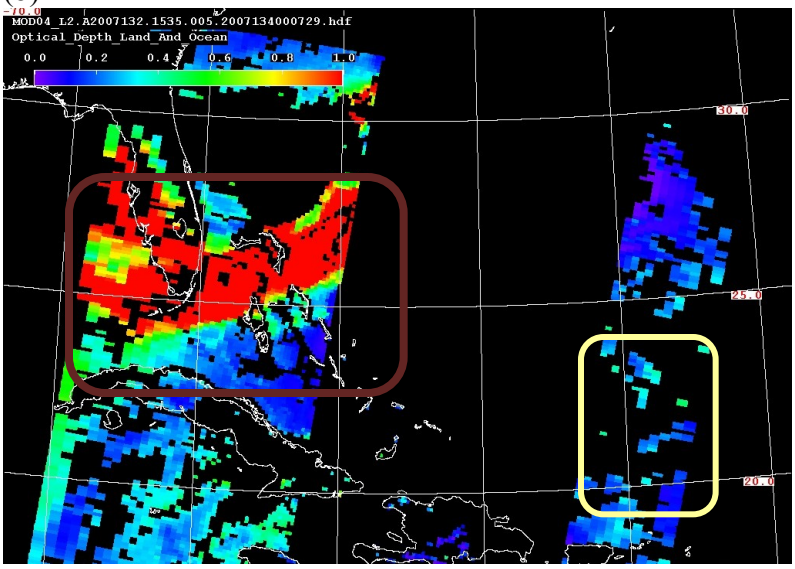

Fig. 4.14. Case Day 3 (a) MODIS visible imagery of smoky and non-smoky clouds and (b) MODIS AOT upwind from smoky and non-smoky clouds with smoky clouds in darker outline.

(a)

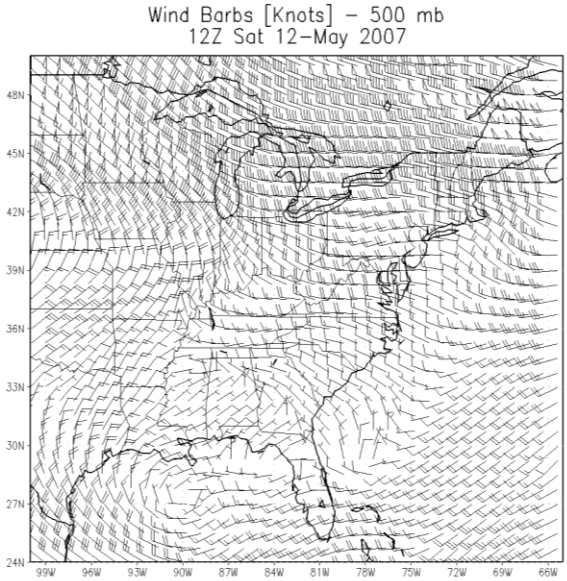

(b)

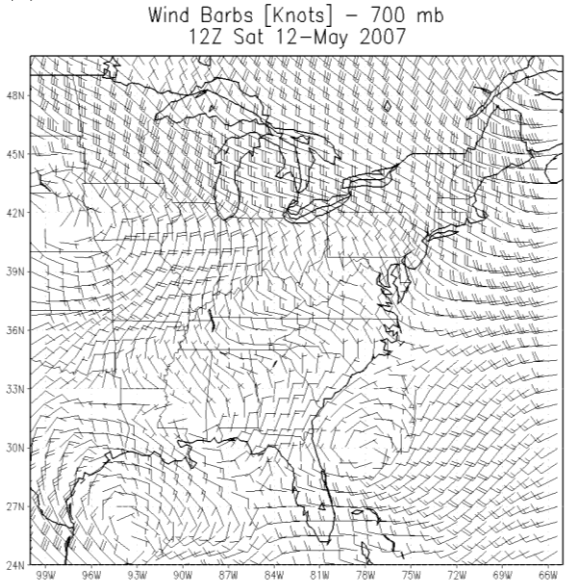

(c)

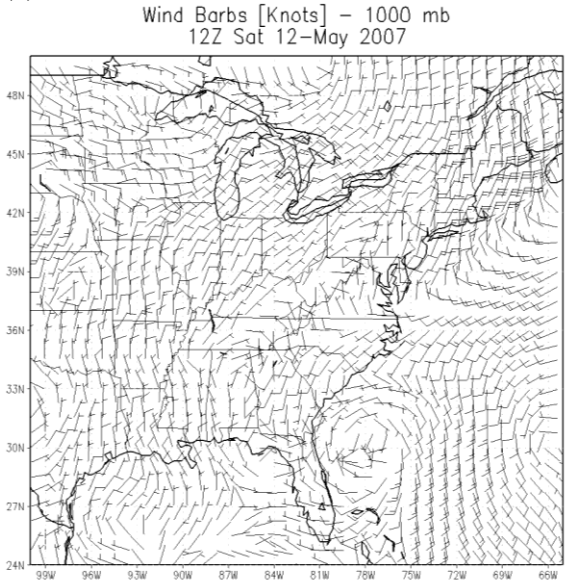

Fig. 4.15. Case Day 3 NARR wind barbs at (a) 500 hPa, (b)700 hPa, and (c) 1000 hPa.

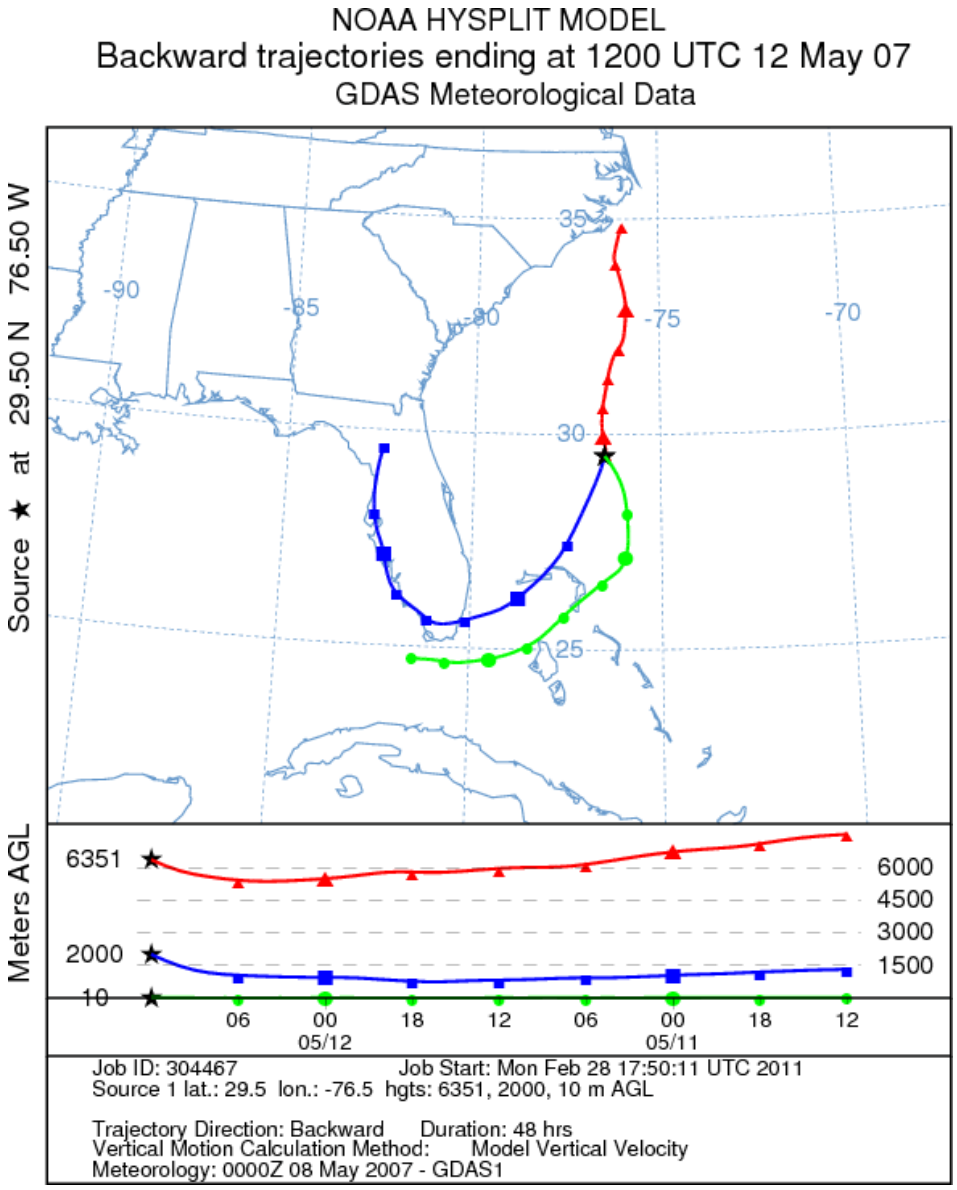

Fig. 4.16. Case Day 3 HYSPLIT model 48 hour backward trajectories from smoky clouds.

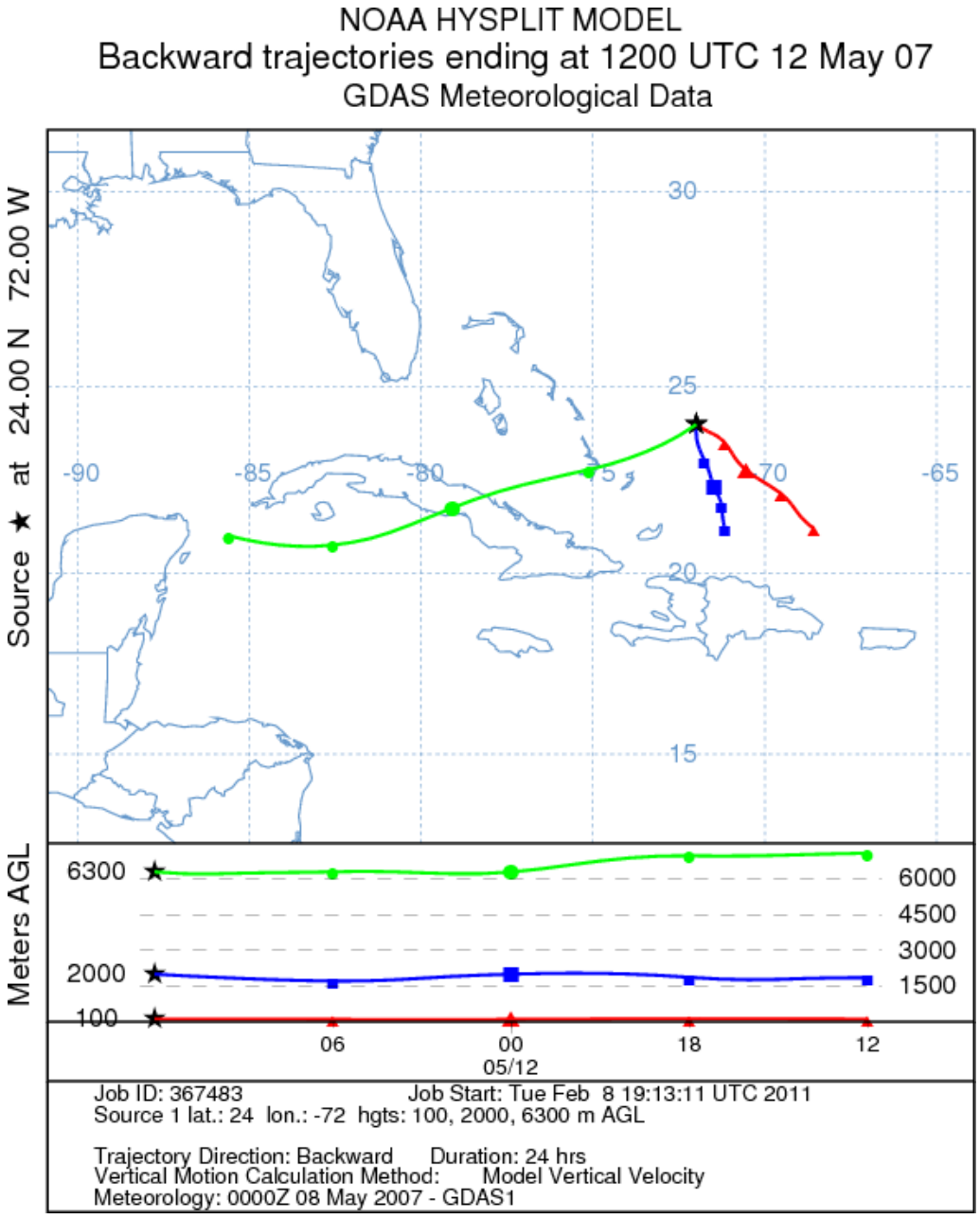

Fig. 4.17. Case Day 3 HYSPLIT model 24-hour backward trajectories for non-smoky clouds.

(a)

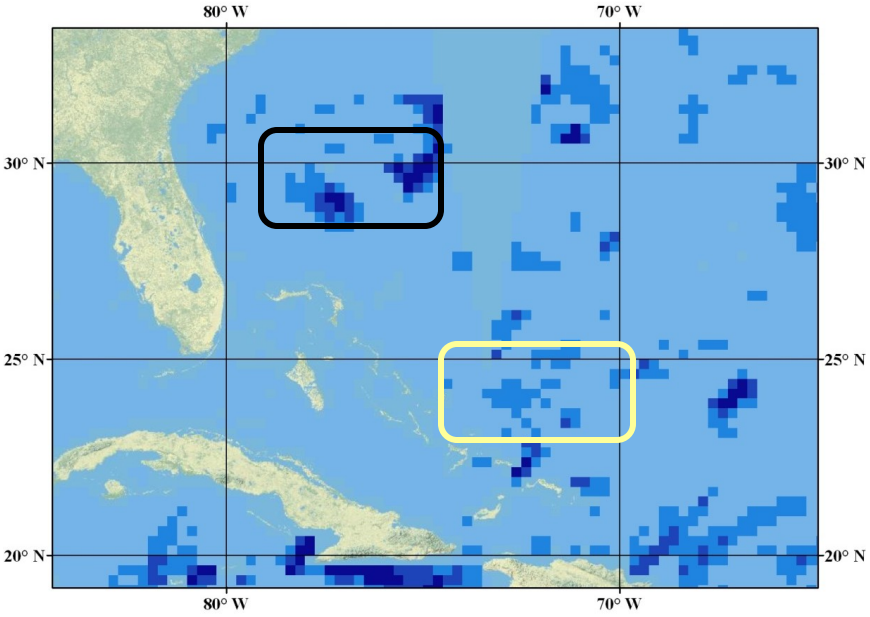

(b)

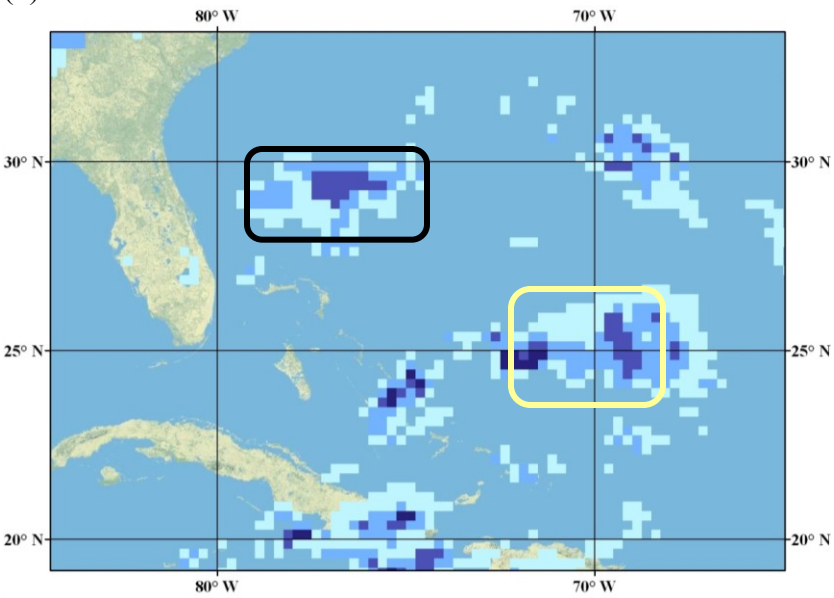

Fig. 4.18. Case Day 3 (a) AMSR CLW for smoky and non-smoky clouds and (b) TRMM TMI 3B42 values for smoky and non-smoky clouds with smoky clouds in darker outline.

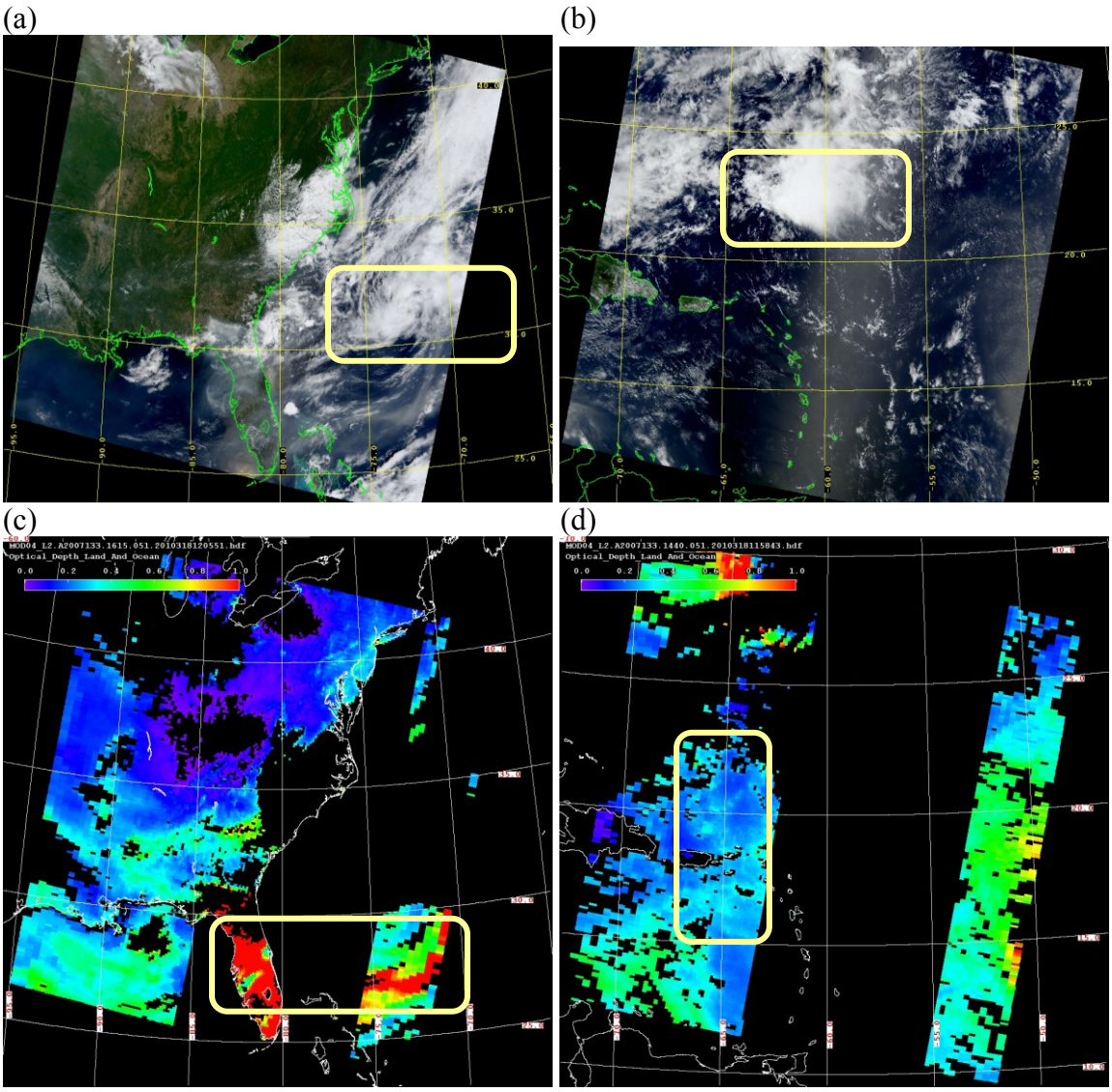

Fig. 4.19. Case Day 4 (a) MODIS visible imagery for smoky clouds and (b) non-smoky clouds and (c) MODIS AOT upwind from smoky clouds and (d) non-smoky clouds.

(a)

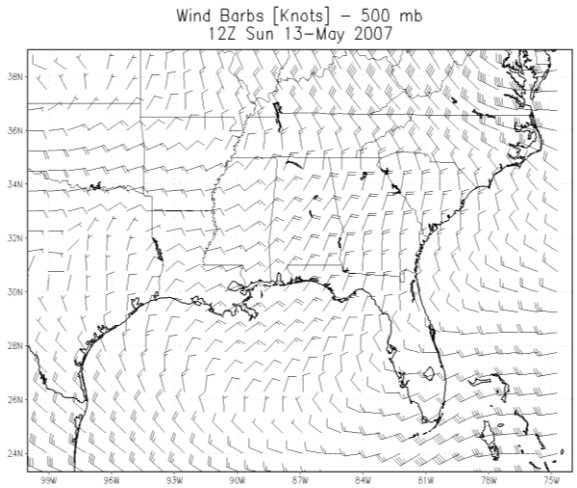

(b)

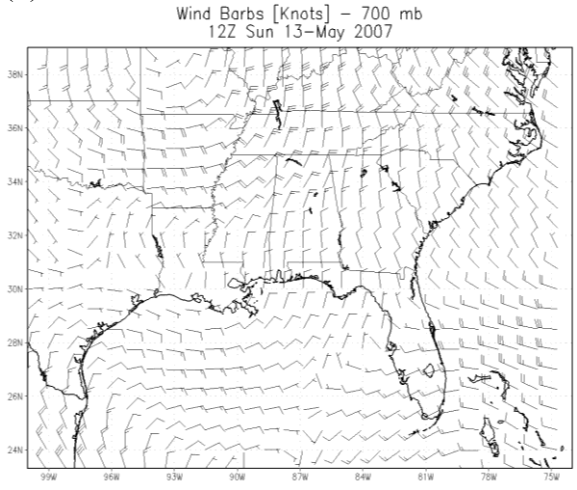

(c)

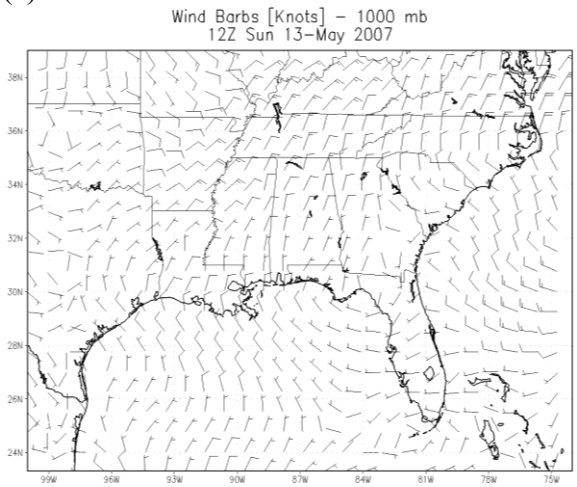

Fig. 4.20. Case Day 4 NARR winds at (a) 500hPa, (b) 700hPa, (c) and 1000 hPa.

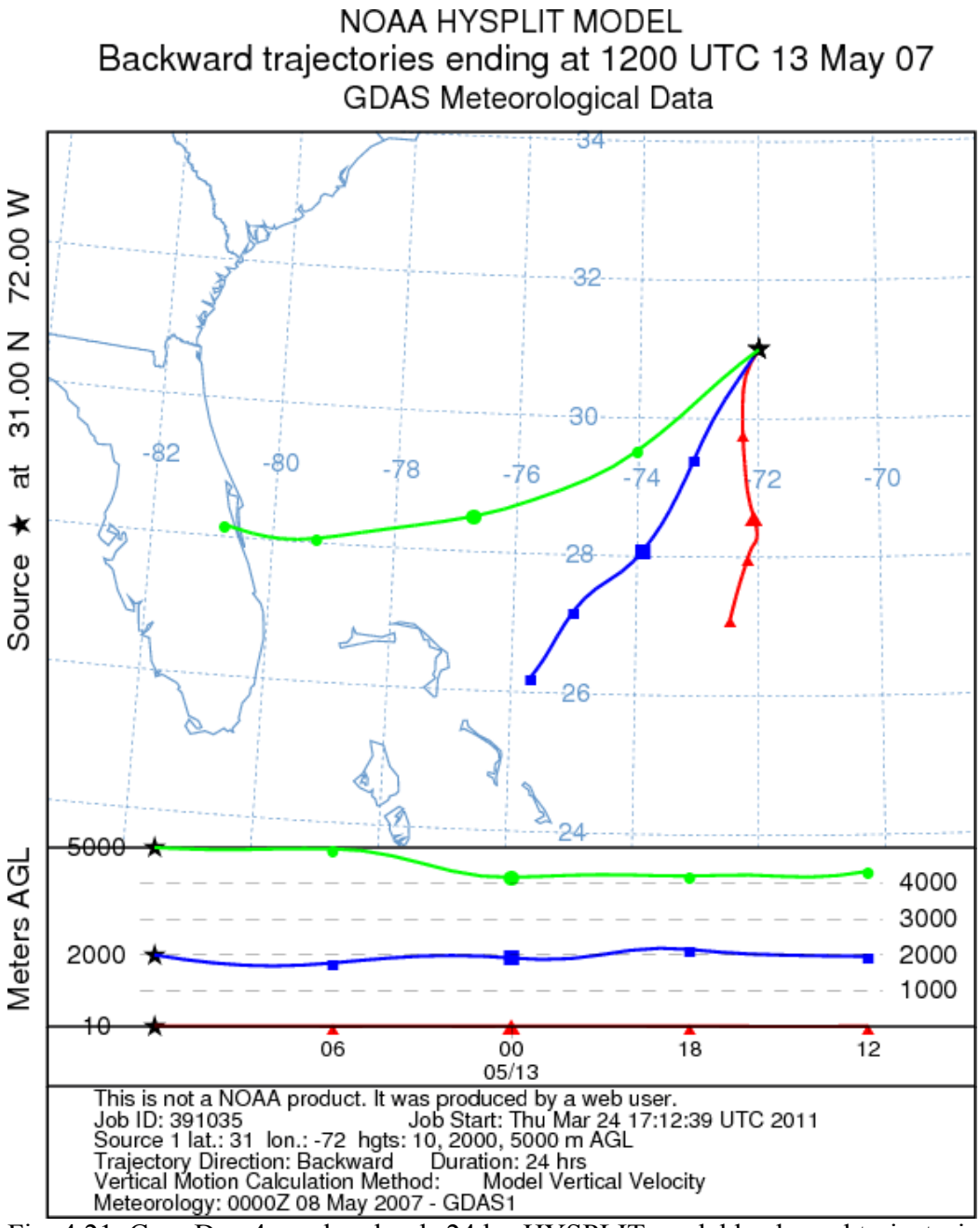

Fig. 4.21. Case Day 4 smoky clouds 24 hr. HYSPLIT model backward trajectories at 10 m, 2000 m, and 5000 m.

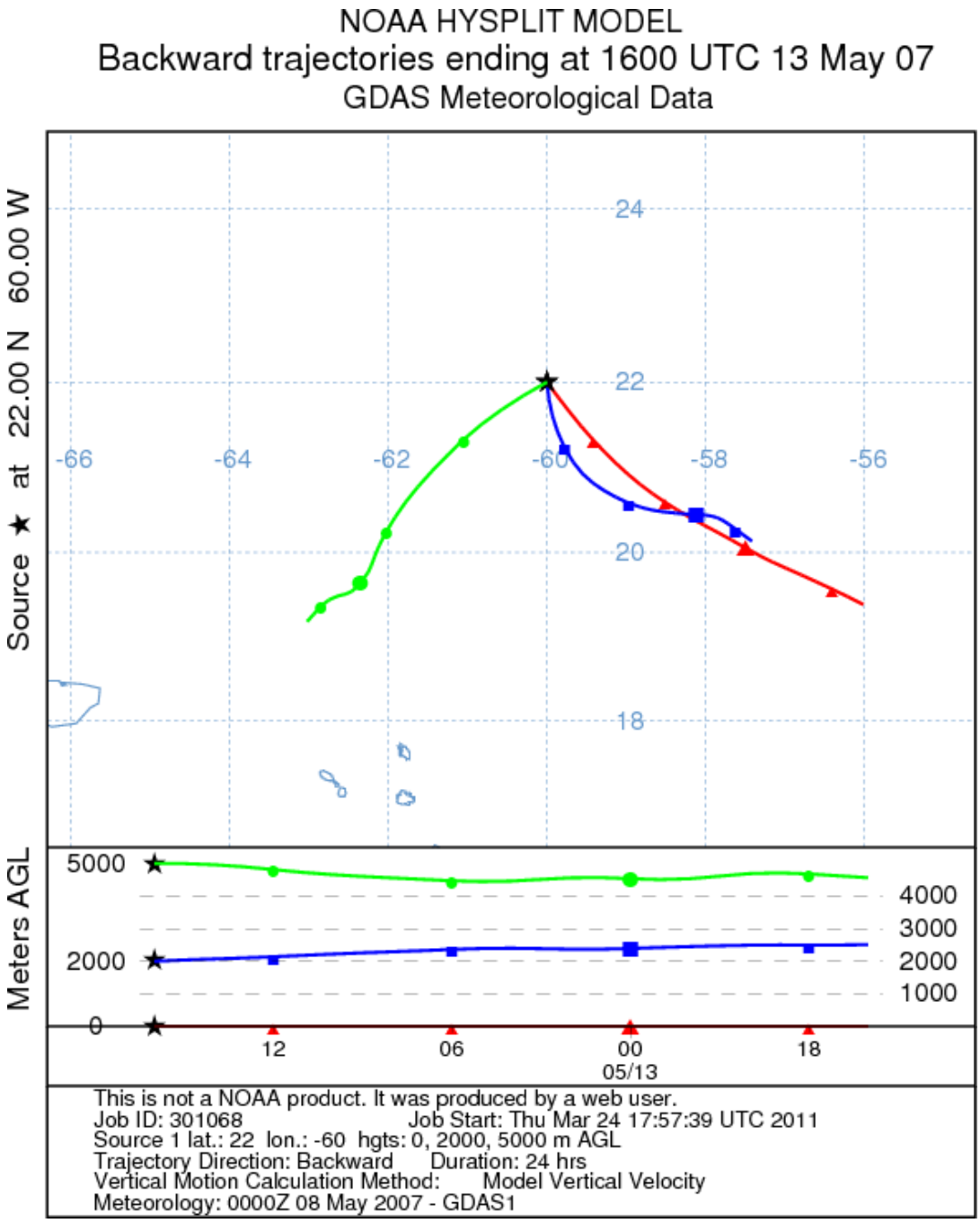

Fig. 4.22 . Case Day 4 non-smoky clouds 24 hr. HYSPLIT model forward trajectories at 10 m, 2000 m, and 5000 m.

(a)

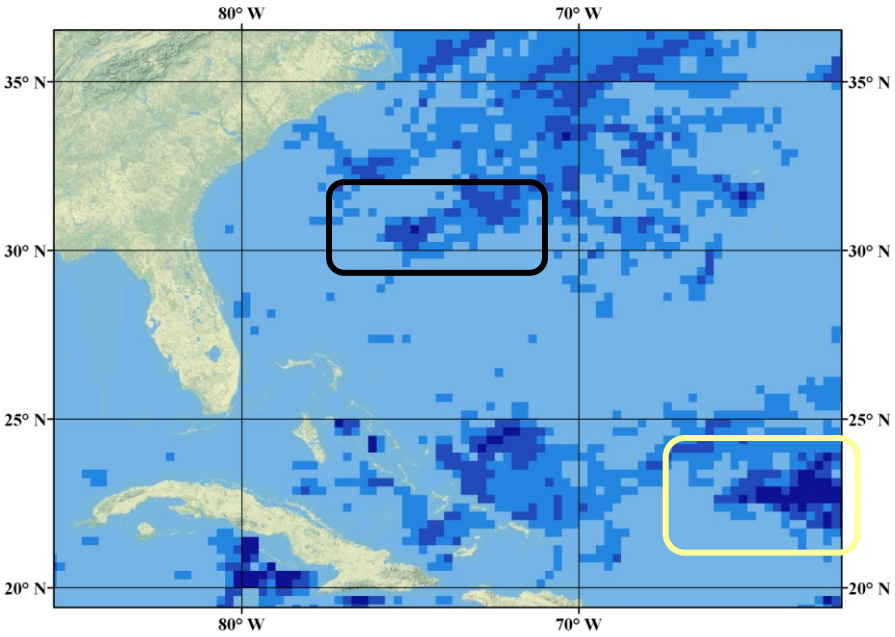

(b)

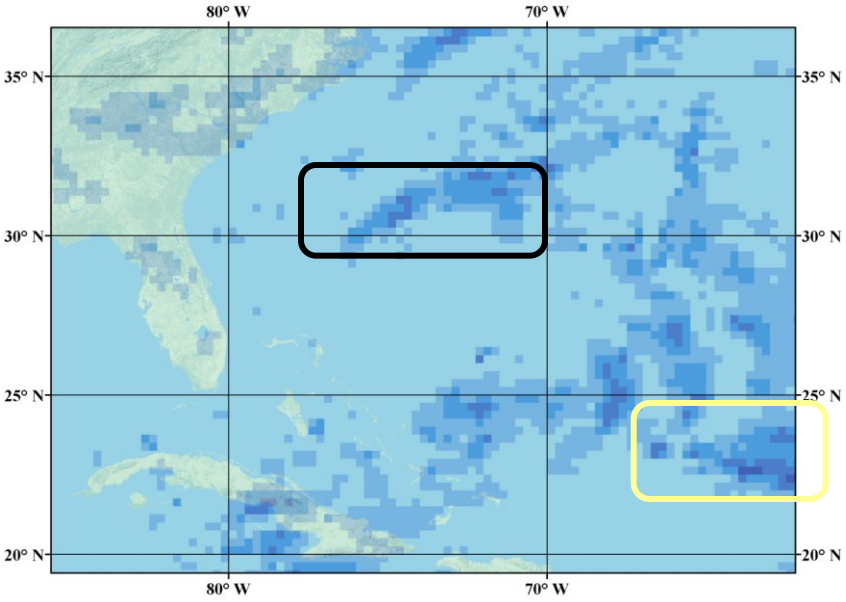

Fig. 4.23. Case Day 4 (a) AMSR CLW for smoky and non-smoky clouds and (b) TRMM TMI 3B42 values for smoky and non-smoky clouds with smoky clouds in darker outline.

(a) (b)

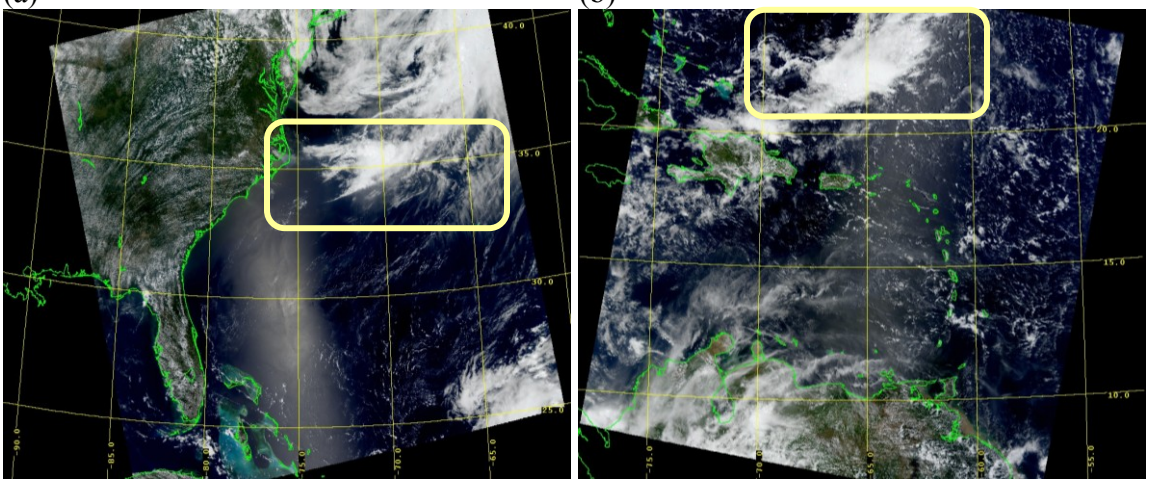

(c)

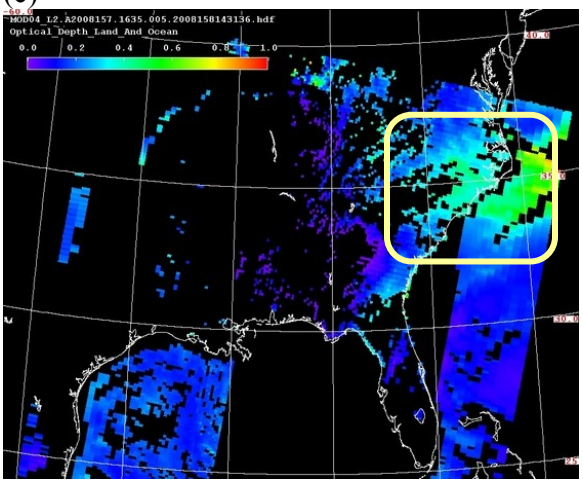

(d)

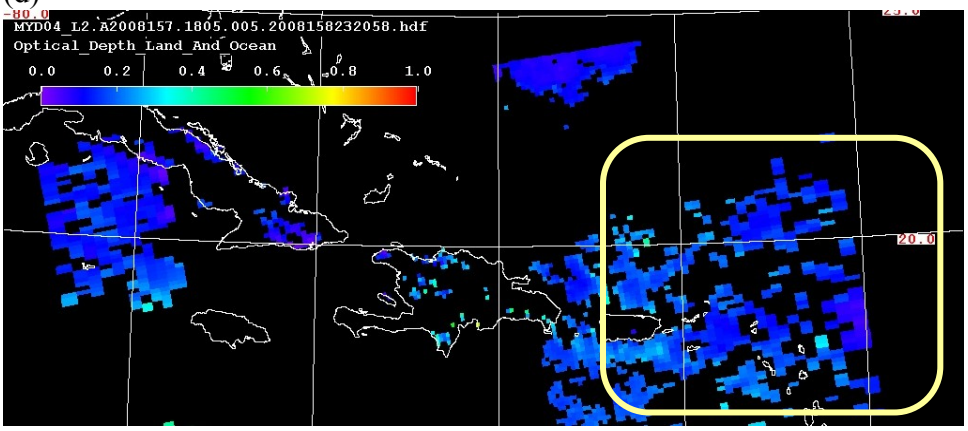

Fig. 4.24. Case Day 5 (a) MODIS visible imagery for smoky clouds and (b) non-smoky clouds and (c) MODIS AOT upwind from smoky clouds and (d) non-smoky clouds.

(a)

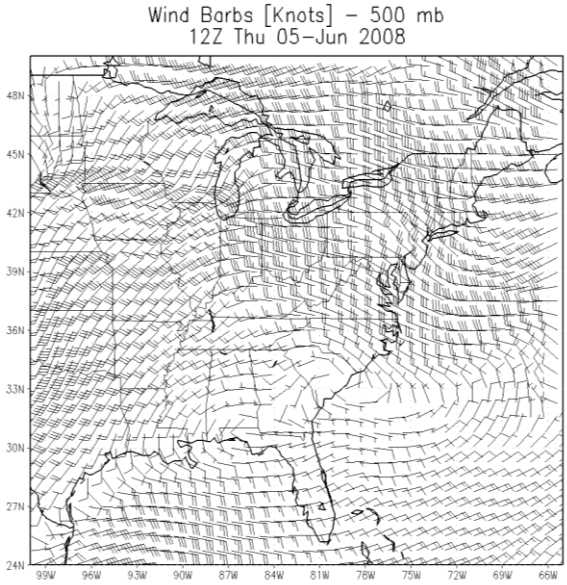

(b)

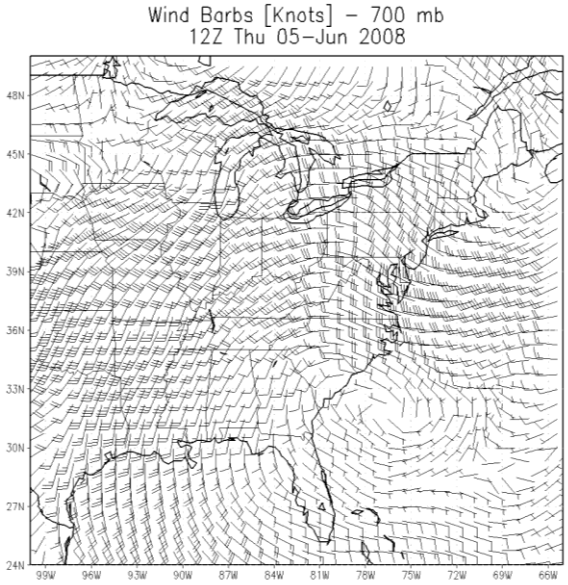

(c)

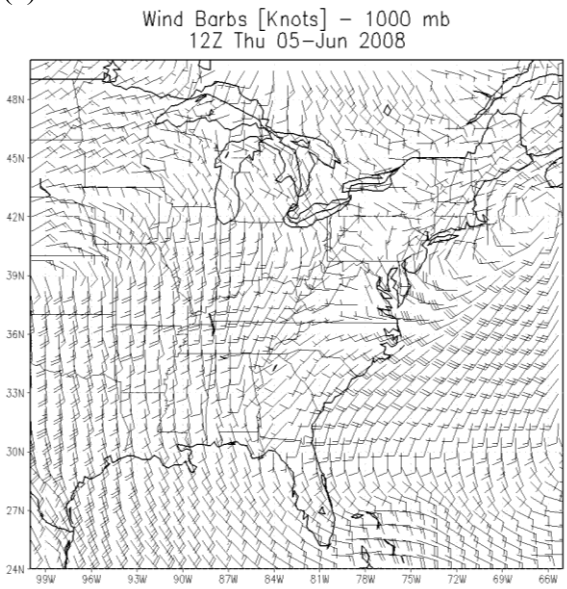

Fig. 4.25. Case Day 5 NARR wind barbs at (a) 500 hPa, (b) 700 hPa, (c) 1000 hPa.

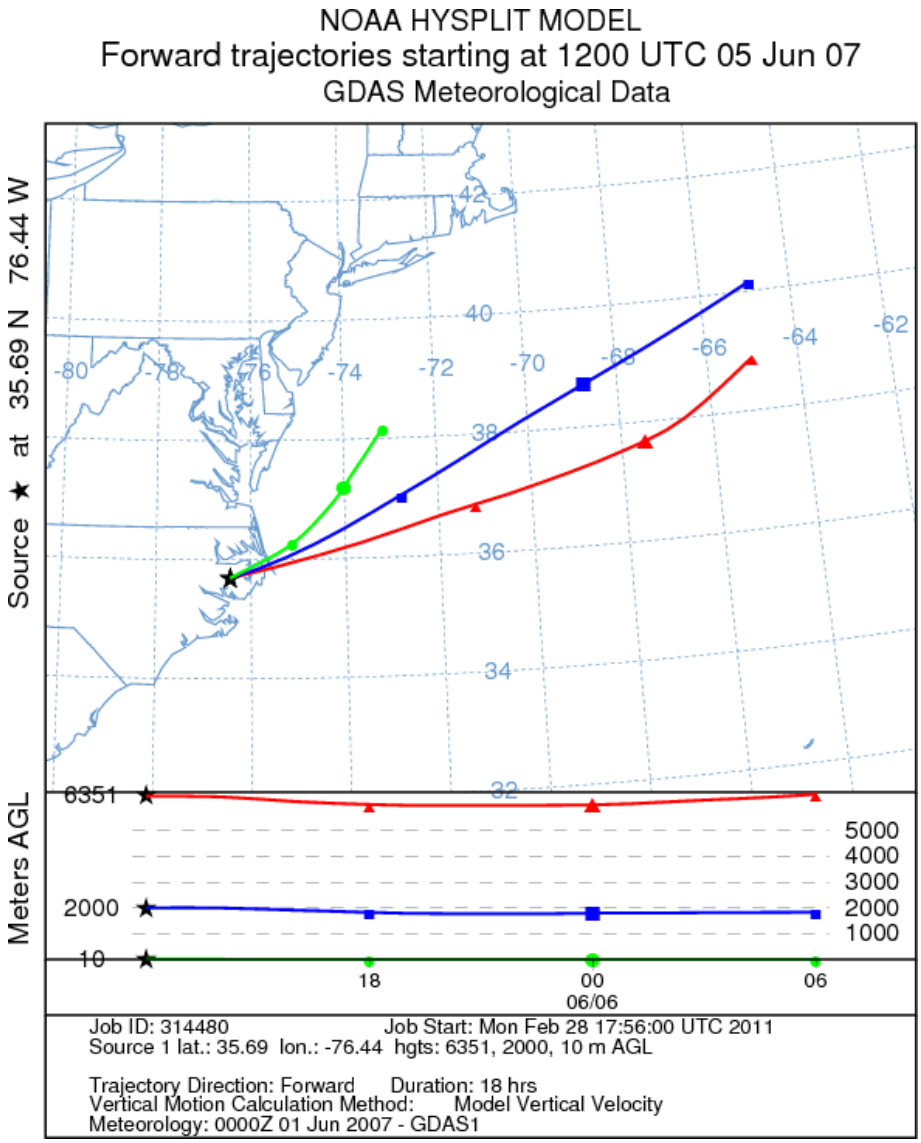

Fig. 4.26. Case Day 5 HYSPLIT model 18 hour forward trajectories from Hyde County, NC fire.

(a)

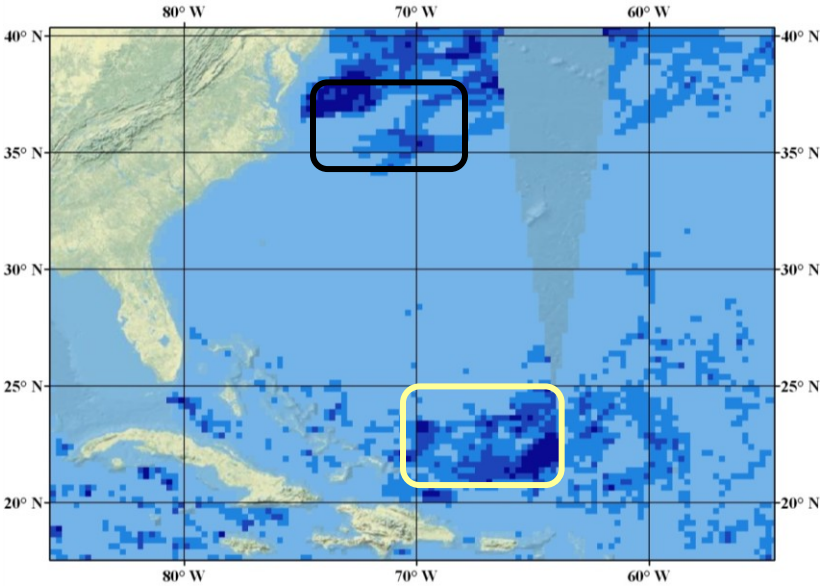

(b)

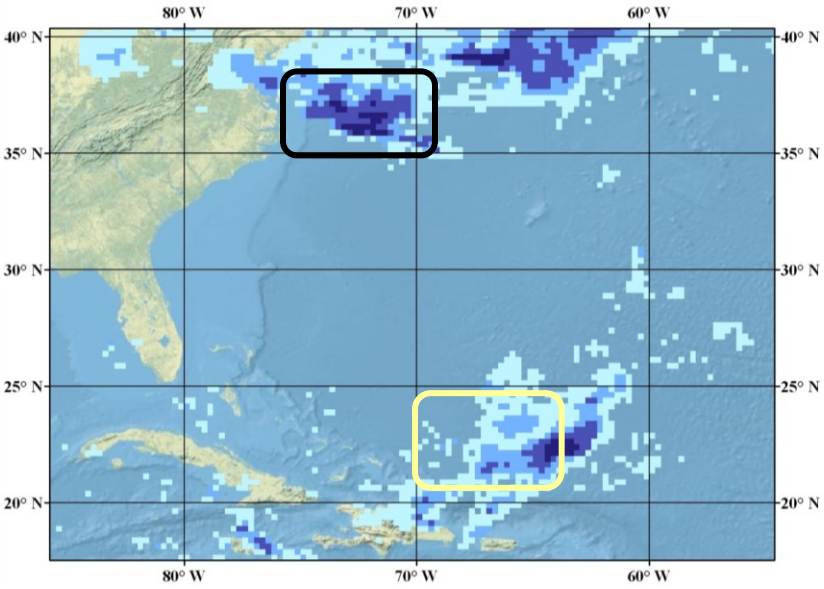

Fig. 4.27. Case Day 5 (a) AMSR CLW for smoky and non-smoky clouds and (b) TRMM TMI 3B42 values for smoky and non-smoky clouds with smoky clouds in darker outline.

(a) (b)

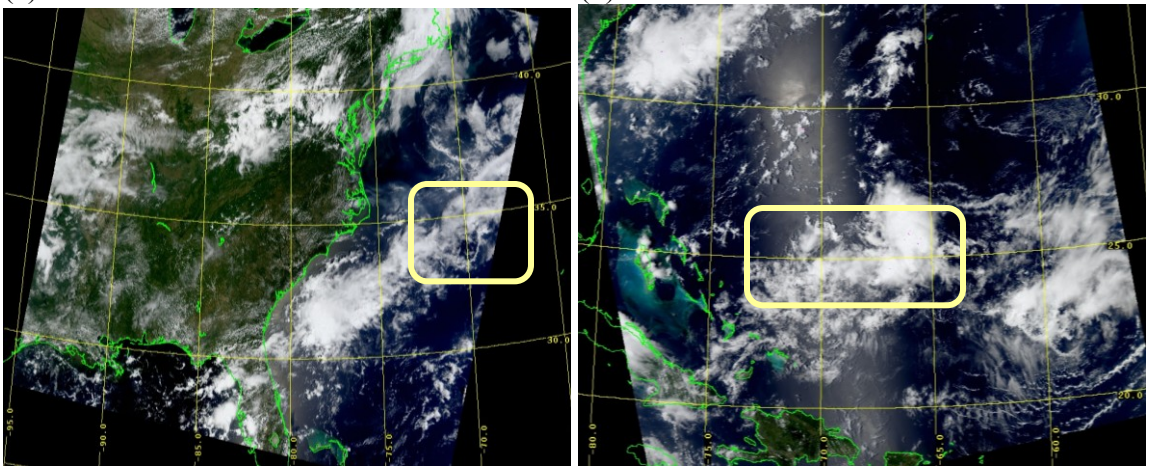

(c)

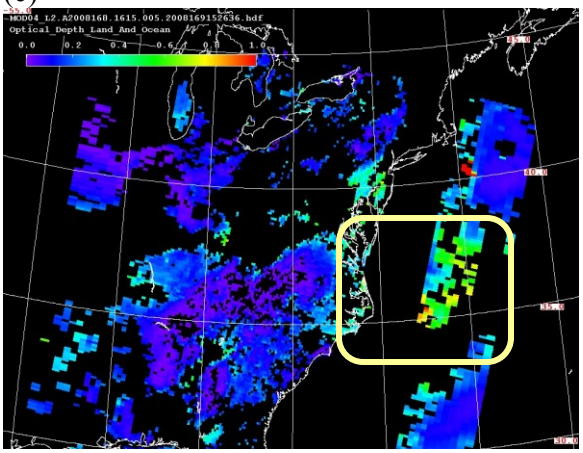

(d)

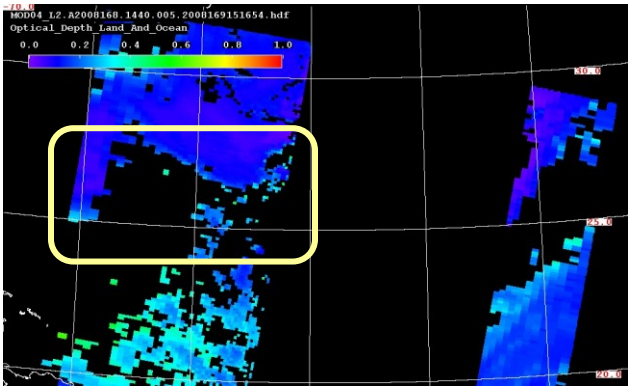

Fig. 4.28. Case Day 6 (a) MODIS Visible imagery for smoky and (b) non-smoky clouds and MODIS AOT upwind from (c) smoky clouds and (d) non-smoky clouds.

(a)

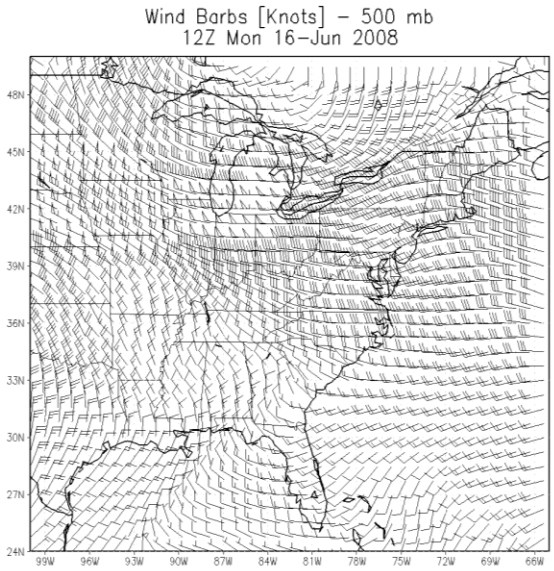

(b)

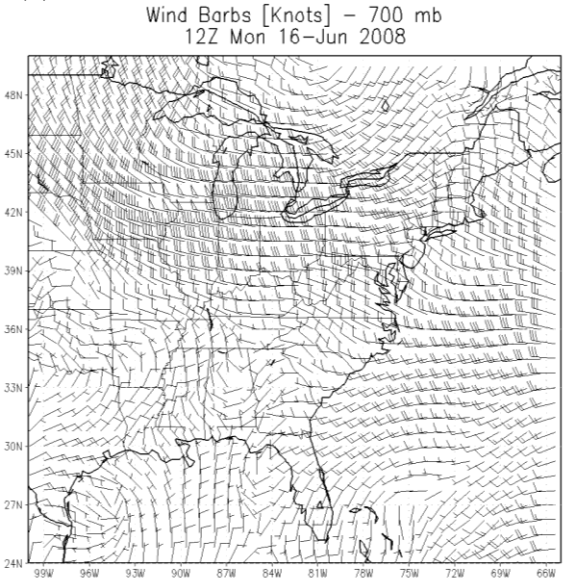

(c)

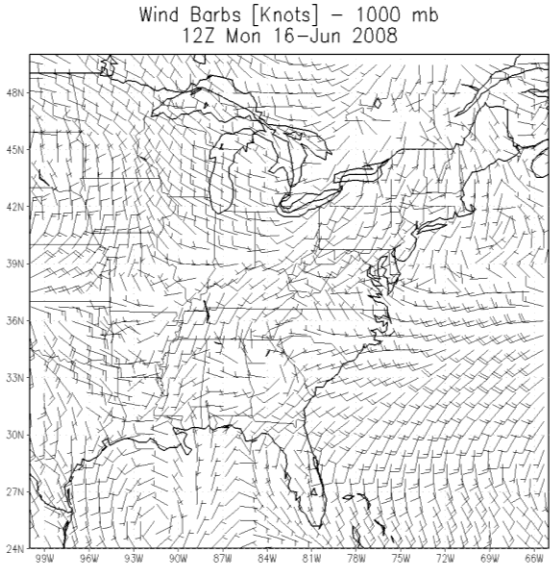

Fig. 4.29. Case Day 6 NARR wind barbs at (a) 500 hPa, (b)700 hPa, and (c) 1000 hPa.

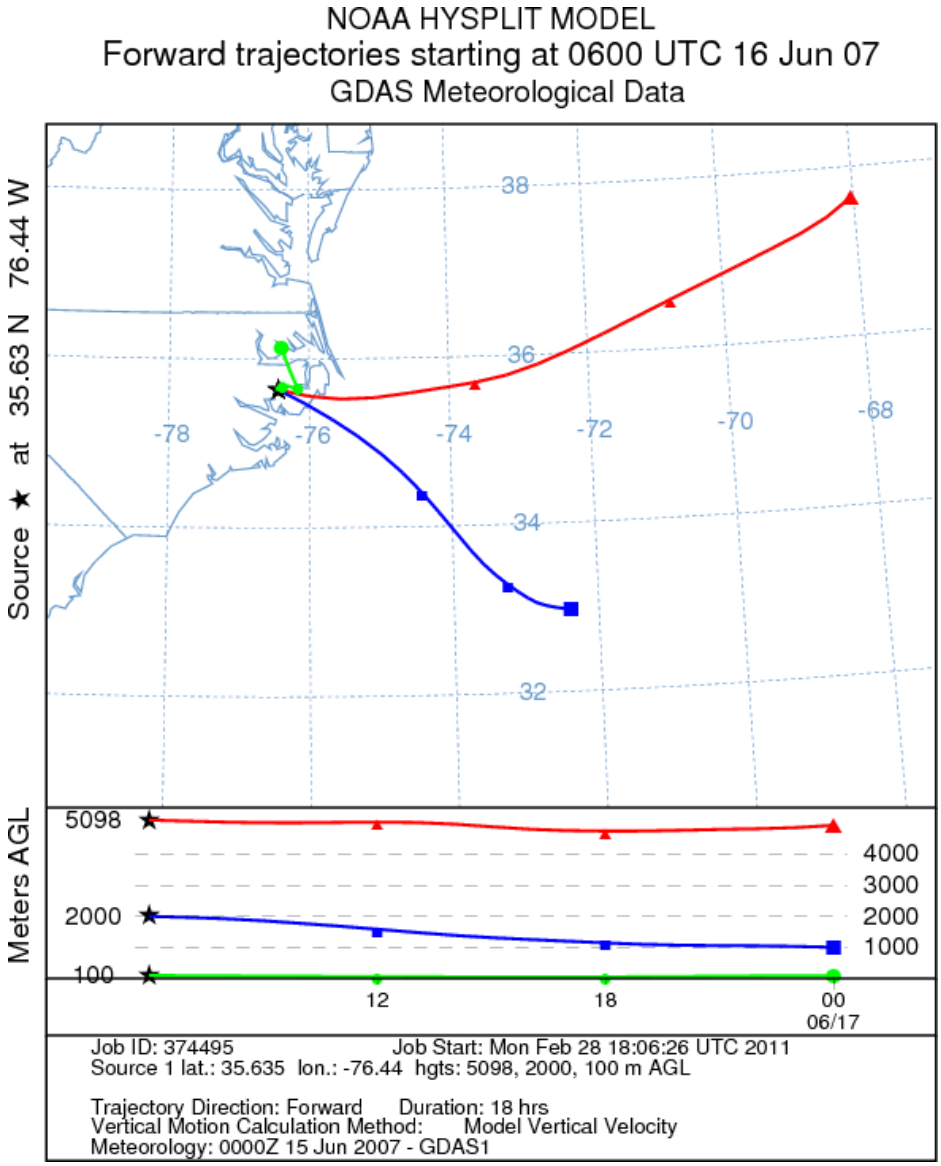

Fig. 4.30. Case Day 6 HYSPLIT model 18 hour forward trajectories from Hyde County, NC fire.

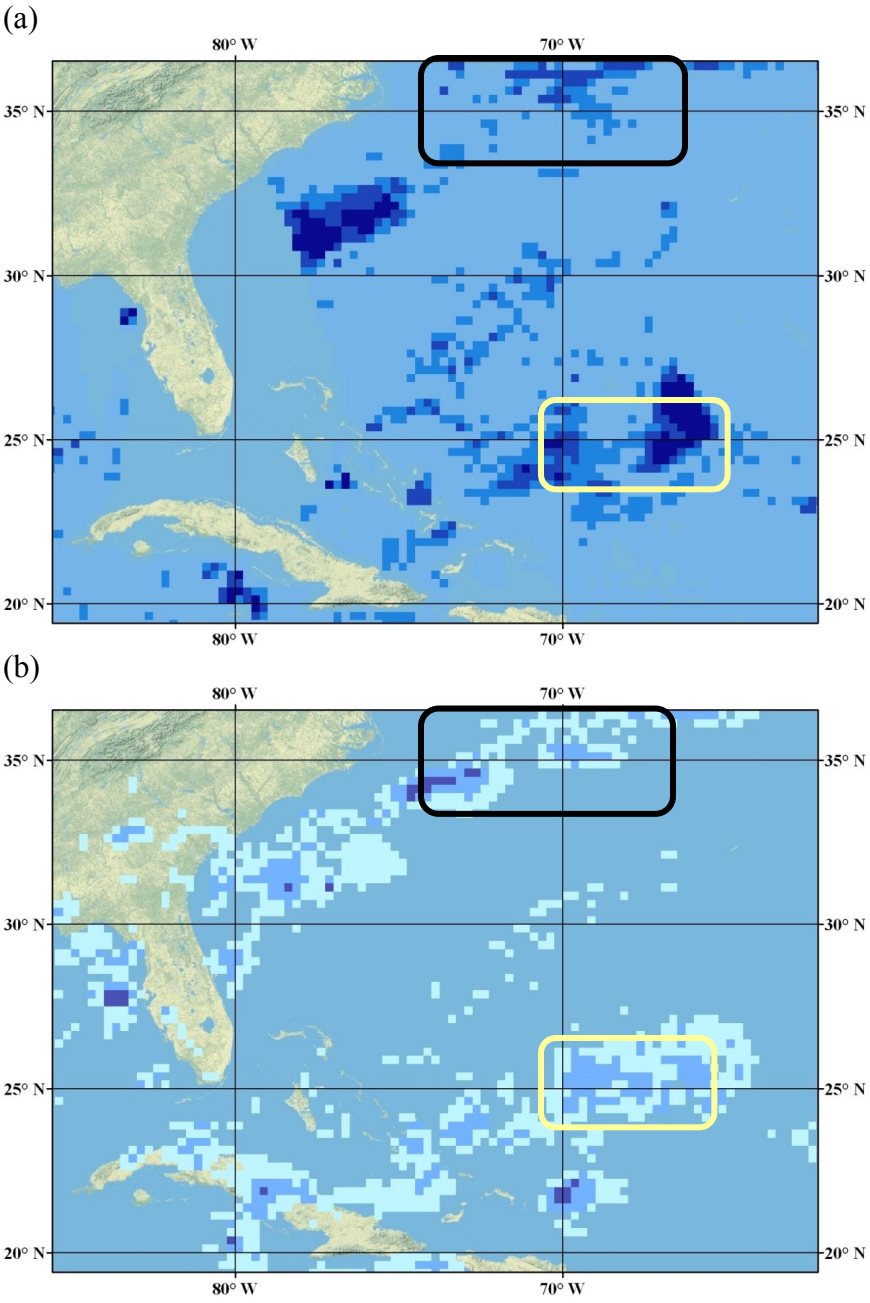

Fig. 4.31. Case Day 6 (a) AMSR CLW for smoky and non-smoky clouds and (b) TRMM TMI 3B42 values for smoky and non-smoky clouds.

CHAPTER 5

CONCLUSIONS AND FUTURE WORK

This study analyzed forest fire aerosol forcing of precipitation through a case day analysis. Six case days were analyzed giving a range in atmospheric and fire conditions. Four case days from 2007 and two cases from 2008 were analyzed. The 2007 cases analyzed fires in South Georgia and North Florida, four of which were associated with the historic Georgia Bay Complex fire. The 2008 cases analyzed fires from eastern North Carolina and eastern Virginia. Several satellite products were used including MODIS Aerosol and Cloud products, TRMM TMI PR_{rate}, and AMSR CLW. NARR winds and HYSPLIT model trajectories were used to estimate smoke plume transport.

Availability of data proved to be the most cumbersome obstacle in finding case days as only 3 years of SMARTFIRE and about 10 years of consistent satellite data were available. This study found that forest fire aerosols rarely interacted with precipitating clouds in the study area. This is partly due to the infrequency of large fires occurring in these states. Southeastern U.S. fires are highly dependent on inter-annual variability of precipitation. Wet years have very low numbers of class F and G fire days as evidenced by the 2009 fire statistics (Fig. 4.4). In drought years, there may be a substantial increase in the number of large fire days as seen in the 2007 fire statistics (Fig. 4.3).

This study initially set out to analyze shallow clouds as well as deep clouds. After analyzing nearly 100 fire days, six case days for this study were found. None of the case days

included shallow precipitating clouds. Other studies suggest that shallow clouds experience suppression of precipitation when aerosols are introduced (Rosenfeld 1999, Rosenfeld 2000, Andreae et al. 2004, Rosenfeld et al. 2006, Rosenfeld et al. 2008). The introduction of aerosols may explain why none of the smoky clouds studied here are shallow. The aerosols may have caused a substantial decrease in precipitation efficiency leading to no precipitation in the shallow clouds influenced by the forest fire aerosols.

Another important finding from this study was from the cloud effective radius analysis. In all six cases, the smoky clouds had lower effective radii when compared to the clean clouds for the same day. This is an expected outcome based on previous findings (Kaufman and Fraser 1997, Martin et al. 1994, Pawlowska and Brenguier 2000, Taylor and McHaffie 1994). As the forest fire aerosols enter a cloud, they introduce additional CN for which water binds to. The result of this is smaller droplets because the water available in the cloud is distributed over increased CCN. This finding also reaffirms the presence of increased aerosols in the smoky clouds. In a few of the cases the smoky clouds were able to have the same ability as their non-smoky proxies to precipitate the available CLW. Studying cloud effective radius alone does not explain aerosols impact on precipitation.

The primary objective of this study was to determine forest fire aerosol forcing of precipitation in the study area. The results of this study are somewhat inconclusive on the response to the introduction of large amounts of aerosols into deep, cold tropical and sub-tropical clouds. In three Case Days, 5, and 6) low amounts of forest fire aerosols (median AOT ~0.80-0.90) interacted with the smoky clouds. In these cases, aerosols showed little impact on the ability for the smoky clouds to precipitate based on the CREP ratios. These three cases had an average CREP median ratio of 1.05. In the three other Case Days (2, 3, and 4) large amounts of

wildfire aerosols (median AOT ~ 1.9-3.3) interacted with the smoky clouds. These three cases suggest the ability to affect the smoky clouds ability to precipitate the available cloud liquid water when significant amounts of forest fire aerosols are present.

Smoke plume dispersion plays a role in the magnitude of the median AOT values. In the three high smoky cases, the smoke plumes were well intact and showed little dispersion. The two three smoke cases also had large amounts of acreage burning (>100 km^2). In the three less smoky cases, there was evidence the smoke had been dispersed likely due to changing wind directions the day leading up to the case day and the day of the case day. In these cases, less acreage was being burned as well.

Evidence from these six case days suggests there are three conditions that must be present in order for forest fire aerosols to have an impact of precipitation in deep clouds. Smoke plumes from the fires must have low dispersion, and the point source fires much be burning a large amount of acreage. This leads to high AOT values upwind from the clouds. In the cases presented here, the relationship suggests median AOT values must be 1.50 or greater to have a significant impact on the clouds ability to precipitate the available CLW. Whether a negative or positive relationship exists between AOT and precipitation is inconclusive based on the precipitation proxy used here.

While deep, marine clouds have been largely unstudied, previous research suggested the results of this study would indicate a negative forcing (Rosenfeld 1999). This study examined deep, marine clouds, while an earlier study examined forest fire aerosols on deep clouds off the Australian coast and its affect on precipitating clouds (Rosenfeld 1999). That study consisted of one case and indicated wildfire smoke interacted with clouds and suppressed precipitation while non-smoky clouds nearby precipitated efficiently. Smoky clouds had to reach a height of -10°C

before they began precipitating (Rosenfeld 1999). The results of this study suggest that very cold top clouds (~40°C) do not display a clear relationship between aerosols and the precipitation efficiency proxy. In the three smokiest cases, two of the smoky clouds precipitated less of the available CLW compared to their non-smoky case days. In the other case high smoke day, the smoky clouds precipitated more of the available CLW than the non-smoky clouds. This apparent discrepancy required additional parameters to be examined.

The results from this thesis finds some consilience in prior research on deep, convective clouds that indicate that the introduction of aerosols into terrestrial convective clouds causes an increase in precipitation amount (Andreae et al. 2004, Grell et al. 2010, Ntelekos et al. 2009). This thesis also suggests that a decrease in precipitation may occur when extremely cold top clouds elevate a significant amount of the CCN above the level of homogeneous nucleation through intense updraft. This is suggested by Case Days from 9 May 2007 and to a greater extent, 12 May 2007. The only evidence to substantiate this hypothesis is the extremely high ice to liquid ratios in these two cases as well as the substantial decrease in CREP. This hypothesis needs further evidence to substantiate it. This outcome has been produced by model studies but it has been difficult to find this phenomenon in observations (Rosenfeld and Woodley 2000, Cui et al. 2006, Khain et al. 2001).

The findings from this thesis suggest the possibility that deep clouds have different responses to aerosols as the cloud evolves over time. This is an important finding for future research. One snap shot of a cloud in time may not capture the true response of the cloud over its life span. An initial suppression of precipitation early in its lifespan appears to give way to increased precipitation but can lead to a subsequent suppression of precipitation if intense updrafts elevate too much of the CCN above the homogenous nucleation level. This finding also

has important ramifications for regional and global climate models. Parameterization of aerosols and their effect of precipitation in these models may not capture the true forcing of the aerosols.

The methodology used in this study raised questions regarding the methodology used in previous studies. This study demonstrated the wide spectrum of aerosol forcing possible within deep clouds. Observational and remote sensing studies in the future must analyze several events or cases to begin to reach meaningful conclusions. Analyzing any one of these case days independently would be inappropriate and any conclusions drawn should not be done so based entirely on the findings from that one case day. These studies still have their importance, as they are able to confirm or reject findings from modeling studies and other similar observational studies. Model simulations should not be considered independently, but should be confirmed using observational studies that replicate the model simulation.

There are undoubtedly shortcomings of this study including the use of a precipitation efficiency proxy instead of a more accurate measurement of precipitation efficiency. When conducting research using case days, conclusions must be made with some caution because the sample size is often low. The six cases days found in these three years do not represent the full range of aerosol and weather scenarios. In some of the cases, the non-smoky clouds are a significant distance from the smoky clouds. This is an unavoidable consequence as the smoke was widespread and the closest non-smoky clouds were quite some distance. This was necessary to avoid smoke intrusion in the non-smoky clouds. Future research would focus on finding additional cases in the Southeast going back to 2002, when some of the remotely sensed products used here were first available.

Other future research related to this study would include analyzing lightning data to determine if this could support any of the theories on the ice/liquid ratio discrepancies presented

here. Recent research suggests that forest fire aerosols have the ability to alter stability profiles (Menon et al. 2002). Research into the stability in the case days above could help substantiate some of the findings here. These case days could be analyzed under the theoretical framework of a dynamic mesoscale weather model and a biomass burning emissions model to see if the results seen here are replicated by the model. May 2007 was a historically smoky period for the study region. A future objective of this study is to compare a monthly CREP value between May 2007 and a collection of other lower aerosol months. This would help eliminate the problems with analyzing individual events and would provide important insight to how large, long-live forest fires may effect precipitation over a monthly time period.

Future technological advances may be able to improve this study by providing more detailed smoke plume information as the plume travels through time. Higher resolution data will likely become available in the future which would provide more accurate and precise cloud and precipitation data. The advancement of LIDAR technology to more affordable means will help make in-cloud aerosol measurements more accessible. The ability to detect aerosol loads from within these precipitating clouds would be the single more important advancement for more accuracy in the findings of this study.

This study was novel in its attempt to examine forest fire aerosols over a relatively large spatial extent. This study also examined an area largely unstudied in terms of aerosol impacts on precipitation. Deep clouds over oceanic regions are sparse in the academic record as well. This area of research is important because of the role aerosols play both in mesoscale dynamics and global circulation. Clouds influenced by forest fire aerosols off the southeastern U.S. Atlantic Coast were found in this study to have the following:

- Significant AOT (>1.50) must be present to have an impact on precipitation in deep clouds.
- Smoky plumes must have low dispersion to produce significant AOT (>1.50)
- Shallow, precipitating clouds influenced by the forest fire aerosols could not be found over the three-year period. This is either due to coincidence or the fact that precipitation is largely suppressed in this cloud regime.
- Forest fire aerosols cause a decrease in the cloud effective radius in the smoky clouds.
- Cloud lifecycle may play an important role on the response of precipitation to aerosols. This can have important ramifications in cloud and weather models due to parameterization schemes for aerosols and precipitation.

This thesis finds convincing more evidence with regard to aerosol effects on cloud properties (effective radius, ice/liquid phase) than with regard to precipitation (CREP). These findings are similar to Jin and Shepherd (2008). It is recommended that future studies include multiple cases due to the variability identified in the six case days in this thesis. Furthermore, future studies ideally would analyze clouds through their life cycle to better understand how aerosols affect each stage of the cloud life cycle.

REFERENCES

Albrecht, B.A., 1989: Aerosols, cloud microphysics, and fractional cloudiness. *Science*, **245**, 1227-1230.

Andreae, M.O., E.V. Browell, M. Garstang, G.L. Gregory, R.C. Hariss, G.F. Hill, D.J.Jacob, M.C. Pereira, G.W. Sachse, A. W. Setzer, P.L. Silva Dias, R.W. Talbot, A.L. Torres, and S.C. Wofsy, 1988: Biomass-burning and associated haze layers over Amazonia. *J. Geophys. Res.*, **93**, 1509-1527.

Andreae, M.O., E. Atlas, H. Cachier, W.R. Cofer, III, G.W. Harris, G. Helas, R. Koppmann, J.P. Lacaux, and D.E. Ward, 1996: Trace gas and aerosol emission from savanna fires. *Biomass Burning and Global Change*, edited by J.S. Levine, pp. 278-295, MIT Press, Cambridge, MA.

Andreae, M.O., and P. Merlet, 2001: Emission of trace gases and aerosols from biomass burning. *Global Biogeochemical Cycles*, **15**, 955-966.

Andreae, M.O., D. Rosenfeld, P. Artaxo, A.A. Costa, G.P. Frank, K.M. Longo, and M.A.F. Silva-Dias, 2004: Smoking rain clouds over the Amazon. *Science*, **303**, 1337-1342.

Berg, W., T. L'Ecuyer, and C. Kummerow, 2006: Rainfall climate regimes: The relationship of regional TRMM rainfall biases to the environment. *J. Appl. Meteor Climatol*, **45**, 434-445.

Bevan, S.L., P.R.J. North, W.M.F. Grey, S.O. Loa, S.E. Plummer, 2009: Impact of atmospheric aerosol from biomass burning on Amazon dry-season drought. *J. Geophys. Res.*, **114**, D09204.

Crutzen, P.J., A. C. Delany, J. Greenburg, P. Haagensen, L. Heidt, R. Lueb, W. Pollock, W. Seilor, A. Wartburg, and P. Zimmerman, 1985: Tropospheric chemical composition measurements in Brazil during the dry season. *J. Atmos. Chem.*, **2**, 233-256.

Crutzen, P.J. and M.O. Andreae, 1990: Biomass Burning in the Tropics: Impact on Atmospheric Chemistry and Biogeochemical Cycles. *Science*, **250**, 1669–1678.

Cui, Z., K.S. Carslaw, Y. Yin, and S. Davies, 2006: A numerical study of aerosol effects on the dynamics and microphysics of a deep convective cloud in a continental environment. *J. Geophys. Res.*., **28**, D05201.

Draxler, R.R. and Rolph, G.D., 2003. HYSPLIT (HYbrid Single-Particle Lagrangian Integrated Trajectory) Model access via NOAA ARL READY Website (http://www.arl.noaa.gov/ready/hysplit4.html). NOAA Air Resources Laboratory, Silver Spring, MD.

Eagen, R.C., P.V. Hobbs, and L.F. Radke, 1974: Measurements of cloud condensation nuclei and cloud droplet size distributions in the vicinity of forest fires. *J. Appl. Meteor.*, **13**, 553-557.

Georgia Forestry Commission (GFC), 2007: Georgia Wildfires of 2007 Summary of Facts and Costs of Recovery, (http://www.gfc.state.ga.us/GFCNews/documents/GFC2007FireFacts.pdf).

Graber, E.R. and Y. Rudich, 2006: Atmospheric HULIS: How Humic-Like Are They? A Comprehensive and Critical Review. *Atmos. Chem. Phys.*, **6**, 729-753.

Grassi, H., 1975: Albedo reduction and radioactive heating of clouds by absorbing aerosol particles. *Beitr. Z. Phys. Atmos.*, **48**, 199-210.

Grell, G., S.R. Freitas, M. Stuefer, and J. Fast, 2010: Inclusion of biomass burning in WRF-Chem: impact of wildfire on weather forecasts. *Atmos. Chem. Phys. Discuss.*, **10**, 30613-30650.

Haywood, J., and O. Boucher, 2000: Estimates of the direct and indirect radiative forcing due to tropospheric aerosols: A Review. *Rev. Geophys.*, **38**, 513-543.

Johnson, D.B., 1982: The role of giant and ultragiant aerosol particles in warm rain initiation. *J. Atmos. Sci.*, **57**, 1497-1514.

Jin, M., and J.M. Shepherd, 2008: Aerosol relationships to warm season clouds and rainfall at monthly scales over east China: Urban land versus ocean. *J. Geophys. Res.*, **113**, D24S90.

Kaufman, Y.J., A. Setzer, D. Ward, D. Tanré, B.N. Holben, P. Menzel, M.C. Pereiera, and R. Rasmussen, 1992: Biomass Burning Airborne and Spaceborne Experiment in the Amazonas (Base-A). *J. Geophys. Res.*, **97**, 14581-14599.

Kaufman, Y.J., 1993: Aerosol optical thickness and atmospheric path radiance. *J. Geophys. Res.*, **98**, 2677-2692.

Kaufman, Y. J. and R.S. Fraser, 1997: The effect of smoke particles on clouds and climate forcing. *Science*, **277**, 1636–1639.

Kaufman, Y.J., D. Tanré, L. Remer, E. Vermote, A. Chu, and B. Holben, 1997: Operational remote sensing of tropospheric aerosol over land from EOS moderate resolution imaging spectroradiometer. *J. Geophys. Res.,* **102**, 17,051-17,067.

Kaufman, Y.J., D. Tanré, and O. Boucher, 2002: A satellite view of aerosols in the climate system. Review. *Nature*, **419**, 215-223.

Kaufman, Y.J., I. Koren, L.A. Remer, D. Rosenfeld, and Y. Rudich, 2005: The effect of smoke, dust, and pollution aerosol on shallow cloud development over the Atlantic Ocean. *Proc. Natl. Acad. Sci.*, **102**, 11207-11212.

Kaufman, Y.J., and I. Koren, 2006: Smoke and pollution aerosol effect on cloud cover. *Science*, **313**, 655-658.

Khain A.P., D. Rosenfeld, and A. Pokrovsky, 2001: Simulation of deep convective clouds with sustained supercooled liquied water down to -37.5 C using a spectral microphysics model. *Geophys. Res. Lett.*, **28**, 3887-3890.

Khain, A. P., N. BenMoshe, A. Pokrovsky, 2008: Factors determining the impact of aerosols on surface precipitation from clouds: An attempt at classification. *J. Atmos. Sci.*, **65**, 1721–1748.

Kiehl, J.T. and K.E. Trenberth, 1997: Earth's annual global mean energy budget. *Bull. Am. Meteorol. Soc.*, **78**, 197-208.

King, M.D., W.P. Menzel, Y.J. Kaufman, D. Tanré, B. Gao, S. Platnick, S.A. Ackerman, L.A. Remer, R. Pincus, and P.A. Hubanks, 2003: Cloud and Aerosol Properties, Precipitable Water, and Profiles of Temperature and Water Vapor from MODIS. *IEEE Trans Geosci. Remote Sens.,* **41**, 442-458.

Koren, I., Y.J. Kaufman, L.A. Remer, and J.V. Martins, 2004: Measurements of the effect of Amazon smoke on inhibition of cloud formation. *Science*, **303**, 1342-1345.

Koren, I., Y.J. Kaufman, D. Rosenfeld, L.A. Remer, Y. Rudich, 2005: Aerosol invigoration and restructuring of Atlantic convective clouds. *Geophys. Res. Lett.*, **32**, 2886-2897.

Larkin, N.K., S.M. O'Neill, R. Soloman, S. Raffuse, T. Strand, D.C. Sullivan, C. Krull, M. Rorig, J. Peterson, and S.A. Ferguson, The BlueSky smoke modeling framework, 2009: *Intl. J. Wildland Fire*, **18**, 906-920.

Levin, Z., and W. Cotton (Eds.), 2009: *Aerosol Pollution Impact on Precipitation: A Scientific Review*, Springer, New York, NY, pp. 407.

Lin, J.C., T. Matsui, R.A. Pielke Sr. and C. Kummerow, 2006: Effects of biomass-burning-derived aerosols on precipitation and clouds in the Amazon Basin: A satellite-based empirical study. *J. Geophys. Res.,* **111**, D19204.

Lohmann, U. and J. Feichter, 2005: Global indirect aerosol effects: a review. *Atmos. Chem. Phys.*, **5**, 715-737.

Martin G.M., W. Johnson, and A. Spice, 1994: Parameterization of Bulk Condensation in Numerical Cloud Models. *J. Atmos. Sci.,* **51**, 1728-1739.

Menon, S., J. Hansen, L. Nazarenko, and Y. Luo, 2002: Climate Effects of Black Carbon Aerosols in China and India. *Science,* **297**, 2250-2253.

Mesinger, F., G. DiMego, E. Kalnay, K. Mitchell, P.C. Shafran, W. Ebisuzaki, D. Jovic, J. Woollen, E. Rogers, E.H. Berbery, M.B. Ek, Y. Fan, R. Grumbine, W. Higgins, H. Li, Y. Lin, G. Manikin, D. Parrish, and W. Shi, 2006: North American Regional Reanalysis. *Bull. Amer. Meteor. Soc.*, **87**, 343-360.

Newton, C. W., 1966: Circulations in large sheared cumulonimbus. *Tellus,* **18**, 699-711.

Ntelekos, A.A., J.A. Smith, L. Donner, J.D. Fast, W. J. Gustafson Jr., E.G. Chapman, and W.F. Krajewski, 2009: The effects of aerosols on intense convective precipitation in the northeastern United States. *Quart. J. Roy. Meteor. Soc.*, **135**, 1367-1391.

NWS National Hurricane Center (NHC), 2011, NHC Archive of Hurricane Seasons, [Available online at http://www.nhc.noaa.gov/pastall.shtml.]

Pawlowska, H., and J.L. Brenguier, 2000: Microphysical properties of stratocumulus clouds during ACE-2. *Tellus*, **52**, 868–887.

Penner, J.E.(Coordinating lead author), 2001: *Climate Change 2001: The Scientific Basis [Working Group 1 to the Third Assessment of Report of the Intergovernmental Panel on Climate Change (IPCC),* Cambridge Univ. Press, 289-348.

Phillips, V.T.J., A. Pokrovsky, and A. Khain, 2007: The Influence of Time-Dependent Melting on the Dynamics and Precipitation Production in Maritime and Continental Storm Clouds, *J. Atmos. Sci.*, **64**, 338-359.

Radke, L.F. and P.V. Hobbs, 1969: An automatic cloud condensation nuclei counter. *J. Appl. Meteor.*, **8**, 105-109.

Radke, L.F. and P.V. Hobbs, 1976: Cloud condensation nuclei on the Atlantic seaboard of the United States. *Science*, **193**, 999-1002.

Ramanathan, V., P. Crutzen, J.Kiehl, and D. Rosenfeld, 2001a: Aerosols, climate and the hydrological cycle. *Science*, **294**, 2119-2124.

Ramanathan, V., and 39 other authors, 2001b: Indian Ocean Experiment: An integrated analysis of the climate forcing and effects of the great Indo-Asian haze. *J. Geophys. Res.*, **106**, 28371-28398.

Ramanathan, V., C. Chung, D. Kim, T. Bettge, L. Buja, J.T. Kiehl, W.M. Washington, Q. Fu, D.R. Sikka, and M. Wild, 2005: Atmospheric Brown Clouds: Impacts on South Asian climate and hydrological cycle. *Proc. Natl. Acad. Sci. U.S.,* **102**, 5326-5333.

Reid, J.S. and P.V. Hobbs, 1998: Physical and optical properties of young smoke from individual biomass fires in Brazil. *J. Geophys. Res.*, **103**, 32,013-32,030.

Reid, J.S., R. Koppmann, T.F. Eck, and D.P. Eleuterio, 2005: A review of biomass burning emission. Part II: Intensive physical properties of biomass burning particles. *J. Atmos. Chem. Phys.*, **5**, 799-825.

Roberts, G.C., M.O. Andreae, J. Zhou, and P. Artaxo, 2001: Cloud Condensation nuclei in the Amazon Basin: "Marine" conditions over a continent? *Geophys. Res. Lett.*, **28**, 2807-2810.

Roberts, G.C., P. Artaxo, J. Zhou, E. Swietlicki, and M.O. Andreae, 2002: Sensitivity of CCN spectra on chemical and physical properties of aerosol: A case day from the Amazon Basin. *J. Geophys. Res*., **107**, 8070.

Rodgers, E., T. Black, B. Ferrier, Y. Lin, D. Parrish, and G. DiMego, 2001: Changes to the NCEP Meso Eta Analysis and Forecast System: Increase in resolution, new cloud microphysics, modified precipitation assimilation, modified 3DVAR analysis. NWS Technical Bulletin 488, NOAA/NWS.

Rosenfeld, D., 1999: TRMM observed first direct evidence of smoke from forest fires inhibiting rainfall. *Geophys. Res. Lett.*, **26**, 3105-3108.

Rosenfeld, D., 2000: Suppression of rain and snow by urban and industrial air pollution. *Science*, **287**, 1793-1796.

Rosenfeld, D., and G. Gutman, 1994: Retrieving microphysical properties near the tops of potential rain clouds by multispectral analysis of AVHRR data. *Atmos. Res.*, **34**, 259-283.

Rosenfeld, D. and W.L. Woodley, 2000: Convective clouds with sustained highly supercooled liquid water down to -37.5°C. *Nature*, **405**, 440-442.

Rosenfeld, D., I.M. Lensky, J. Peterson, and A. Gingis, 2006: Potential impacts of air pollution aerosols on precipitation in Australia. *Clear Air and Environ. Quality*, 40:43-49

Rosenfeld, D., U. Lohmann, G.B. Raga, C.D. O'Dowd, M. Kulmala, S. Fuzzi, A. Reissell, and M.O. Andreae, 2008: Flood or drought: How do aerosols affect precipitation? *Science*, **321**, 1309-1313.

Satheesh, S.K. and V. Ramanathan, 2000: Large differences in tropical aerosol forcing at the top of atmosphere and Earth's surface. *Nature*, **405**, 60-63.

Shepherd, J.M., 2005: A review of current investigations of urban-induced rainfall and recommendations for the future. *Earth Interact.*, **9**, 1-27.

Sinha, P., P.V. Hobbs, R. J. Yokelson, D. R. Black, S. Gao, and T.W. Kirchstetter, 2003: Distributions of trace gases and aerosols during the dry biomass burning season in southern Africa. *J. Geophys. Res.*, **108**, 4536.

Smith, D.M., M.S. Akhter, J.A. Jassim, C.A. Sergides, W.F. Welch, and A.R. Chughtai, 1989: Studies of the structure and reactivity of soot. *Aerosol Sci. Tech.*, **10**, 311-325.

Stevens, B. and G. Feingold, 2009: Untangling aerosol effects on clouds and precipitation in a buffered system. *Nature*, **461**, 607-613.

Tanré, D., Y.J. Kaufman, M. Herman, and S. Mattoo, 1997: Remote sensing of aerosol over oceans from EOS-MODIS. *J. Geophys. Res.,* **102**, 16,971-16,988.

Tao, W-K., D. Johnson, C-L. Shie, J. Simpson, 2004: The atmospheric energy budget and large-scale precipitation efficiency of convective systems during TOGA COARE, GATE, SCSMEX, and ARM: Cloud-resolving model simulations. *J. Atmos. Sci.*, **61**, 2405–2423.

Taylor, J. P., and A. McHaffie, 1994: Measurements of cloud susceptibility. *J. Atmos. Sci*., **51**, 1298-1306.

Teller, A. and Z. Levin, 2006: The effects of aerosols on precipitation and dimensions of subtropical clouds: A sensitivity study using a numerical cloud model. *Atmos. Chem. And Phys.*, **6,** 67-80.

Twomey, S., 1960 On the nature and origin of natural cloud nuclei. *Bull. Obs. de Puy de Dome*, **1**, 1-5.

Twomey, S., 1977: The influence of pollution on the shortwave albedo of clouds. *J. Atmos. Sci.*,**34**, 1149-1152.

Warner, J., and S. Twomey, 1967: The production of cloud nuclei by cane fires and the effect on cloud droplet condensation. *J. Atmos. Sci.*, **24**, 704-706.

Warner, J., 1971: Smoke from sugar-can fires and rainfall. Proceedings, International Conference on Weather Modification, Canberra, Australia, American Meteorological Society, 191-192.

Wentz, F.J. and T. Meissner, 2004 (updated daily): AMSR-E/Aqua Daily L3 Global Ascending/Descending .25x.25 deg Ocean Grids V002, [2007-2009]. Boulder, Colorado USA: National Snow and Ice Data Center. Digital media.

Yin, Y., Z. Levin, T.G. Reisin, and S. Tzivion, 2000: The effects of giant condensation nuclei on the development of precipitation in convective clouds- A numerical study. *Atmos. Res.*, **53**, 91-116.